TECHNISCHE UNIVERSITÄT WIEN

Institut für Computertechnik
Institute of Computer Technology

Master's Thesis

Simulation oriented grey-box model for weather dependent heat demand of households

by

Benedikt Herold

ORCID: 0009-0006-8465-6286

Submitted to the

Institute of Computer Technology

Department of Electrical Engineering and Information Technology

TU Wien

In Partial Fulfillment of the Requirements for the Degree of a

Diplom-Ingenieur (Dipl.-Ing.)

Supervised by

Univ.Ass. Dipl.-Ing. Dr.techn. Ralph Hoch

Ao.Univ.Prof. Dipl.-Ing. Dr.techn. Thilo Sauter

Vienna, Austria

20th March 2025

Abstract

The building sector is a major contributor to global greenhouse gas emissions, with heat demand accounting for a predominant portion, especially in residential areas. Achieving climate-neutral heat supply involves reducing CO_2 emissions through the integration of on-site renewable energy sources, such as photovoltaic (PV), and heat pump (HP) technologies, within sector coupling strategies that combine electricity, heating, and cooling. While these approaches offer potential for reducing emissions and improving energy efficiency, their widespread deployment in urban areas increases decentralized loads on electrical distribution networks, requiring accurate forecasting of both heat demand and electrical load to ensure grid stability. Given the complexity of predicting energy demand in this dynamic environment, simulation models are essential for forecasting grid behavior, as large-scale physical testing is often impractical for system planning and management.

This thesis develops a grey box model (GBM) for simulating residential heat demand and HPs for load prediction and flexibility management aimed at grid-oriented optimization. Implemented within the BIRFOST simulation environment, the model serves as an efficient and versatile tool for calculating flexibilities in heat demand and HP performance based on room temperature flexibilities in residential households. Additionally, the model incorporates dynamic thermal mass modeling with assumptions of uniform temperature distribution within the building structure, enhanced by empirical corrections from Finite Difference Analysis.

The validation of the proposed model emphasizes its impact on the low-voltage grid level dynamics, rather than precise replication of individual household heat demand. Using the WPuQ dataset, the model demonstrates strong accuracy, with a deviation of less than 5 % in simulating aggregated annual heat demand. Its dynamic behavior aligns with expectations, showing rapid temperature drops in the evening when heating is disabled, followed by gradual reductions due to the building's high thermal mass. The model achieves efficient real-time performance, with a simulation time for one step at 2 ms per building, including a forecast for the next 24 hours, supporting its application in real-world scenarios to optimize heating flexibility for grid stability and carbon reduction. Additionally, the model demonstrates HP flexibility through local and cross-location optimization strategies, leveraging on-site renewable energy sources like PVs, drawing parallels between HP systems and battery storage setups.

Consequently, the proposed GBM provides a foundation for future studies on heating systems, sector coupling, and the flexibility these systems offer in terms of load balancing and grid management. Its capability to predict future energy demand scenarios, accounting for variables such as weather patterns and urban settlement characteristics, facilitates the development of more advanced control strategies and energy system optimization. Additionally, the model's flexibility potential for cross-location optimization, demonstrated in this thesis, highlights its significance in maintaining grid stability and reducing greenhouse gas emissions, thereby contributing to efforts to mitigate climate change.

Kurzfassung

Der Gebäudesektor, insbesondere der Wärmebedarf in Wohngebieten, trägt erheblich zu globalen Treibhausgasemissionen bei. Um eine klimaneutrale Wärmeversorgung zu erreichen, müssen CO2-Emissionen durch die Integration von lokal verfügbaren erneuerbaren Energiequellen und Wärmepumpentechnologien im Rahmen von Sektorkopplungsstrategien gesenkt werden. Der Einsatz dieser Technologien in städtischen Gebieten führt jedoch zu erhöhten dezentralen Lasten in den elektrischen Verteilungsnetzen, weshalb eine präzise Vorhersage des Wärmebedarfs und der resultierenden elektrischen Last erforderlich ist.

In dieser Arbeit wird ein Grey-Box-Modell zur Simulation des Wärmebedarfs von Wohngebäuden und Wärmepumpen entwickelt, das für die Lastprognose und die Bestimmung des Flexibilitätspotentials im Kontext einer netzorientierten Optimierung verwendet wird. Das Modell wird in der Simulationsumgebung BIRFOST implementiert und stellt ein effizientes Werkzeug zur Berechnung von Flexibilitäten im Wärmebedarf sowie der Wärmepumpenleistung basierend auf Temperaturflexibilitäten in Wohnräumen dar. Eine dynamische Modellierung der thermischen Masse wird integriert, wobei eine gleichmäßige Temperaturverteilung innerhalb der Gebäudestruktur angenommen wird, welches mit Finite Differenzen Methode verifiziert wird.

Bei der Validierung liegt der Fokus auf dem aggregierten Lastverhalten auf Niederspannungsebene und nicht auf der exakten Nachbildung des Wärmebedarfs einzelner Haushalte. Die Simulation des jährlichen aggregierten Wärmebedarfs mehrerer Gebäude zeigt eine hohe Genauigkeit mit einer Abweichung von weniger als 5 %, basierend auf dem WPuQ Datensatz. Das dynamische Verhalten des implementierten Modells entspricht den Erwartungen, mit einem raschen Temperaturabfall am Abend nach Abschaltung der Heizung und einer langsameren Absenkung durch die hohe thermische Kapazität der Gebäudestruktur. Das Modell erreicht eine Echtzeitfähigkeit mit einer Simulationszeit von 2 ms pro Gebäude, einschließlich einer Vorhersage für die nächsten 24 Stunden, was den Einsatz in realen Szenarien zur Optimierung der Heizungsflexibilität für die Netzstabilität ermöglicht.

Zusätzlich zeigt das Modell die Flexibilität von Wärmepumpen durch lokale und standortübergreifende Optimierungsstrategien, die erneuerbare Energiequellen wie Photovoltaik nutzen und Parallelen zu Batteriespeichern ziehen. Das implementierte Grey-Box-Modell bildet eine Grundlage für weiterführende Analysen von Heizsystemen und Sektorkopplungsstrategien und trägt zur Optimierung von Energiesystemen bei. Durch die Vorhersage des Wärmebedarfs in zukünftigen Szenarien, die Wetterbedingungen und Siedlungsausbau berücksichtigen, werden fortschrittliche Steuerungsstrategien unterstützt. Das Flexibilitätspotential des Modells zur standortübergreifenden Optimierung bietet zudem einen wesentlichen Beitrag zur Aufrechterhaltung der Netzstabilität und zur Verringerung der Treibhausgasemissionen, was zur Einschränkung des Klimawandels beiträgt.

Acknowledgment

My sincere gratitude goes to my supervisors Ralph Hoch and Thilo Sauter, for their support in shaping my Master's thesis. I also wish to emphasize the intellectual guidance and help I received from my colleagues in the Energy & IT group, namely Thomas Reisinger and Stefan Wilker, and I am truly grateful for their assistance.

In addition to the supervision of my thesis, heartfelt thanks go to my friends and fellow students for their ongoing support, both academically and emotionally, throughout the demanding years of my academic journey. Without the necessary friendships and social connections, this time would not have been as meaningful as it was.

My family deserves special thanks for their support during my education, as well as their help in proofreading my thesis. In particular, my sister Natalie has been a great help in reviewing my work. I would like to express special gratitude to my wife Daniela, who has supported me through the often though times and has always stood by my side.

Contents

List of Tables

List of Figures

Acronyms

A.S.I. Austrian Standards International.

ANNs artificial neural networks.

BBM black box model.

CC community controller.

CO_2 carbon dioxide.

COP coefficient of performance.

CREEM Canadian Residential Energy End-use Model.

DIN Deutsches Institut für Normung.

DMU decision making unit.

EC energy community.

EER energy efficiency ratio.

ET East Tyrol.

EU European Union.

GBM grey box model.

GUI graphical user interface.

HD heat demand.

HDM heat demand model.

HP heat pump.

ISO International Organization for Standardization.

MERRA-2 Modern-Era Retrospective analysis for Research and Applications, Version 2.

NASA National Aeronautics and Space Administration.

PV photovoltaic.

SHC specific heat capacity.

SLPs standard load profiles.

SVMs support vector machines.

TO Tyrolean Oberland.

VDI Verein Deutscher Ingenieure.

WBM white box model.

Chapter 1

Introduction

1.1 Motivation

The rise in energy demand, particularly in the residential and commercial sectors, presents a growing concern, as it directly contributes to increased carbon dioxide (CO_2) emissions. Energy consumption within buildings constitutes approximately 36 % of global energy usage and 39 % of the energy related CO_2 emissions. [1] The residential sector is expected to experience an annual increase of 2.1 % in energy consumption from 2012 to 2040 world wide and a 50 % increase from 1995 to 2050 within the European Union (EU). [1, 2] At the European level, the Energy Performance of Buildings Directive aims to reduce greenhouse gas emissions in the building sector by 80-95 % by 2050, relative to 1990 levels. [3] This objective has driven policies promoting the adoption of nearly zero energy buildings, which maximize the utilization of on-site renewable energy sources, such as photovoltaic (PV). [4]

A substantial proportion of energy demand in buildings is attributed to heating, which represents a significant share of the overall energy consumption. In Germany, the government's goal of a climate-neutral heat supply by 2045 is spurring the installation of heat pump (HP) systems as a key solution. To meet the first milestone of having 65 % of heating systems powered by renewable energy by 2028, financial incentives are being offered to support the replacement of existing heating systems by the government. [5] The increasing prevalence of HPs, which form part of sector coupling strategies to integrate electricity, heating, and cooling, will substantially increase decentralized loads in electrical distribution networks, particularly in urban areas. This trend requires an accurate prediction of heat demands and electrical loads to ensure grid stability. [6]

Due to the inherent complexity in predicting energy demand, simulation becomes a critical tool. The challenge of accurately simulating heating and cooling requirements is compounded by the fact that physical testing on a large scale grid is often not feasible. [7] To address the growing energy demand, it is imperative to integrate renewable energy sources efficiently, while simultaneously ensuring grid stability and minimizing carbon emissions. [8] Sector coupling, exemplified by the use of HP systems, represents a promising solution but necessitates detailed simulations of both heat and electrical demand to ensure the reliability and sustainability of energy systems. [9]

While various organizations, including International Organization for Standardization (ISO), Austrian Standards International (A.S.I.), Deutsches Institut für Normung (DIN), and Verein Deutscher Ingenieure (VDI), provide diverse stan-

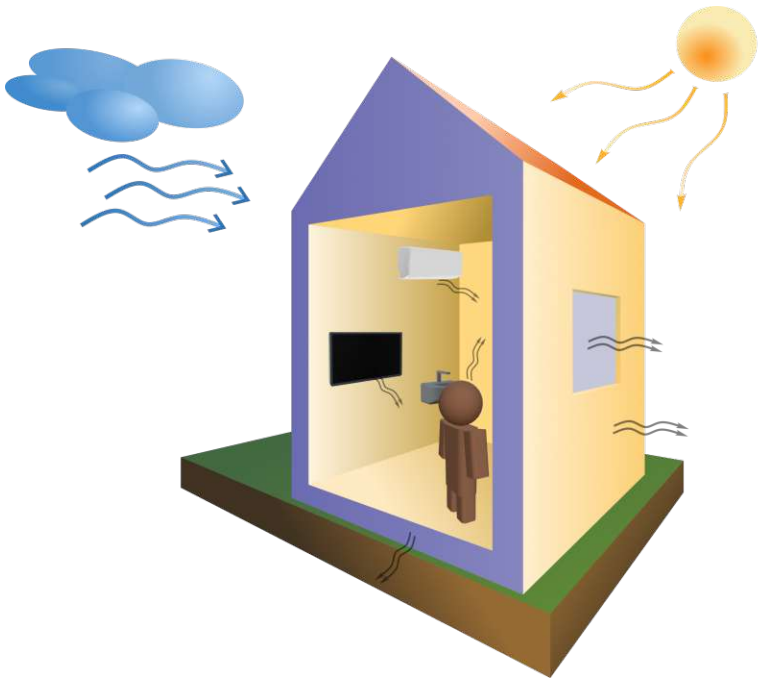

Figure 1.1: Illustration of a building with different internal and external factors influencing the heat demand, affecting the electrical power load of HPs, thereby resulting on the energy load on the electrical power grid

dards for heat demand (HD) in buildings, these standards generally focus on either calculating the annual HD or the dimensioning of heating systems based on worst-case scenarios. [10–12] While these guidelines are valuable for establishing the necessary equations for HD calculation, they are insufficient on their own for constructing a comprehensive simulation model. Therefore, models such as the grey box model (GBM), combining both physical or white box model and data-driven or black box model methods, provide more accurate estimates of thermal energy demand on a higher temporal resolution. These simulations are essential for assessing the impact of HPs on the grid and for the development of energy management strategies that optimize both electrical and thermal energy usage. [13]

Another aspect of sector coupling between heat and electricity through heat pump (HP) systems is the potential to leverage the substantial heat capacities of building's structure as a source of flexibility for grid-oriented energy optimization. [14] This flexibility allows for the temporal shifting of energy, and could also facilitate the spatial redistribution of energy, particularly when considering the citizen communities promoted by the EU. [15] For instance, when simulating the energy demand in buildings equipped with a HP, several factors must be taken into account, as illustrated in Figure 1.1, including internal heat gains, such as electrical devices or human heat dissipation, and external environmental variables, such as air temperature and solar irradiation. These factors could result in varying heating requirements across different locations due to regional differences in weather conditions, presenting opportunities for cross-location optimization. GBMs could supply the necessary data to aid in the planning and optimization of energy systems, thereby supporting the achievement of both environmental objectives and the growing energy demand.

1.2 Research Question

In relation to the motivation discussed in Section 1.1, the objective of this thesis is the development of a GBM to estimate and predict the heat demand of a building with respect to the needs for a simulation not only of heat, but also of electricity and the optimization of the grid. That puts the focus on a GBM capable of representing multiple influencing factors, as

illustrated in Figure 1.1, that affect the peak load of electricity grids. Additionally, the model allows for optimization by providing flexibility in temperature control for building heating. In order to integrate this GBM into an existing energy grid simulation, the aim is to facilitate real-time calculations of the HD. This leads to the following research questions for this thesis.

RQ 1: Which factors influencing a household's heat demand significantly affect the overall heat demand profile, particularly in the context of grid-oriented energy optimization?

RQ 2: To what level of detail and using which methods should these factors be estimated to provide a general representation of heat demand while enabling real-time calculation?

A second set of research questions addressed in this thesis concerns the potential benefits of cross-location optimization compared to local optimization under varying weather and building scenarios, using the implemented GBM. This also highlights the need for a dynamic GBM capable of accurately simulating energy shifts for heating, resulting in temperature variations.

RQ 3: What dynamic behavior is required from a grey box model to model temperature changes due to energy shifts for optimization purposes?

RQ 4: What potential does cross-location optimization offer over local optimization, particularly by leveraging different weather conditions across various locations?

In order to validate the proposed GBM and address the research questions, several validation methods are suggested. First, the GBM is compared to actual HD data from a dataset. To ensure alignment with the measured data, the simulation setup must accurately reflect real heating systems, considering household characteristics and weather data. The second method conducts a simulation with local optimization to investigate the dynamic behavior of the model. The final step involves performing a cross-location optimization, where two settlements with distinct weather conditions are simulated, and the energy shift potential between them is analyzed.

The focus of the validation process is not on exact replication of the measured HD data at the individual household level, but rather on the overall influence on the electric grid. The primary objective of the GBM is to facilitate the simulation of future scenarios, even in the absence of measurement data for direct comparison. Therefore, it is essential that the simulation produces results that are both expected and comprehensible, particularly in terms of the flexibility of the HD.

1.3 Structure of the Work

This thesis is structured in seven chapters, with Chapter 1 *Introduction* serving as the motivation and overview of this work. It is followed by Chapter 2 *State of the Art*, which provides an overview of relevant standards in heat demand (HD) calculation, HD models, and data, as well as a review of simulation environments and the project context of this thesis.

Chapter 3 *Heat Energy Contributors* examines the various factors influencing household HD and discusses approximations for these factors. This includes the static contributions, such as heat transmittance or solar irradiation, hot water generation, as well as the dynamic behavior associated with thermal capacitance. Chapter 4 *Model Implementation*

presents the structure and architecture of the model, along with a detailed description of the methods implemented. It also discusses the integration of the model into the simulation environment, as well as solutions for generating HD flexibility and HD predictions for the optimization algorithm.

Chapter 5 *Model Analysis* and Chapter 6 *Flexibilities and Optimization Potential* outline the validation methods. Chapter 5 begins with a comparison between the simulated GBM and measurement data from a dataset, analyzing both yearly and daily HD profiles. Chapter 6 focuses on the dynamic behavior and flexibility in HD provided by the GBM for local optimization, as well as the potential for cross-location optimization.

Finally, Chapter 7 *Summary* provides an overview of the thesis and its results, addressing the proposed research questions. This Chapter also suggests potential future improvements to the GBM, emphasizing the addition of functionalities required for specific scenarios and enhancing the behavior of the heat demand model.

Chapter 2

State of the Art

In this chapter standards for HD calculation, existing models, heat demand data, simulation environments for HD and the project context of this thesis are discussed. Due to the importance of the heat and energy demand, there are many different approaches and models for estimating and predicting the energy demand of individual households or entire communities. This can be achieved by different methods and includes various details, which in turn leads to an extensive state of the art with different classifications and ways of creating HD profiles. Therefore the question of why a further model is necessary in this area is raised, but precisely because of the abundance of approaches it becomes clear that there is no general solution. An adapted model is necessary for each problem to focus on the relevant aspects and details.

2.1 Standards for Heat Demand Calculation

Many organizations have developed different standards for calculating energy requirements and heating loads. Often they are derived from a committee, sometimes they are based on best practice techniques that reflect the latest advances in technology, but all have their own innovations and represent different methods.

2.1.1 International Organization for Standardization

The International Organization for Standardization (ISO) reviews standards every 5 years to make sure all information is up to date and without mistakes. The one ISO standard listed in this thesis is embedded within the set of Energy Performance of Buildings Directive standards in the context of the modular structure as set out in ISO 52000-1 for assessing the energy performance of new and existing buildings. [16]

ISO 52016-1:2017 - Energy performance of buildings — Energy needs for heating and cooling, internal temperatures and sensible and latent heat loads

This standard is a part of the ISO 52000-1 family with part 1 specifying calculation methods for the assessment of energy need for heating and cooling, based on hourly or monthly calculations, the latent energy need for (de-)humidification, based on hourly or monthly calculations, the internal temperature and the conditions of the supply air to provide the necessary humidification and dehumidification. The calculation methods can be used for both residential and non-

residential buildings, which can also be analyzed for their different thermal zones. The calculations can be based on the assumption that the thermal zones are thermally coupled or not. [17]

The calculation methods were developed for the calculation of basic energy loads and requirements without interaction with specific building services systems and for the calculation of system specific energy loads and requirements including interaction with specific systems. The hourly calculation methods can also be used as a basis for calculations with more extensive system control options. [17]

2.1.2 Austrian Standards International

The Austrian Standards International (A.S.I.) develops ÖNORM documents based on international standards from organizations like ISO with the purpose of implementing them on an Austrian level. This can lead to standards directly derived from other standards or to a new set of definitions as a combination of many other standards or regulations to be implemented. [18]

ÖNORM EN ISO 52016-1 - Energetische Bewertung von Gebäuden - Berechnung des Energiebedarfs für Heizung und Kühlung, Innentemperaturen sowie der Heiz- und Kühllast in einem Gebäude oder einer Gebäudezone - Teil 1: Berechnungsverfahren (ISO 52016-1:2017)

Derived directly from the corresponding ISO standard, this standard implements the same definitions targeted for Austria. It mainly translates the English standard in order to enable a barrier-free implementation of the standard. [10]

ÖNORM EN 12831 - Heizungsanlagen in Gebäuden - Verfahren zur Berechnung der Norm-Heizlast

This standard is mainly based on regulations and specifies methods for calculating heat loss for standard cases under target conditions. It contains a method for calculating the heat load for standard cases under target conditions. Standard cases are the majority of all buildings encountered in practice with a limited room height, for which it is assumed that they are heated to a steady state under the set point conditions. The standard heat load is essential for dimensioning the heating system when designing new buildings and renovating old buildings with a new heating system and building envelope. [18]

2.1.3 Verein Deutscher Ingenieure

The Verein Deutscher Ingenieure (VDI) publishes technical guidelines, available in German and English, offering practical, expert-driven solutions for various industries based on other standards or best practice techniques, reflecting the latest advancements in technology. Compiled by around 10,000 voluntary experts from science, industry, and public administration, the VDI guidelines include checklists and tables for easy implementation. With over 600 committees, VDI plays a crucial role as a regulator in Germany. [19]

VDI 2067 - Economic efficiency of building installations - Effective energy demands for heating drinking water

This standard provides calculations for the energy demand of heating drinking water, focusing on the energy needs for personal hygiene and home hygiene. It serves as a foundation for comparative cost accounting in the energy supply

industry and aims to make energy demands more transparent by distinguishing between values related to buildings, individual energy use, systems, and energy supply. This allows users to clearly compare different solutions for buildings and systems. [20]

VDI 4655 - Reference load profiles of residential buildings for power, heat, and domestic hot water as well as reference generation profiles for photovoltaic plants

This guideline is newer and tries to combine the demands for heating drinking water with the other heat and power demands in a residential building. The standard covers the demand for electricity, space heating and domestic hot water in residential buildings, providing data for existing buildings and low-energy houses. It applies to single-family homes with up to six occupants and multi-family houses with up to 25 units, including electricity generation data from PV systems. The standard offers reference load profiles for designing electricity and heat generators, such as combined heat and power systems, heat pumps and solar thermal systems, and helps assess their economic efficiency. It also supports system efficiency testing, design criteria, simulations and calculations for heat and power storage systems. [12]

2.1.4 Deutsches Institut für Normung

The Deutsches Institut für Normung (DIN) is an independent platform for developing standards in Germany and globally. It collaborates with industry, science, the public sector, and civil society to address future challenges. A standard outlines requirements for products, services, or processes, promoting clarity, trade facilitation, and exports extending regulation requirements. DIN ensures market acceptance through broad participation, transparency, and consensus, allowing anyone to propose standardization and enabling all relevant parties to contribute their expertise. [21]

DIN V 4108 - Wärmeschutz und Energie-Einsparung in Gebäuden

This standard describes the terms used for the thermal balance of a building and the procedure for calculating the annual heating and heating energy requirements, taking the boundary conditions into account that are to be applied in Germany. The method is applicable to residential buildings and to buildings that have to be heated to certain indoor temperatures. The pre-standard is suitable to provide calculation rules for computer programming. [11]

2.2 Heat Demand Models

There are various methods for modeling heat demand (HD) in residential buildings, but most of them are designed either for large energy systems with low spatial resolution and therefore little optimization potential, or for very small systems with high resolution but insufficient performance characteristics. [22] These methods can be characterized in three main categories, which are data-based models, physical-based models and grey box model (GBM) as a combination of the above approaches. In reality, almost every method is a mixture of data- and physical-based and thus a GBM, but some of them have their focus on the data characteristics or the physical processes behind the model.

The data-based models, also known as black box model (BBM), require large datasets in order to sufficiently represent the energy demand at a detailed view with spatial resolution on households level and are not able to extrapolate simulation results as well as physical-based models, also known as white box model (WBM). This is due to their limited robustness to changes, as slight differences in the physical parameter of the model can lead to significant changes in the

model behavior. But BBMs can have great advantages in simulation time and development costs as well as higher accuracy in the defined scope compared to WBMs, which require a deep understanding of the underlying physical process. [23]

The grey box model (GBM) tries to combine advantages of both techniques by providing some abstraction with estimations regarding actual data and on the other hand implementing important and relevant dependencies with physical models, that can be tuned and extrapolated for different scenarios.

2.2.1 Data-based models

The data-driven models or BBM can consist of different internal structures. The calculations are not derived from physical processes and are only used to reproduce the reference data provided to generate the BBM. [1] They can be classified as two main types of techniques, the static models and the machine learning approaches, which are listed below.

Static method

For a static model, standard load profiles (SLPs) are often used for large-scale modeling of energy systems. These SLPs are derived from historic data from the 1980s and therefore may not reflect current energy demands. Another issue with these profiles is the lack of variance and spatial resolution, as there is only one profile for each weekday, season and building type. They are designed to represent multiple households for energy provider and grid operator but do not represent single household profiles. [22]

In order to overcome the lack of variance in profiles, measured public available data as described in Section 2.3 is used to get a higher spacial resolution. [24] Another solution is using stochastic bottom-up methods to derive from single household profiles to aggregated grid profiles. [25, 26]

A more elaborate approach is done by authors in [27] implementing Canadian Residential Energy End-use Model (CREEM) using several available datasets for energy consumption, housing prices and weather conditions in Canada. From this, 16 house archetypes were developed and simulated. The various data sets, as well as actual energy billing data, were then used to evaluate and adjust the profiles for different regions and building types. After several cycles of adjusting the profiles and comparing them to the data sets from different sectors, the estimations matched with those from other studies such as [28] for Canada.

A similar idea was implemented by [29] using SLPs in combination with detailed global temperature datasets from NASA MERRA-2 and high resolution population data to diversify the profiles for more spatial resolution on energy density maps. This approach leads to very robust and detailed data for big regions, but is not suitable for single household profiles and optimization analysis.

These models can be describe as statistical methods that correlate energy and heat consumption with the influencing variables. Although they are still empirical models developed from historic data, they implement a statistical regression model of a sort and thus build the bridge to the machine learning approaches discussed in the next section. [30]

Machine learning approach

Due to the complexity and non-linear behavior of HD profiles machine learning algorithms are mostly used and commonly applied with support vector machines (SVMs) and artificial neural networks (ANNs) and are a prime example of black box model due to implicit relationship with the physical fundamental principles. [1] But one of the first contributions on using machine learning as a regression model in predicting the HD of a single household was done by authors in [31, 32]. Further work was developed on top by dividing the total load into sub-levels by many authors after that, in order to estimate the demand more accurate and with better tuning opportunities. [30]

A more recent work on regression models for HD profiles was done in [33] focusing more on the thermal inertia of buildings, especially with nightly ventilation in offices. In [34] multiple linear regression and self-regression methods were implemented to predict monthly power energy consumption for large scale public buildings. With the findings in [35] regression models on measurements with the length of one day, one week and three months were associated with prediction errors of 100 %, 30 % and 6 %. It was shown that the dataset size and period greatly influences the quality of these models.

The first set of recent thermal energy demand calculations is based on the SVMs as done in [36] as a pseudo-dynamic model to also account for the thermal inertia of the building. In [37] a prediction of the heat load for consumers connected to district heating system is implemented by short-term multistep-ahead predictive models using SVMs. In order to optimize the SVMs parameters the Firefly Algorithm was used. A similar approach was done by the authors in [38] using also short-term multistep-ahead predictive models devoloped using SVMs coupled with a discrete wavelet transform, showing that this increases predictive accuracy compared with results from ANNs approaches.

Besides support vector machines, the most commonly used artificial intelligence models in the application of building energy prediction are artificial neural networks, due to there good capabilities of solving non-linear problems effectively. [30] One of the first indroduction of ANNs as done in [39], where the results of recurrent ANNs applied to hourly energy consumption data are presented to predict the future heating and cooling energy demand of buildings using only weather data and time stamps. The authors in [40] used the same type of ANNs to predict cooling loads for three office buildings, training the model with data from 1997 to 2000 and testing it with data from 2001.

A more detailed review of ANNs in energy applications in buildings was done 2006 by the author of [41], including solar radiation, wind speed, solar water heating systems, air flow distribution inside a room and many other factors. Building on that in [42], a back propagation neural network is used to predict cooling demand profiles in buildings. In the study the modal trimming method, a global optimization method, was introduced to determine the model parameters. In [43], the influence of weather on energy consumption in different regions is investigated by using a back propagation neural network to predict the heating and cooling loads in different climate zones, represented by heating and cooling degree days, using these variables as input data for the model.

The authors of [44] developed an advanced thermal control method based on ANNs, which consists of a thermal control logic framework, including two predictive and adaptive logics using ANNs, and a system hardware framework. These models take not only air temperature but also humidity into account. In [45], a replacement method based on ANNs was developed to accelerate the prediction of thermal comfort for any member of a building category. The ANNs method uses the data obtained from EnergyPlus, discussed in Section 2.4, simulations for multi-family buildings of linear-type social housing in southern Spain. Both models are generated in the MATLAB environment described in Section 2.4 with

the International Building Physics Toolbox.

2.2.2 Physical-based models

The white box model (WBM) involves detailed modeling of the thermodynamic laws and therefore requires the complete building and environmental parameters and a lot of knowledge for the implementation and parametrization of the physical-based models. [46] The techniques for modeling the heat demand can be static, including only the heat exchange, or dynamic, including the heat capacities of the building mass. The complexity of the WBM varies greatly depending on the degree of accuracy of the modeled processes. Many HD and energy simulation tools for buildings are based on the WBM and the most commonly used ones, including TRYNSIS, EnergyPlus, ESP-r, SUNREL and DOE-2 are covered in Section Section 2.4. Due to the complexity and high cost of implementing physical-based models, most of the literature is based on these tools, either using them to simulate and analyze their own models or improving parts of the methods involved in these tools. [47–53]

In [47] a simple method to account for the radiative heat on the inner surface of external envelopes for improving the accuracy of the "air-to-air" conduction method is introduced. For this purpose, a simplified analytical model to evaluate the impact of internal radiant heat on the cooling load is developed and tested with 5 case studies in EnergyPlus. Authors in [48] present a dynamic model for thermal transient analysis and its application to a simplified test case considering solar irradiation and internal radiation for modeling of a typical single-zone building. Their approach uses a state-space representation developed in MATLAB/Simulink.

A three-dimensional, finite-element, heat-transfer computer program was developed in [49] to study ground-coupled heat transfer from buildings. It was used in conjunction with the whole-building energy simulation program SUNREL to analyze ground-coupled heat transfer from buildings. In [50] a dynamic thermal model for a building with an integrated ventilated PV-facade based on TRNSYS was presented and validated against experimental data. Authors in [51] focused on developing an estimation model for the heating and cooling demand of a residential building with different envelope designs using the finite element method.

A simplified building simulation tool to evaluate energy demand and thermal indoor environment in the early stages of building design is introduced in [52], calculating hourly values for the HD and indoor temperature based on weather data. Another approach for a more simplified WBM was discussed in [53] by an iterative methodology to progressively reduce building simulation model complexity with the aim of identifying potential trade-offs between computational requirements such as model complexity and energy estimation accuracy. This approach leads to the idea of grey box model (GBM) trying to make usage of the advantages of WBM without the high computational efforts.

The methods used to implemented the above models are numerical and based on finite element, finite difference and finite volume approaches as the majority of WBMs in literature. These approaches have a well understood theory and already good software support for developing and computation. They also intend to serve a very specific purpose or a small set of data, either time or building quantities, due to high computational effort and the need of high knowledge of the model parameter. On the other hand, they enable the analysis of new scenarios and hypothetical use cases without measurement data. [47–53]

2.2.3 Grey-box models

To overcome the drawbacks of BBM and WBM the GBM try to implement a more generic, but still physical-based approximated approach. They can be mixed or transitional forms of BBMs and WBMs with some sort of simplification and tuning parameters with still physical meaning. A commonly used method of abstraction is the representation of the thermal network of a building with a lumped approach of capacitance and resistance elements, where the definition of parameters is also based on measured data of a real system. [1]

In 1999 the authors in [54] used a GBM to predict building heat moisture systems with high accuracy. To forecast energy usage in heat pump water heaters in [55] an improved GBM was applied, finding that a four-week data interval yielded the best prediction results. Authors in [56] integrated two weather prediction modules into a simplified thermal load model to predict cooling loads. They used a modified grey model for temperature and humidity, and a regression model for solar radiation. The model's performance improved when trained with the predicted weather data.

The following works have all been performed using the capacitance and resistance approach with different amount of resistance and capacitance elements. In [57] a time-series cooling load model is deduced from a simplified resistance–capacitance model to provide an efficient solution with manageable computational requirements. This is done to encounter the thermal capacity of a building envelope delaying conduction heat gains, while the thermal capacity of the whole structure delays radiative cooling loads. Authors in [58] develop a genetic algorithm estimator with 2 resistance and 2 capacitance elements for the estimation of the lumped internal thermal parameters of the building thermal network model, using the operation data collected from site monitoring. To investigate and verify the method, a seven-resistance, five-capacitance model was tested in [59] against a reference model in EnergyPlus using predicted weather data. It was shown that the method can accurately calculate and predict the HD of a building.

Another approach for using a lumped approach of capacitance and resistance elements is in combination of multiple GBMs for various elements of the building. In [60] a transformation of a multi-layer wall into a three resistances and four capacities model in combination with a one resistances and two capacities water loop model for floor heating is introduced. The author in [61] shows the potential of second-order simplified thermal models with improved accuracy due to combination with capacitance and resistance elements approach. In [62] the degree day calculation method introduced by different standards is extended with several transient energy balance equations for external leading to a lumped approach of capacitance and resistance elements. the results are evaluated against simulation in TRNSYS and EnergyPlus. Based on a standard of ISO a GBM is developed in [1] for hourly thermal energy needs in different types of premises. It consists of different resistance–capacitance models for windows and exterior walls as well as energy balance equations for different thermal zones.

These presented models show the potential for grey box model approaches in developing computational more reasonable methods for accurate HD simulations. With a well adapted GBM for the respective parameter and resolution requirements, a GBM can also be used for larger applications beyond a household for different scenarios without measurement data.

2.3 Heat Demand Data

In order to develop data-based models or to validate white box models and grey box models a sufficient set of real measurement data is required. As with many private data, the availability of data on household level is limited. To provide an overview of the available data three different data sets are listed in the following section.

2.3.1 Simbench

The SimBench project [63] aims to create a benchmark dataset for grid analysis, planning, and operation management. This dataset will allow the development of new methods and solutions without relying on proprietary grid data, ensuring comparability, transparency, and consistency in the field. It includes electrical parameters for static modeling of electric grids across a range of voltage levels, from low to extra-high voltage. The dataset features 13 basic grids, all of which can be interconnected and come in three future scenario variants. [63]

This dataset is not a collection of real data, but a hypothetical definition of different settlements and load profiles in order to make research in this field comparable. While electric load profiles and also heat pump profiles are included in the future scenarios of the dataset, it has no basis for verification of a heat demand model (HDM). The benefit of using SimBench settlements is the enabling of other authors to compare their models with the same settlements and parameters, making results more replicable and open the possibility for benchmarking the simulators. [64]

2.3.2 WPuQ Dataset

As part of the WPuQ project authors in [65] generated a dataset on electrical single-family house and heat pump load profiles in Germany, Hamelin in Lower Saxony. The district comprises 68 single family homes built around 2000, all of them meeting low-energy standards with a heating requirement of 45 to 50 kWh/m^2a. Each house is equipped with a water-to-water heat pump connected to a cold local heating network and solar thermal systems for water heating. The heat pumps have a thermal output of 7.4 to 11.3 kW and have a 6 kW heating rod for support. They operate with water temperatures of 10 to 12°C on the primary side and 35°C on the secondary side and use underfloor heating for space heating. Solar thermal systems with 4-6 m^2 collectors provide hot water in summer, which is supplemented by the heat pump if there is insufficient solar energy. [65]

Separate measurements were carried out in 38 households as well as an aggregated measurement in the substation that supplies all 68 households. The installation of the measurement technology began in 2017 and the data has been available for most households since May 2018. Separate electricity meters were installed for the household and heat pump consumers, while the electricity consumption of the pumps in the heating circuit and the solar thermal system was recorded via the heat pump meter. For households with a ventilation system, their electricity consumption was also recorded via the heat pump meter. [65]

All data is available on the Zenodo platform. The entire dataset consists of seven hierarchical HDF5 files per year, with five files containing measurement data and two additional files containing weather data and temperatures from a nearby district heating network. Each of the five measurement files provides similar information in different aggregations. For simplicity, the data is aggregated at four temporal resolutions of 10 s, 1 min, 15 min and 60 min, with one file containing spatially aggregated profiles of all households in individual profiles. The original sampling interval is 10 s. In the HDF5 format, the datasets are organized in groups, each consisting of up to three nodes, top level, middle level and bottom

level, that categorize the data. [65]

2.3.3 Aggregated Heat Pump Profile

Authors in [66] used data from German distribution system operators of standardized load profiles for heat pumps to generate their own aggregated profile for the energy demand of heat pumps. The hourly demand of electricity for a heat pump is listed depended on the ambient temperature. This results in a two dimensional dataset with time and ambient temperature as input data.

The data is used in [66] to analyze the shift and optimization potential when offering more flexibility from HD profiles with shedding load. Based on the electricity generation from renewable energy sources, applications provide demand responses. These results show, that this reduces limitations of renewable energy sources.

2.3.4 Data from Simulation Tools

In many of the works presented in the previous section, no real data is used as a basis, but simulated data from recognized tools such as TRYNSIS or EngeryPLUS, described in Section 2.4. The reason for this is due to the difficulty of obtaining data and the fact that it often does not exist for special scenarios. [1, 57–62]

This method enables a very good comparison of new implemented models, as the environmental and influencing factors can be set identically between the comparison data. However, the reference to reality is lost, not only due to possible errors in the calculation of reference models, but also in the perhaps unrealistic assumption of parameters. This is not noticeable when configuring models, but is then usually evident in deviations from real data. This type of validation is therefore only useful for certain requirements.

2.3.5 Energieausweis

The Energieeinsparverordnung, which came into force in February 2002 as the third amendment to the Wärmeschutzverordnung, aims to reduce the energy consumption of buildings by an average of 30 % and cut CO_2 emissions. The 2007 revision introduced the Energieausweis, which is mandatory for existing buildings in all EU member states. This certificate, which is based on various DIN standards, informs interested parties about the energy efficiency of a building. It identifies the causes of energy losses in the building envelope and systems technology and estimates the heating energy requirement, taking into account climate and standard consumption data. However, the energy performance certificate does not reflect actual consumption. [67]

With the data provided by the Energieausweis the parameter of a GBM could be defined and simulated. In order to validate a model the results should then not be compared to the theoretical energy demand in the Energieausweis, but to the actual measured consumption profile. Since the scope of this thesis is not to replicate the HD of a singular household perfectly, but match the profile of a community and multiple buildings, such a comparison is not effective or significant.

2.4 Simulation Environments

There are many energy demand simulation tools and environments for the integration of heat demand models. Some of the most commonly represented ones in literature are discussed in this section, including the BIFROST simulation environment used for this work. The available options differ in terms of implementation and use case. Some are primarily intended for the energy or thermal analysis of buildings, while others support a variety of application areas. They can also differ in terms of simulation duration, with TRNSYS and MATLAB, depending on the implementation, in particular being used for detailed simulations over short periods of time and the others mainly for dynamic simulations of buildings and systems over longer periods of time, such as whole years. [68]

2.4.1 MATLAB/Simulink

MATLAB combines a desktop environment for iterative analysis and development processes with a programming language in which you can directly formulate matrix-based mathematics. It includes the Live Editor for creating scripts that combine program code, output and formatted text in an executable notebook. It is a very powerful tool for many areas of application, with heat demand simulation being a small part of it. Together with the Simulink it allows for model-based design to take the development of complex systems to a graphical level by placing models at the center of all processes throughout the entire development process. It is frequently used in science and industry for implementing own models and controllers as well as for using toolboxes for existing methods. [69] Although it is not specifically designed for HD simulations, it is often used to implement the HDMs discussed above. [47, 48]

One of those Toolboxes is The International Building Physics Toolbox in Simulink introduced in [70] for the purpose of modular structuring of standard building elements, using the graphical programming language Simulink. It is an open-source package that is also used in other works for modeling HD. [44, 45]

Besides the implementation of physical-based models MATLAB also allows for the implementation of artificial neural networks (ANNs). With the help of the Deep Learning Toolbox and the Statistics and Machine Learning Toolbox, both deep and shallow neural networks can be created. [71] In [44, 45] this is used to develop and simulate the presented ANNs.

2.4.2 TRNSYS

TRNSYS is a flexible, graphically based software environment used to simulate the behavior of transient systems. The vast majority of simulations focus on evaluating the performance of thermal and electrical energy systems, but TRNSYS can also be used for modeling other dynamic systems such as traffic flows or biological processes. It is a component-based software package that evolves with new technologies over time. The standard library includes around 150 models, including pumps, multi-zone buildings, wind turbines, electrolyzers, weather data processors, economic routines and heating, ventilation as well as air conditioning systems. It is used in [50, 62] for generating validation data and simulating different analyzed scenarios together with EnergyPlus. [72]

2.4.3 EnergyPlus

EnergyPlus is an energy simulation program for the entire building that can be used to model energy consumption for heating, cooling, ventilation, lighting, process loads as well as water consumption in buildings. Some of the notable fea-

tures and capabilities of EnergyPlus include solutions of different thermal zone conditions, heat balance-based solution of radiant and convective effects, sub-hourly user-definable time steps, a model that accounts for air movement between zones and illuminance and glare calculations. EnergyPlus is a consol based program that can read and write input to text files. This tool was used in [59] for generating a reference model. [73]

2.4.4 ESP-r

ESP-r (Environmental Systems Performance - Research) is a building performance simulation modeling tool developed at the University of Strathclyde Glasgow. In carrying out its assessments, the system is capable of modeling heat, air, moisture, light and electricity flows at a spatial and temporal resolution specified by the user. The tool has been developed for the Linux operating system but has the ability to run on Windows directly or via the Cygwin environment. [74]

2.4.5 SUNREL

SUNREL is an energy audit tool for residential buildings that uses comprehensive thermal models to provide hourly information on energy consumption. This diagnostic tool is used to estimate different influencing factors in the design of energy-efficient residential buildings, where energy consumption depends primarily on the interaction between the building, its occupants and the local environment. [75]

2.4.6 DOE-2

DOE-2 is a freeware building energy analysis program that can predict energy consumption and energy costs for all types of buildings. DOE-2 uses a description of the building layout, construction, operating schedules, conditioning systems, and consumption rates provided by the user, along with weather data, to perform an hourly simulation of the building and estimate consumption bills. The DOE-2 program is a console based program that requires experience to use effectively, but offers great flexibility to researchers and experts. Together with DOE-2 a complete interactive Windows implementation called eQUEST is available, with additional wizards and graphical user interface to assist in the use of DOE-2. [76]

2.4.7 BIFROST

BIFROST [77] is a simulation platform with a web-based interface designed for building, designing and managing communities. It enables the connection of external simulation modules to its core, which processes these modules in a specific order and integrates the data they provide into the central data model. In this way, specialized domain models can work together and achieve the desired results at the end of each simulation cycle. [78]

Figure 2.1 displays the web-based graphical user interface (GUI) of the simulation environment, with an exemplary settlement, showing different buildings and landscape elements. Together with the 2.5-D design, this GUI allows for first glance analysis of data, enabled by the option to display plots of different variables. After the computation, a finished simulation can be played to show the course of variables or display some events, like switching of lights, movement of cars or power outage, based on the simulated data. To contribute to that, the visual landscape elements do not serve a simulation purpose but are solely intended to represent an urban landscape.

Figure 2.1: The web-based interface of the BIFROST simulation environment with an exemplary settlement, showing different buildings and landscape elements, as well as the plot illustration of variables within the GUI

While the other described simulation environments primarily focus on processing and calculating data, BIFROST also enables a highly intuitive and visual representation of events. The goal is to convey data and results in a manner that can highlight problems and solutions, even for individuals who are less familiar with the subject area. Therefore, the representation of the settlements is designed to be as visually realistic as possible, offering the additional capability to replay and present already simulated results.

BIFROST consists of several modules that provide various functions. In addition to the core module, there is a building model that includes households, commercial properties and municipal buildings. This module is split up into different sub modules including a Load Class, Battery Class, Photovoltaic Class and Heat Pump Class, which provides the information about the consumed electricity due to HD. Therefore the grey box model developed in this thesis is connected to this Class.

Furthermore a weather generator module simulates the weather conditions for a specific date and location and a community controller (CC) manages mergers of several households and other properties as energy communities. The CC handles the exchange of flexibilities between all the participants of the energy community, including the controller, member buildings, community batteries and the higher-level controller. With predictions from the members for the next 24 h the CC optimizes the schedule of each participant to minimize the grid load for each energy community. [78]

The structure of the BIFROST simulation setup in combination with the GBM introduced in this thesis is shown in Figure 2.2. This also includes a decision making unit (DMU) discussed in Section 2.5 with two BIFROST instances. It is used for the decision making on higher levels and plays the role of the higher-level controller for the CC. The illustration 2.2 shows the gap that is covered by the HDM in order to make a decision at the highest level based on the energy balances.

2.5 Project Context

This thesis is part of the EnergyDec project [79] funded by the Klima- und Energiefonds and FFG (Austrian Research Promotion Agency) and carried out under the Energy Research Program 2020 “Energieforschung (e!MISSION)”, with the aim of using a decision making unit to decide on different scenarios on a global level. The idea is to use various

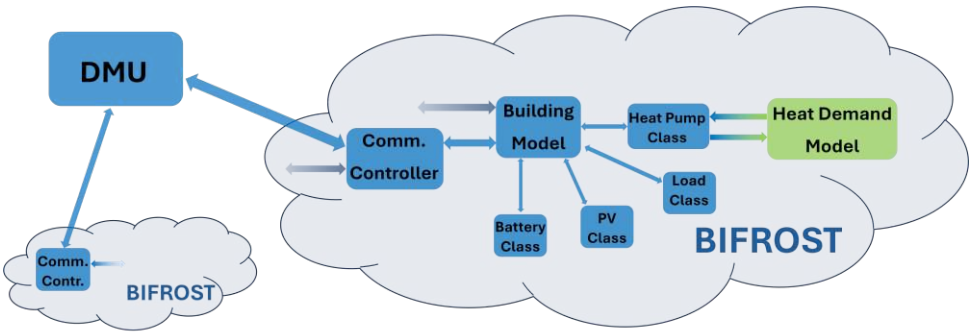

Figure 2.2: The structure of a BIFROST simulation including the sub models needed for the HDM introduced in this thesis, with the DMU and a second BIFROST instance for the analysis of cross-location optimization

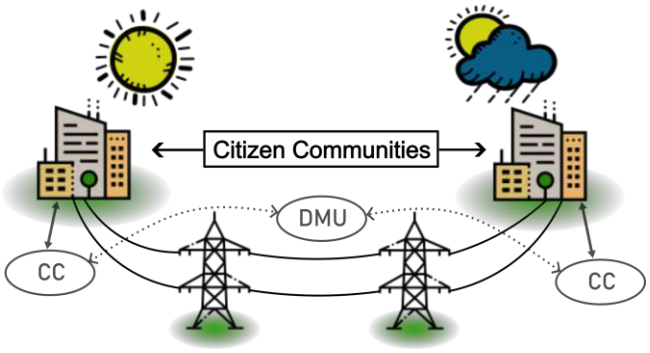

Figure 2.3: The goal of the EnergyDec project with two energy communities in different location, forming a citizen community, and the local optimization with CCs and a cross-location optimization with a DMU

optimal schedules for different objectives calculated by the community controller on a local level in order to make a decision at a higher level as to which schedule should be selected in the next time step for each location. This also involves cross-location optimization beyond single sites and using information from multiple locations to optimize the energy balance at a supra regional level.

HD plays an important role here, as this will have the greatest influence on various energy requirements in different locations due to weather conditions. By taking weather influences into account, an even better energy balance can be drawn across several sites than just across a single energy community as illustrated in Figure 2.3. With a DMU already implemented as part of this project, the influence of a more detailed GBM can be investigated for this area of application. [80]

The simulation and implementation of the project and the required DMU is in BIFROST as illustrated in Figure 2.2, with the structure presented in Section 2.4. This allows modular setups and the use of already implemented solutions for the optimization of energy communities using an CC as well as the weather module for different scenarios.

Chapter 3

Heat Energy Contributors

To address the first two research question ***RQ1*** and ***RQ2*** defined in Section 1.2 on the aspects of a household's heat demand (HD), this chapter discusses various contributors in terms of their influence on the total HD and makes estimates in order to meet the requirements of the computational effort. There are three factors to consider when calculating the energy balance in relation to the heat and temperature of a building.

On the one hand, there are the static contributions from the current weather and other influencing factors as discussed in Section 3.1. These aspects are unaffected by the past and are based only on present values, so therefore they can be considered and balanced statically.

On the other hand, hot water generation and the associated hot water demand also play an important role. For the simulation, this would also be considered a static factor, but as the system for supplying and generating hot water can differ from that for heating the building, this aspect is dealt with separately in Section 3.2 and not aggregated to one HD. Even when using a heat pump for the generation of both the hot water and the heating system, they may vary in temperature levels with heating often only 35°C and hot water up to 60°C, thus resulting in different efficiency factors and electrical power demands.

The final contribution to the thermal calculation of a building is the temperature behavior. This is associated with a dynamic model as described in Section 3.3, as both the air and the building substance represent a thermal mass with heat capacities and different coupling to the indoor air temperature. This requires a calculation of temperature changes based on heat balances as well as coupling processes between different building elements and addresses the final two research question of the dynamic behavior of energy shifts due to optimizations in the simulation.

3.1 Static Contributors

Different factors are discussed in this section for the static contributions to the heat balance. Even if some contributions, such as heat transmission, correspond to a dynamic process, they are considered in a steady state and therefore calculated statically. A static approximation can be found for many dynamic processes in this section, which simplifies calculations and reduces computation times. It is important that the characteristics of the influencing factors are not lost in the process so that a realistic profile of the HD can still be obtained.

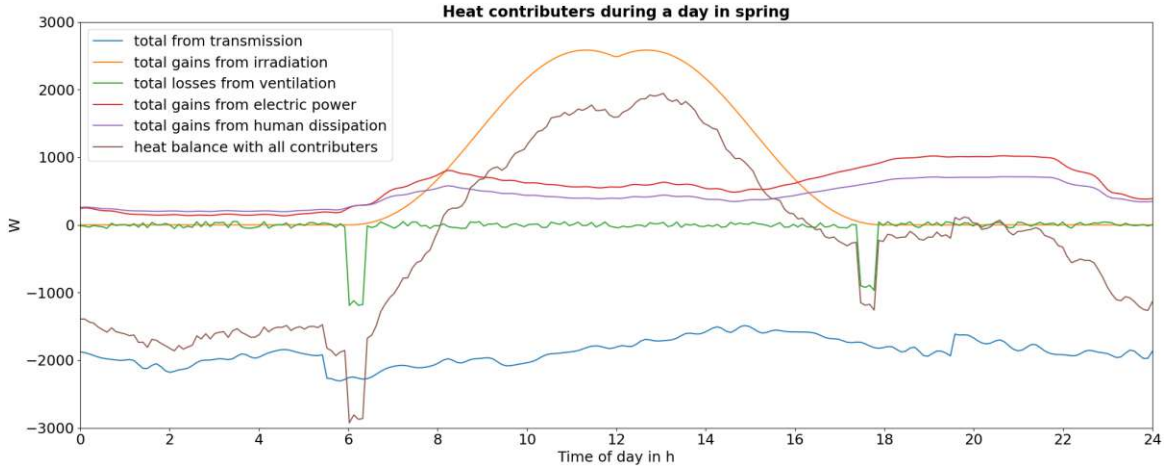

Figure 3.1: Illustration of a possible day profile with the different heat contributes discussed in Section 3.1 of a 4 person household and a living area of 100 m^2 on two floors, with temperatures of 2-10°C and a maximum solar elevation of 40°

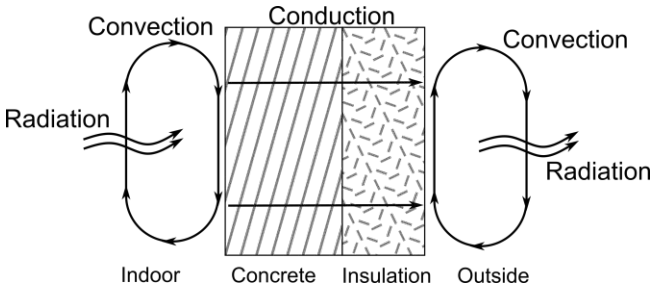

Figure 3.2: Illustration of the thermal transmission due to thermal conduction, radiation and convection on a cross section of an exterior wall with insulation

An overview of the factors considered and a possible daily course of a classic 4 person household and a living area of 100 m^2 on two floors in early spring at temperatures between 2 and 10°C is shown in Figure 3.1. The contributions shown are described in more detail in the respective subsections and the basis for their calculation is provided. It is clear that all the factors illustrated have a relevant contribution to the heat balance of the building with different characteristics, which can also vary greatly over the year and environmental influences.

3.1.1 Thermal Transmittance

Heat transmission is a collective term for all forms of heat transport, thus describing the total heat losses or gains between the building and its surroundings. The term includes thermal conduction, thermal radiation and thermal convection as the three forms of heat transport. In Figure 3.2 the three different forms are illustrated on a cross section of an exterior wall with insulation.

Thermal conduction

Thermal conduction is the transfer of heat within a body through interaction between particles. In macroscopic terms, the individual particles are at rest and are not transported. The ability of a material to transport heat through thermal conduction is specified with the thermal conductivity λ in W/m K giving a relation between the resulting heat flow per Kelvin and Meter of the material. Equation 3.1 shows the calculation for the heat flow $\dot{Q}$ through a flat wall like illustrated in Figure 3.2 with an area A and different layers with the thickness s_i and the thermal conductivity λ_i for a temperature difference ΔT. [81]

Material	Density ρ in kg/m^3	Thermal conductivity λ in W/m K	Spec. heat capacity in kJ/kg K
Concrete	2400.0	2.10	0.9
Brick	1000.0	1.00	0.9
Steel	7850.0	50.00	0.5
Wood	60.0	0.13	1.7
Glass	2500.0	0.90	0.7
Glass wool	120.0	0.05	0.8
Wood wool	400.0	0.09	2.1
Cotton	81.0	0.06	1.7
Mineral wool	120.0	0.04	0.8
Polystyrene	25.0	0.03	1.4
Gravel	1800.0	0.70	0.8
Soil	1500.0	1.20	1.0
Rubber	1100.0	0.16	1.5
Water	997.0	0.60	4.2
Air	1.2	0.02	1.0

Table 3.1: Thermal conductivities, densities and specific heat capacity of relevant materials for heat conduction in buildings from data of [81] and [82]

$$\dot{Q} = A\frac{\Delta T}{\sum_i^n \frac{s_i}{\lambda_i}} \tag{3.1}$$

In Table 3.1 some of the relevant thermal conductivities together with the density are listed based on the data of [81] to give an overview of the magnitude for different materials. In general, a trend can be seen that conductivity also increases with increasing density. Especially the difference between building materials like concrete and bricks compared to insulating materials shows the importance of preventing thermal bridges as discussed in Section 3.1.6.

Thermal Radiation

Thermal radiation is a form of energy transport through electromagnetic waves. Heat is transferred without a medium for transmission and takes place between all objects. Often only the thermal radiation in one direction is considered, as in Figure 3.2, but in fact the colder bodies also radiate to the warmer ones and the net energy flow is created by the differences in intensities. The intensity depends on the respective temperature of the body and follows the Stefan-Bolzmann law. The heat emitted is proportional to T^4, the absolute temperature. It is therefore clear that higher temperatures quickly lead to greater thermal radiation intensity and therefore emit significantly more energy to colder objects. [81]

The net heat flow $\dot{Q}_{1,2}$ between two surfaces A_i with temperature T_i can be determined using formula 3.2, where ϵ_i gives the emission coefficients, σ is the Stefan-Bolzmann constant and $\theta_{1,2}$ is a dimensionless geometric quantity that indicates what proportion of a surface radiation meets the counter surface under consideration at an angle. [81]

$$\dot{Q}_{1,2} = \epsilon_1\epsilon_2\sigma\theta_{1,2}\left({T_1}^4 - {T_2}^4\right)A_1 \tag{3.2}$$

In order to generate a more convenient form for approximating the thermal radiation between two objects like a wall with a surface of A and its surroundings equal to thermal conduction, equation 3.3 is used to simplify the calculation with one parameter α_r and a linear temperature difference ΔT. Since thermal radiation is proportional to T^4 with T_W

being the temperature of the wall and T_S being the temperature of the surrounding, a at first inconvenient parameter b is used, with the benefit of generating a linear equation together with a parameter C to combine all dependencies. [81]

$$\dot{Q}_{1,2} = \alpha_r \cdot \Delta T = C\, b \cdot \Delta T\ , \quad b = \frac{{T_W}^4 - {T_S}^4}{\Delta T} \tag{3.3}$$

Thermal convection

In convection, the heat flow is created by the movement of liquids or gases. These transport the energy in the form of temperatures together with a mass flow. Convection usually refers to when these liquids or gases hit a solid body and release or absorb the heat from it. [81] This phenomenon is illustrated in 3.2 at the boundary surfaces between the wall and the inside or outside air. In this case the convection is lead by gases. For the calculation of the heat flow $\dot{Q}$ in the gas a simple equation 3.4 can be used by relating the heat transport to the mass transport $\dot{m}$ and the temperature difference ΔT with the specific heat capacity c. [83]

$$\dot{Q} = \dot{m}\, c\, \Delta T \tag{3.4}$$

The movement of the fluid or gas can by passive, meaning driven by density differences due to temperature differences, or active by applying movement with fans or opening windows and using the wind. In this section the passive convection is analyzed for heat transmission through walls. The estimation of the convention involves complex fluid dynamics with laminar and turbulent flow in order to predict the movement along surfaces. As introduced in [81] a approximation is done to combine the effects into one parameter α_c. With this estimation the heat transfer $\dot{Q}$ along a surface A can be calculated with equation 3.5, with the surface temperature T_S and the air temperature T_A.

$$\dot{Q} = \alpha_c A\, (T_S - T_A) \tag{3.5}$$

U-Value

In order to estimate the entire thermal transmission of a object like illustrated in Figure 3.2, all three heat transfer forms need to be included. All of them are can be expressed in a linear equation as done in 3.1,3.3 and 3.5 with the heat transfer $\dot{Q}$ proportional to the difference in temperature ΔT.

The thermal radiation and convection take place on both sides of the object and are often combined into one parameter $\alpha = \alpha_r + \alpha_c$. Depending on the position of the associated surfaces there are common values for this parameter that are used in the literature. This eliminates the need to analyze thermal radiation and convection, both of which are very time consuming calculations, and still allows for a very good approximation of these contributions. The values for different surfaces are listed in Table 3.2 and depend only on the location and orientation, but not on the material of the surface. [81]

If you combine the heat transfer coefficient α on both sides with the thermal conductivity, it makes sense to consider the inverse problem not of heat transfer but of thermal resistance R. There it makes sense to sum up all resistance

Surface Location	Heat transfer coefficient α in $\mathrm{W/m^2\,K}$
Outside surface of building	25.0
Walls inside	7.7
Floor to the top	7.7
Floor to the bottom	5.9

Table 3.2: Heat transfer coefficient of different surfaces in a building from data of [81]

contributors, which are the inverse of the previous discussed parameters. This leads to equation 3.6 calculating the total thermal transmittance or U-value, with α_i on the inside and α_o on the outside and the thermal conductivities λ_k for the materials with a thickness of s_k. [81]

$$u = \frac{1}{\frac{1}{\alpha_i} + \sum_k^n \left(\frac{s_k}{\lambda_k}\right) + \frac{1}{\alpha_o}} = \frac{1}{R} \tag{3.6}$$

With the determined U-value, the calculation of thermal transmittance becomes fairly simple after the U-value is determined for all components and does not change. The total heat flow can be obtained by multiplying the U-value with the current difference in temperatures ΔT and the area A of the surface as shown in equation 3.7

$$\dot{Q} = u\,\Delta T\,A \tag{3.7}$$

3.1.2 Solar Irradiation

Solar radiation is a relevant thermal contribution to the heat balance of a building. The intensity and duration of the irradiation on the material is important, but also the angle and direction of the radiation. The resulting heat gains can vary greatly due to the surface and geometry of the irradiated material, which means that the heat gain from radiation through a window onto a surface inside the building is significantly higher than when the exterior wall experiences irradiation from the outside.. [84]

The general solar radiation corresponds fairly closely to solar constant and follows a specific spectrum defined by the absorption due to water vapor, CO_2, ozone and dust. However, the effective solar radiation is highly dependent on local weather conditions, especially clouds and results in direct and diffuse solar radiation. [81]

Direct Irradiation

Direct solar irradiation is the amount of solar radiation that strikes a surface directly. This direct radiation is directional and changes with the time of day and season as well as weather and cloud conditions. To calculate the effective direct irradiation I_{ds} on a surface according to equation 3.8, the cosine of the angle η at which the surface is hit must be taken into account and multiply with the direct radiation I_{dir}. [81]

$$I_{ds} = I_{dir} \cdot \cos\eta \tag{3.8}$$

In order to go from solar irradiation to the heat gain for the building, a type of absorption factor is required that takes both reflection and cooling by the ambient air, in the case of external walls, into account. Reflection can vary depending

on the material and color, but is relatively negligible compared to cooling by the ambient air, especially at low ambient temperatures, leading to an absorption factor of just a couple of percent. [85, 86]

For window areas this changes due to the transmission through the glass and the usage of almost the entire solar irradiation as gains. In this case only the reflection of the glass needs to be considered as well as some reflection from the inside surface back through the glass, leading to an absorption of up to 70 %. [81]

For both applications the heat gain from a surface due to direct irradiation can be calculated with equation 3.8 for the effective direct irradiation I_{ds} and the absorption factor ϵ and area A of the surface under investigation. This leads to the following equation for the heat gains of a building under direct irradiation. [85]

$$P_{direct} = \sum_{i}^{n} I_{ds,i} \epsilon_i A_i \tag{3.9}$$

Diffuse Irradiation

When solar radiation passes through the atmosphere, it is scattered by molecules and dust. This and the reflection from other objects result in non directional radiation, which leads to diffuse irradiation on buildings. Weather conditions can affect diffuse and direct radiation in the same way, such as thick clouds reducing both, or they can have opposing effects. Dust and water vapor can increase diffuse radiation by scattering more light while reducing direct radiation. [81]

Even though the diffuse radiation is not directional, it can still have intensity differences between the South and North sides of a building of 20-30 % . This has an influence on the analysis of the thermal zones of a building and its rooms, but can be neglected when estimating the overall thermal balance of a building. [84, 86]

In the case of non directional irradiation, the resulting heat gains can be calculated by adding the diffuse irradiation I_{diff} multiplied by the absorption factor ϵ and the area A of the investigated surface for all surfaces of the building, as it is done in equation 3.10. This looks similar to the calculations in equation 3.9, but the irradiation is no longer dependent on the surface under investigation. [86]

$$P_{diff} = \sum_{i}^{n} I_{diff} \epsilon_i A_i \tag{3.10}$$

Solar Irradiation Approximation

The effect of higher absorption gains due to windows can lead to higher solar gains during the winter when the sun is lower and hits window surfaces more direct, although the solar radiation on the building is lower overall. This is illustrated by Figure 3.3 with a very large window front facing South only, to show this effect more clearly. By combining this with shading the windows in summer, an even greater difference in window gains can be achieved between the seasons. This means the irradiation through windows and on exterior walls must be simulated individual and cannot be combined to one contributor.

For the simulation a cuboid building with a square normalized side surface of 1 m^2 and a front surface twice as long was assumed with no material differences between roof and walls. Half of the South side was simulated as window with 80 %

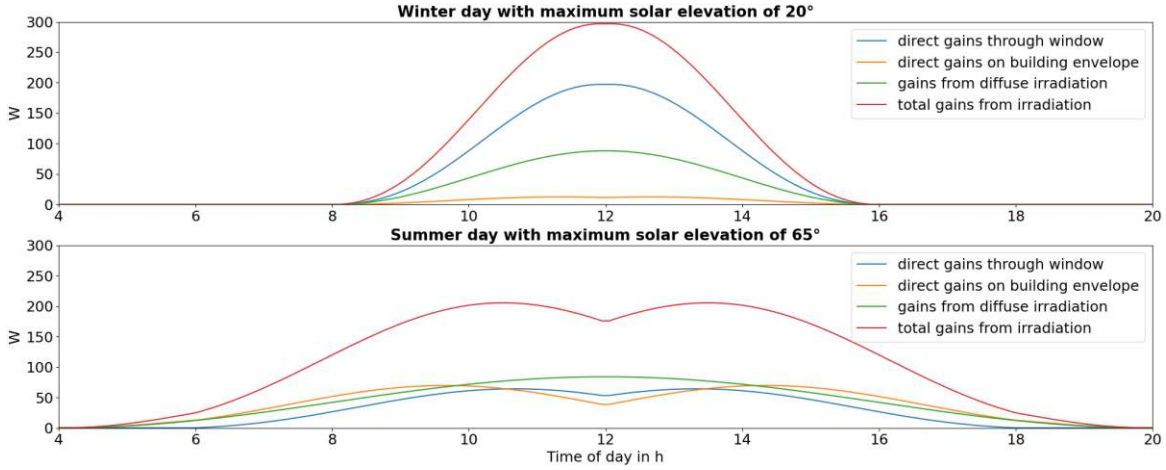

Figure 3.3: Comparison of day profile for solar irradiation gains between a winter day and a summer day. With a maximum solar elevation of 20° and a maximum diffuse and direct irradiation of 90 W and 300 W for the winter day and with a maximum solar elevation of 65° and a maximum diffuse and direct irradiation of 100 W and 900 W in the summer

shading during the summer, resulting in 70 % absorption during winter and 14 % during summer for the window area. For the solar gains of the building envelope, a low absorption factor of 4 % was selected in winter and a factor of 10 % in summer due to the higher outside temperatures. The calculation was done according to equations 3.9 and 3.10.

Figure 3.3 also shows the contribution of diffuse radiation, which combines the gains through the windows and the building envelope, if the differences in radiation between the North and South sides of a building are neglected. It can be seen that in this extreme case the total gains from solar radiation can be higher in winter than in summer. It also shows that the distinction between window area and building envelope is important in order to estimate the different behavior and to include the diffuse radiation in the calculation.

In addition Figure 3.3 shows that even with shading of the window area and an absorption of only 14 % in summer, which is almost as low as the absorption of the normal exterior wall, the windows have a major influence on the heat gains of a building. Solar radiation is also not at its highest at midday in summer, but in the morning and afternoon on the East and West sides of the building. This is mainly due to the greater influence of solar radiation at a shallower angle. The same behavior can also be observed in other models and in real data. [81]

3.1.3 Electrical Power Consumption

Due to the conservation of energy the electrical power consumption of a household is converted into another form of energy. Temporarily, this can be in the form of mechanical energy, light or directly into heat, with most of the mechanical energy being converted into heat due to friction and light and other forms of radiation are absorbed and converted into heat. [87]

This leads to the conclusion that almost all electricity consumption, with the exception of consumption in the garden, such as a water pump for the pool or outdoor lighting, as well as the power required by the heat pump itself, is ultimately converted into heat. It is estimated that up to 90 % of electricity is converted into heat and added to the heat balance of a building.

People	Building volume	Volume per person	Percentage of volume	Method 1	Method 2
2	$200\,m^3$	$14\,m^3/h$	$0.75 \cdot 20\,\%$	$28.0\,m^3/h$	$30.0\,m^3/h$
2	$200\,m^3$	$36\,m^3/h$	$0.75 \cdot 50\,\%$	$72.0\,m^3/h$	$75.0\,m^3/h$
4	$300\,m^3$	$14\,m^3/h$	$0.75 \cdot 20\,\%$	$56.0\,m^3/h$	$45.0\,m^3/h$
4	$300\,m^3$	$36\,m^3/h$	$0.75 \cdot 50\,\%$	$144.0\,m^3/h$	$112.5\,m^3/h$
6	$450\,m^3$	$14\,m^3/h$	$0.75 \cdot 20\,\%$	$84.0\,m^3/h$	$67.5\,m^3/h$
6	$450\,m^3$	$36\,m^3/h$	$0.75 \cdot 50\,\%$	$216.0\,m^3/h$	$168.8\,m^3/h$

Table 3.3: Estimation of hourly air volume exchanged for ventilation based on two different methods using either the amount of people (Method 1) or the volume of air inside a building (Method 2)

3.1.4 Ventilation of the Building

Ventilation of the building is necessary for a comfortable indoor climate. However, due to leaky building components, especially in old buildings, the air flow can be higher than necessary for the indoor climate, but for renovated and new buildings, active ventilation is usually required. With intens and short ventilation, heat is only released in the form of material transport, hot air leaves the building and cold air flows in. This means that the losses Q_{air} can be represented directly by the air volume V_{air}, the temperature difference ΔT between inside and outside and the volume specific heat capacity of air $cv_{air} \approx 1.3\,kJ/m^3K$ as shown in equation 3.11. [81]

$$Q_{air} = V_{air} cv_{air} \left(T_a - T_i\right) = V_{air} cv_{air} \Delta T \tag{3.11}$$

Different methods are commonly used to estimate the volume of air. On the one hand, a person related volume of around 14-36 m^3/h can be assumed. [81] Another methods is introduced by the A.S.I. using an estimation based on the volume of the entire building, assuming that 75 % of it is air and 20-50 % of it are exchanged every hour. [10] In Table 3.3 some exemplary values of the hourly volume of air that is exchanged are listed for comparison of both methods with method 1 being based on the people and method 2 based on the volume of the building. In the end, the actual exchange depends heavily on the respective usage behavior and cannot be represented with either of the two methods. However, for an average estimate, both are in the same range of values.

A regular household may not ventilate evenly throughout the day, but opens the windows in the morning and evening after and before going to bed. A concentrated air exchange in the morning and evening is therefore assumed, with a varying time and intensity.

3.1.5 Human Heat Dissipation

At first glance the dissipated heat from human may seem negligible in relation to the entire building, but especially in nearly zero energy buildings, this factor is not irrelevant. The DIN states, that each person dissipates between 100 and 200 W depending on their activity, for sports this can go up to 400 W. [88] The amount of heat generated by a few people is therefore comparable to an electric radiant heater and is therefore quite relevant in the heat balance.

Of course, people only give off heat while they are at home and depending on the activity, therefore a occupancy model is needed to take these contributions into account. This model can be a static day profile, a statistical model with a probability distribution or also any other method of estimation like ANNs. These estimates can be very complex and extensive, but should be kept simple in this thesis, as a summarized view of households can compensate for the fluctuations and can also be assumed with a random distribution of a standard usage profile. [89, 90]

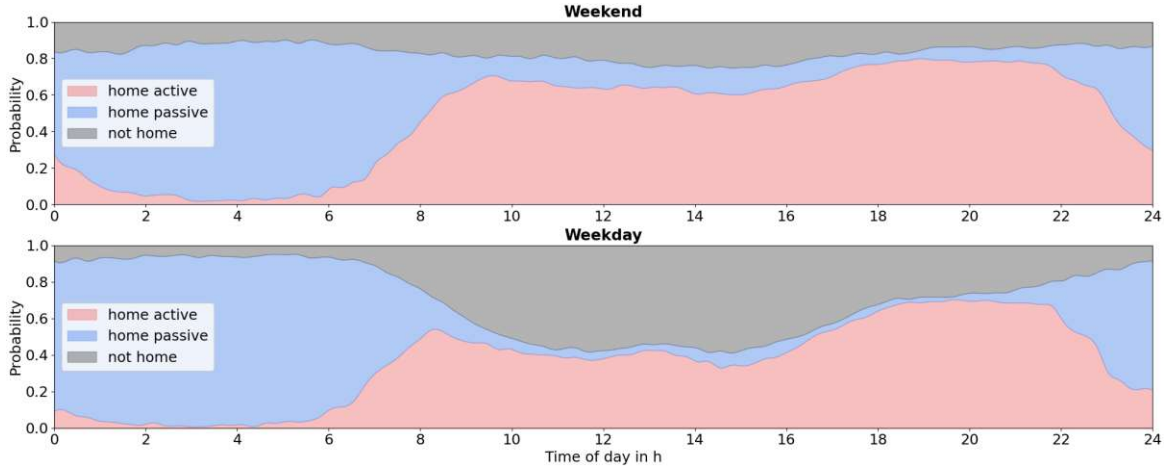

Figure 3.4: A probabilistic occupancy model with data from [89, 90] for a weekday and weekend with distinction between active and passive activities at home

A possible probabilistic occupancy model is shown in Figure 3.4 and illustrates the daily behavior of residents on a weekday and at the weekend with distinction between active and passive activities at home. The data is taken from [89, 90] and was used to create this graphic.

3.1.6 Thermal Bridges

Thermal bridges can occur if materials with better thermal conductivity are used across an insulation layer. For example, floor slabs with balconies can be extended from the interior to the exterior, thus penetrating the insulation of the building envelope. [81] The additional thermal conduction that occurs should not be underestimated when calculating the losses and can make a considerable contribution, due to the large differences in thermal conductivity between concrete and insulation as mentioned in Section 3.1.1.

Since thermal bridges represent thermal conduction, the contributions can be recorded as a thermal bridge correction value ΔU_{TB} and added to the calculated U-value from Section 3.1.1. This is possible because for a heat balance assessment it is not relevant where these additional losses occur. As a result, there is no further contribution in the calculation and only a correction in the parameters needs to be made. For detailed analyses, however, thermal bridges are difficult to consider, as they often cause mold growth through selectively cold spots and the thermodynamic analysis of heat diffusion through different building materials is not straightforward. [81]

3.1.7 Space Heating

Space heating is a control variable in the heat balance of a building. While the other factors must be considered as fixed, the heating can be used to influence the balance and thus control the room temperature. There are different forms of space heating, which can be divided into categories of heat generation, heat distribution and categories of heat dissipation.

In terms of generation, a distinction can be made as to whether the system works centrally for an entire building or group of buildings or decentralized for different parts and rooms. Furthermore, a distinction can be made in the form of energy provided for heat production. For example, different fuels can be burned in boilers, solar energy can be used through solar thermal heating, heat pumps can be used to efficiently convert electricity into heat, or heat consumption

of the district heating network. [81]

The distinction in heat transport can be listed in systems that transport heat in air, water or steam, or use other cooling or heating fluids like air conditioning units. The advantages of water as a heat transfer medium are its high specific heat capacity and the resulting low volume and mass transports required to transfer sufficient heat. In contrast, air as heat transport also makes it possible to control the air quality in the room by supplying fresh air or regulating the humidity. [81]

The last distinction that can be made is in relation to the heat output to the building. Two categories are decisive here. On the one hand, there are heating systems that transfer heat directly to the air, such as radiators or air fans, and on the other hand, there are systems that transfer heat indirectly to the room by heating the building material, such as floor heating systems. These two differ mainly in their dynamic behavior when controlling the room temperature, with floor heating having a much greater time constant for temperature changes, but they also vary in their temperature of the heating system. Radiators need a much higher temperature in order to dissipate sufficient heat into the room, while floor heating systems are coupled closely to the building materials with good heat conduction and can make use of a lot bigger area, resulting in less temperature required for the system. [87]

For this thesis, the type of heat transport is neglected, as the focus is on the amount of heat to be provided. For the grey box model itself the form of heat generation is not relevant, but the type of heat dissipation matters to the dynamic of the model as described previously. Therefore a coupling directly to the air temperature of the room is assumed. Since the influence of HD on the electrical power grid is to be investigated, only heat pumps are considered for heat generation when integrating the GBM into the simulation environment.

3.1.8 Wind

Wind can also have a relevant influence on the heating requirements of buildings. Due to leaks, cold air can be forced into the interior with the pressure difference, leading to increased demand. This behavior is particularly noticeable in older buildings and is not so important for new buildings. For new buildings, the ventilation requirement is significantly higher than the joint leakage rates. But it is precisely during ventilation that the wind speed has a major influence on the air exchange rate and thus on the energy lost. High wind speeds in winter, which occur at higher altitudes in rural areas or in urban areas with taller buildings, are particularly relevant for the HD. As this work assumes a uniformly high building density and does not focus specifically on alpine buildings or skyscrapers, wind was not taken into account in the loss calculation for a building. [81]

3.2 Hot Water

Hot water makes an important contribution to a household's heating demand. As hot water preparation must function independently of the heating requirement, these contributions are also treated separately. Often the systems for providing hot water differ from the heating system or work at a different temperature level in the case of heat pumps. In the following section, the aspects for determining the energy demand for hot water generation are discussed.

Scenario of sanitary installations		Hot water demand per person per day in l/d	Hot water demand per person per year in m^3/a
Shower, sink and additional washing by hand	min	19	6.5
	max	51	17.5
Shower and bathtub, sink and additional washing by hand	min	26	8.8
	max	58	19.9
Medium bathtub, sink and additional washing by hand	min	37	12.7
	max	60	20.6
Large bathtub, sink and additional washing by hand	min	52	17.9
	max	75	25.8

Table 3.4: Scenarios of sanitary installations with the respective personal hot water demand from data of [20]

3.2.1 Hot Water Demand

Hot water demand varies greatly and depends on the number of people in a household, but also on habits and existing installations, such as bathtubs, showers, sinks and others. For different applications, there is detailed information on what flow rates are required, with manufacturers often required to specify and document the water consumption of their appliances. However, since user behavior is ultimately decisive in terms of duration of use and usage frequency, the detailed information on consumption is no longer relevant, as these uncertainties weigh more heavily. [87]

Estimates must therefore be made on the basis of empirical values in order to calculate the actual hot water requirements of households. Table 3.4 shows four scenarios of sanitary installations with the respective personal hot water demand of 40-60°C. The data was taken from the VDI 2067 standard, as this is the common calculation basis for building planning in central Europe. [20] It is clear that the range of minimum and maximum values is further apart than the mean values of the different scenarios. This clearly shows the uncertainties that have to be considered for individual people. However, for several people and, even more importantly, different households, the mean values can then reflect good consumption and thus provide information about the hot water demand of larger communities.

In addition to the daily hot water demand, the temporal distribution over the day is also relevant in the simulation presented in this thesis. Since the accumulated demand is already subject to a high degree of uncertainty, the time profile of an individual person is of course even more diverse.

However, a general profile for the hot water demand in a household can be created for an aggregated view. Such a profile is shown in Figure 3.5 with the data from [87] for residential apartment blocks. To simulate the fluctuations and uncertainties for individual households, it is easiest to work with uncertainty factors or a superimposed noise. [91]

3.2.2 Heat Capacity of Water

When heating water for hot water consumption, the amount of energy required is decisive for the heating demand of a household. The density and specific heat capacity (SHC) of the water are needed to calculate the energy required from the volume of water and the initial temperature of the water. The energy Q required to heat a volume V of water with the initial temperature T_s to the final temperature T_f is calculated using the equation 3.12. The conversion from the volume V to the mass of the water, which is required for the SHC c, is carried out using the density ρ of the water. [92]

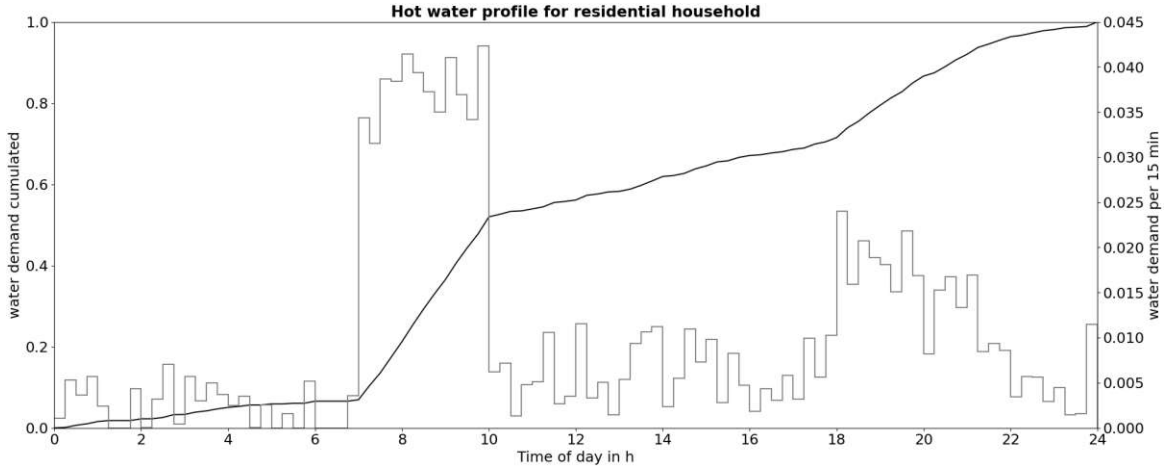

Figure 3.5: Daily hot water distribution for a residential household with the cumulated demand over a day and demand in 15 min resolution from data of [87]

$$Q = \int_{T_s}^{T_f} \rho\, V\, c(t)\, \mathrm{dt} \tag{3.12}$$

Since the SHC itself depends on the temperature, this must be integrated. The density is also a function of the temperature, but it is assumed that it is an iso-process in which the mass remains constant. Therefore, the density is only used at a certain temperature T_f in order to calculate the mass from the final volume V of water required and doing this before the integral. The value of the SHC of water is shown in Figure 3.6a with data from [93] for the temperature range from 0 °C to 100 °C in its liquid form, the density used for water at 60 °C is $0.983\,\mathrm{kg/l}$.

Due to the computational effort required for calculating the integral in equation 3.12, a constant value for the specific heat capacity is desired, which leads to the product shown in equation 3.13. In Figure 3.6b an analysis of the energy required to heat water to 60 °C is carried out using equations 3.12 and 3.13. The static SHC value of $4.183\,\mathrm{kJ}/kg\,K$ used is also marked in the Figure 3.6a. [92]

$$Q = \rho\, V \cdot\ c\,(T_f - T_s) \tag{3.13}$$

As seen in the figures 3.6, the error due to the approximation is very small, with the static SHC selected to have an relative error of 0 for starting temperatures between 5-10 degrees, which is most likely for tap water. At very low temperatures, the error is greatest due to the high deviation of the SHC at temperatures close to 0°C. But even in the most unfavorable case, the relative error for the approximation is less than 0.1 %, which speaks in favor of this approximation.

3.2.3 Power Demand

As for the heating system, a heat pump is also assumed in this thesis for the generation of hot water. However, since heating systems with HP are operated due to better efficiency, at lower temperatures of 35 °C and hot water is usually required up to 60 °C, the hot water demand must be treated separately. It can often be generated by the same heat pump, but the conversion factor to electrical power is lower at higher water temperatures. [81]

By combining the required heat of the hot water and the heating, the information of the efficiency of the HP would

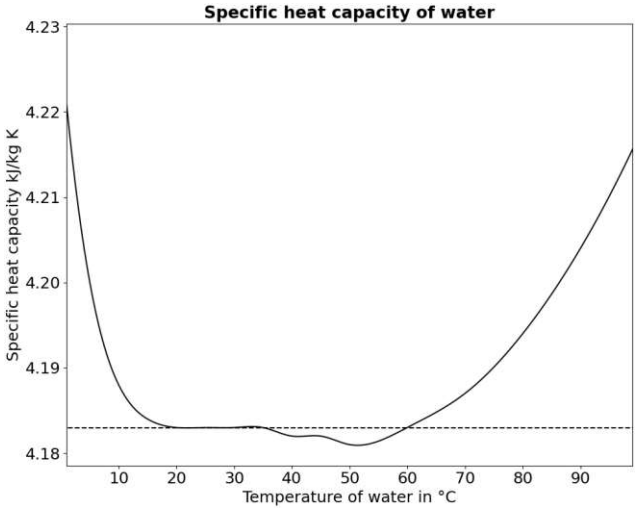

(a) The specific heat capacity of water for the temperature range from 0 °C to 100 °C in its liquid form

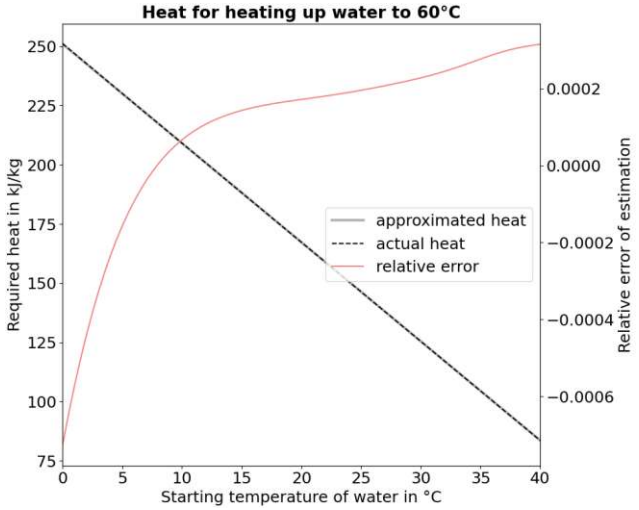

(b) Relative error between approximated and actual energy required to heat water to 60 °C

Figure 3.6: Comparison of an approximation of water heating based on temperature-dependent specific heat capacity based on data from [93] and the approximation of a constant specific heat capacity

be lost. Therefore, in the introduced model in this thesis, the required heat with the corresponding efficiency is first converted separately into electrical energy and only then combined into an total energy demand.

3.3 Dynamic Behavior

In sections 3.1 and 3.2, different influencing factors for the static heat demand were discussed. This involved contributions that depend on the current condition and environmental parameters. However, a dynamic consideration of heat capacities is necessary for the consideration of the HD. Fluctuations in the heat balance can lead to cooling or heating of the building, changing the temperatures, which must be compensated for at a later point in time.

In this section, the influencing factors for the dynamic behavior of a building with regard to its temperature profile are analyzed. The heat capacities of the existing components are relevant here, as are the couplings between them.

3.3.1 Thermal Capacities

An unequal heat balance in a system results in temperature changes. The extent of the temperature increase or decrease is defined by the specific heat capacity (SHC) already discussed in Section 3.2. Using similar considerations, a constant value for SHC can also be assumed here.

Equation 3.14 gives the relationship between the temperature change ΔT and the heat balance Q for homogeneous bodies. Together with the density ρ of a material, the SHC c in relation to the mass can also be used to express a heat capacity in relation to the volume V. Relevant values of SHC are listed together with the densities in Table 3.1 from Section 3.1.1. The specific heat capacity differ greatly from each other, especially in combination with the density in relation to the volume. [82]

$$\Delta T = \frac{Q}{V \rho c} \tag{3.14}$$

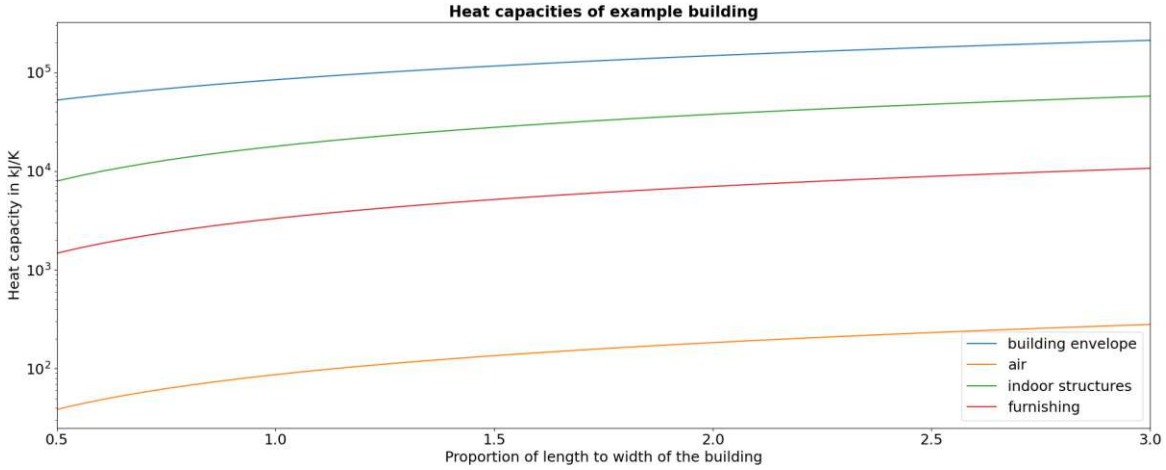

Figure 3.7: Heat capacities, in a logarithm scale, of components for an exemplary building with constant height and width of 5 m, but different lengths

The specific heat capacity differ greatly from each other, especially in combination with the density in relation to the volume. Figure 3.7 shows the heat capacities of the components for an exemplary building with constant height and width, but different lengths. Rough estimates have been made for the thickness of the external walls, the number of walls in the building and the volume of furniture, as it is only a matter of comparing the orders of magnitude.

It is clear that most of the heat capacity of a building is contained in its building substance, the walls and floors, and that air and furniture only make up a small part. Nevertheless, these contributions are important for the dynamic behavior of the room temperature, as the capacities are coupled to the air temperature with different time constants. For example, the heat capacity of the air is directly linked to the temperature change in the room, while walls and furniture can only absorb and release heat with limited power. [87]

3.3.2 Heat Diffusion as Dynamic Thermal Conductivity

For the model introduced in this thesis, a detailed simulation of the processes of heat diffusion is done in order to find a simple and sufficient approximation of the dynamic thermal behavior of a building. In other grey box models discussed in Section 2.2 these processes are often modeled via resistance and capacitance elements. Depending on the detail of the model, several of these element are implemented for the building envelope and internal masses. The exchange of heat between different parts of the building is essential due to the difference in heat capacities described in the previous section and depends on the temperature difference between them as shown in Section 3.1.1. For a dynamic behavior though, the process is not assumed to be in a steady state.

The actual heat and temperature transfer through a medium is defined by the heat diffusion which leads to thermal conduction. This was first discovered by Fourier, who formulated the relation ship between the heat transfer $\dot{Q}$ through an area A due to a gradient in temperature T as shown in equation 3.15. The proportion factor in this equation is given by the thermal conductivity λ. Together with the density and SHC the heat transfer can be expressed as a change of temperature as done in equation 3.16. [82]

$$\dot{Q} = -\lambda A \frac{\mathrm{d}T}{\mathrm{dx}} \tag{3.15}$$

Together with the density and SHC the heat transfer can be expressed as a change of temperature as done in equation 3.16.[82]

$$\frac{\mathrm{d}T}{\mathrm{dt}} = \frac{\lambda}{\rho c}\frac{\mathrm{d}^2T}{\mathrm{dx}^2} \tag{3.16}$$

This description of the heat transfer and temperature changes follows the characteristics of a diffusion process. The idea of the mathematical model underlying a diffusion process is based on the hypothesis that the rate of transfer J_x through a surface is proportional with a diffusion coefficient D to the gradient of concentration C normal to that surface as in equation 3.17. Furthermore the conservation of the diffusion substance leads to the expression in equation 3.18. Combining the two the resulting one dimensional diffusion equation 3.19 is formed that can be extended into three dimension as in 3.20 commonly known as Fick's Second Law. For a constant diffusion coefficient D this equation can be simplified to a linear parabolic partial differential equation 3.21 with the Laplacian of the concentration C. [94]

$$J_x = -D\frac{\partial C}{\partial \mathrm{x}} \tag{3.17}$$

$$\frac{\partial C}{\partial \mathrm{t}} = -\frac{\partial J_x}{\partial \mathrm{x}} \tag{3.18}$$

$$\frac{\partial C}{\partial \mathrm{t}} = \frac{\partial}{\partial \mathrm{x}} \cdot \left(D\frac{\partial C}{\partial \mathrm{x}}\right) \tag{3.19}$$

$$\frac{\partial C}{\partial \mathrm{t}} = \nabla \cdot (D\nabla C) \tag{3.20}$$

$$\frac{\partial C}{\partial \mathrm{t}} = D\,\nabla^2 C \tag{3.21}$$

When interpreting the temperature as a concentration of heat these diffusion equations can be used to calculate the heat transfer due to conduction. By defining the diffusion constant D in equation 3.21 as the coefficient of thermal conductivity λ divided by the heat capacity per volume ρc equations 3.16 and 3.21 describe the same process. This means that well developed and understood methods for diffusion processes can be used to analyze the dynamic thermal behavior of a building, especially the relationship between the room and wall temperatures. [95]

Finite Difference Method

To solve the above equations, the numerical method of finite differences is used. This is a method that has been used for a long time in which the space is discretized into a grid as shown in Figure 3.8. It is robust and is not too computationally intensive for correct conditioning. With the discretization the solution can be calculated for each point individually. To solve the obtained discrete derivatives, an approximation is introduced in which only linear combinations of function values at grid points are used. [96]

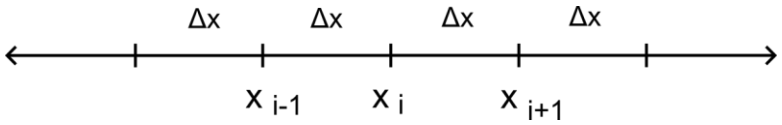

Figure 3.8: One dimensional discretization for the finite difference method of the space

The idea behind this is given by the Taylor series 3.22 which is broken off after the first elements. By expressing the function values of the next x_{i+1} and previous x_{i-1} point with the current point x_i and the discretization step Δx equations 3.23 and 3.24 can be obtained. [97]

$$f(x) = \sum_{n=0}^{\infty} \frac{(x - x_0)^n}{n!} \left(\frac{\partial^n f}{\partial x^n} \right)_{x_0} \tag{3.22}$$

$$f(x_{i+1}) = f(x_i) + \Delta x \left(\frac{\partial f}{\partial x} \right)_{x_i} + \frac{\Delta x^2}{2} \left(\frac{\partial^2 f}{\partial x^2} \right)_{x_i} + \frac{\Delta x^3}{6} \left(\frac{\partial^3 f}{\partial x^3} \right)_{x_i} + \dots \tag{3.23}$$

$$f(x_{i-1}) = f(x_i) - \Delta x \left(\frac{\partial f}{\partial x} \right)_{x_i} + \frac{\Delta x^2}{2} \left(\frac{\partial^2 f}{\partial x^2} \right)_{x_i} - \frac{\Delta x^3}{6} \left(\frac{\partial^3 f}{\partial x^3} \right)_{x_i} + \dots \tag{3.24}$$

By reordering the terms the forward difference and backward difference can by written as done in equation 3.25 and 3.26. By increase the order of error this term decreases more quickly with smaller step sizes Δx. Therefore both representations are added together in 3.27 for the central difference with an better convergence of Δx^2. [97]

$$\left(\frac{\partial f}{\partial x} \right)_{x_i} = \frac{f(x_{i+1}) - f(x_i)}{\Delta x} - \frac{\Delta x}{2} \left(\frac{\partial^2 f}{\partial x^2} \right)_{x_i} - \frac{\Delta x^2}{6} \left(\frac{\partial^3 f}{\partial x^3} \right)_{x_i} - \dots \tag{3.25}$$

$$\left(\frac{\partial f}{\partial x} \right)_{x_i} = \frac{f(x_i) - f(x_{i-1})}{\Delta x} + \frac{\Delta x}{2} \left(\frac{\partial^2 f}{\partial x^2} \right)_{x_i} - \frac{\Delta x^2}{6} \left(\frac{\partial^3 f}{\partial x^3} \right)_{x_i} + \dots \tag{3.26}$$

$$\left(\frac{\partial f}{\partial x} \right)_{x_i} = \frac{f(x_{i+1}) - f(x_{i-1})}{2\Delta x} - \frac{\Delta x^2}{3} \left(\frac{\partial^3 f}{\partial x^3} \right)_{x_i} + \dots \tag{3.27}$$

To get the second order derivative a similar approach can be made, by adding equations 3.23 and 3.24. This results in equation 3.28 with an order of error of Δx^2. The same approximations can be done for derivatives in the other dimensions in order to solve three dimensional partial differential equation. [97]

$$\left(\frac{\partial^2 f}{\partial x^2} \right)_{x_i} = \frac{f(x_{i+1}) - 2f(x_i) + f(x_{i-1})}{\Delta x^2} + \mathcal{O}(\Delta x^2) \tag{3.28}$$

In order to solve the linear parabolic partial differential equation given in equation 3.16 the time derivative also needs to be discretized similar to the space as shown in Figure 3.8. In this case the Taylor series can be broken off after the first two elements to get an approximation of the temperature after a given time interval Δt with the known derivative over time obtained by using 3.16 and 3.28. This leads to equation 3.29 with the calculation of the temperature $T_{j+1}(x_i)$

Material	Diffusion coefficient $\lambda/\rho c$ in cm^2/s
Concrete	9.72 e−3
Polystyrene	8.57 e−3
Air	166.67 e−3

Table 3.5: Diffusion coefficient $\lambda/\rho c$ for concrete, polystyrene and air from the data from Table 3.1

after a given time period Δt from the temperature levels $T_j(x_i)$ at the grid points x_i at the time t_j. [96]

$$T_{j+1}(x_i) = T_j(x_i) + \frac{\lambda}{\rho c} \cdot \Delta t \frac{T_j(x_{i+1}) - 2T_j(x_i) + T_j(x_{i-1})}{\Delta x^2} + \mathcal{O}(\Delta t^2, \Delta x^2) \tag{3.29}$$

Heat Diffusion in Exterior Wall with two Material

Since the biggest heat capacity by far lies in the exterior walls, this is the most relevant factor for long term dynamics of a building. In order to describe the heat transfer and storage between the air inside the room and the exterior walls, a one dimensional simulation based on the finite difference method is done in this section sketched in Figure 3.9a. Given that the envelope of the building usually consists of the building structure itself and an insulation, the simulation was done with a shift between two different diffusion coefficients of the materials.

The diffusion coefficients of the wall and insulation as well as the air are listed in 3.5. It is clear that the air has a much high diffusion and this gets even more significant when considering convection and other movement of the gas. Based on this, it can be assumed that the air is in a steady state compared to the dynamic of the wall and stays at a constant temperature. [98] It is also interesting to see, that the heat diffusion in concrete and polystyrene are nearly the same even with very different thermal conductivity.

Therefor the simulation includes only the exterior wall itself with constant boundary conditions and is based on equation 3.29 and implemented via Python. Boundary conditions can easily be implemented with a numerical approach by forcing the edge points to the constant value and only allowing an update for the inner grid. [96]

For the heat transfer between the air and the concrete the heat transfer coefficient α from 3.2 for indoor walls is used. In order to implement this in the finite difference method a different approach is needed than equation 3.29. Equation 3.18 shows that the change in concentration, or in this case temperature, over time is proportional to the change of flow over space. With this in mind the heat flow between the wall and air is calculated with the heat transfer coefficient and the flow in the wall is modeled via equation 3.25 for the forward difference, resulting in equation 3.30 for the temperature of the first discretized point in the concrete. Since the heat transfer coefficient for the outside of the wall is much higher, the coupling on the outside is assumed to be perfect with the insulation having the exact temperature of the surrounding.

$$T_{j+1}(x_i) = T_j(x_i) + \frac{1}{\rho c} \cdot \frac{\Delta t}{\Delta x} \left(\frac{\lambda \left(T_j(x_{i+1}) - T_j(x_i) \right)}{\Delta x^2} - \alpha \left(T_j(x_i) - T_j(x_{i-1}) \right) \right) \tag{3.30}$$

For a discrete calculation the boundary layer between the two materials of concrete and insulation itself cannot be infinite small and has to consist out of one of the two materials. This boundary point has a mixed diffusion coefficient for the finite difference method as shown in equation 3.31 due to the thermal conductivity $\lambda_{c,p}$ of concrete and polystyrene to both sides and ρc of the discretized point. [96]

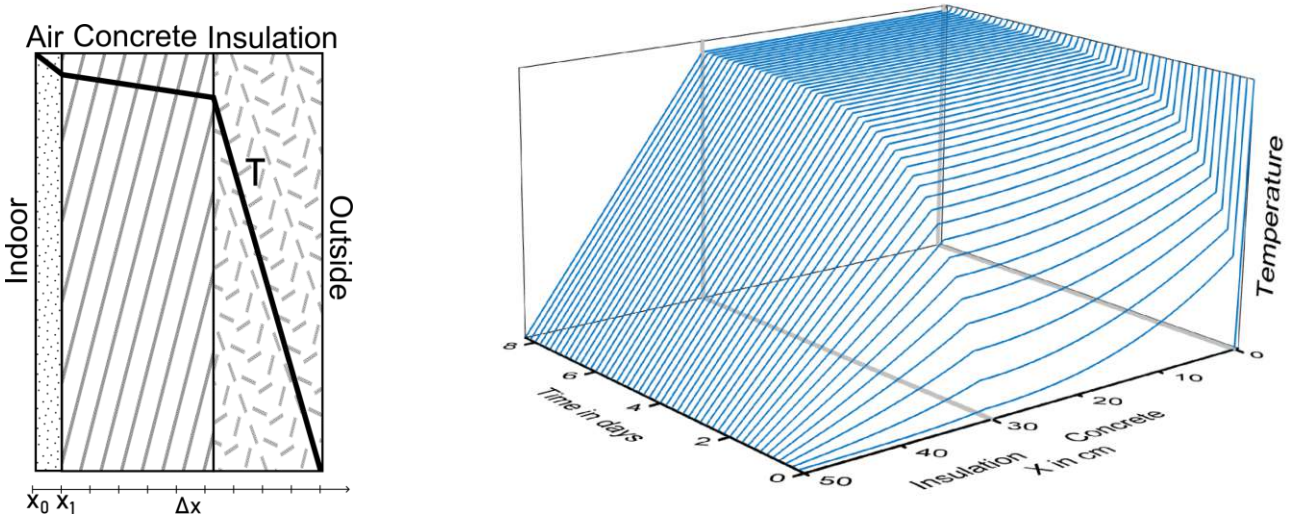

(a) Sketch of the simulated one dimensional region

(b) Temperature, in relation to the temperature difference between inside and outside, in the simulated exterior wall over space in cm and time in days

Figure 3.9: Simulation with finite differences of heat diffusion in an exterior wall with air coupled on the inside of 30 cm concrete and 20 cm polystyrene

$$T_{j+1}(x_i) = T_j(x_i) + \frac{1}{\rho c} \cdot \Delta t \frac{\lambda_p \left(T_j(x_{i+1}) - T_j(x_i)\right) - \lambda_c \left(T_j(x_i) - T_j(x_{i-1})\right)}{\Delta x^2} \tag{3.31}$$

The one dimensional simulation was done for a 30 cm thick concrete wall and 20 cm of polystyrene insulation. For discretization a step Δx of 0.5 cm and Δt of 0.5 s was set. The simulation results are shown in Figure 3.9b for the temperature in the material over time and space. Since the entire process is linear proportional to the temperature difference between inside and outside scaling is irrelevant for the time profile. It can be seen, that the heat transfer into the wall is a process in magnitude of days, with the most change during the first day. It can also bee seen, that almost the entire temperature difference is in the insulation when the materials are saturated and in their steady state. This is expected due to the great differences in thermal conductivity between concrete and polystyrene.

The coupling of air on the inside of the wall is also relevant for the beginning of the diffusion process, as the heat transfer coefficient limits the amount of heat transferred into the wall, resulting in a much slower heat absorption. Overall Figure 3.9b shows the importance of modeling the heat capacities for the building structure dynamical, since the process of saturating to indoor temperatures takes a couple of days.

3.3.3 Capacity Coupling

Due to the time consuming calculations with finite differences an approximation for the process of heat transfer into the wall is needed. In Figure 3.10 the accumulated transferred heat per cm^2 of exterior wall is plotted over the time. Since the simulation was done considering the heat transfer coefficient from the air to the wall the transferred heat into the wall is given by the difference between the air and wall temperature. For a simplified calculation the wall is assumed to have a constant temperature of T_w and a combined heat capacity per cm^2 as c_w and the air a temperature of T_a on the inside. This reduces the diffusion into a simple differential equation 3.32 over time.

$$\frac{\partial T_w}{\partial t} = \frac{\alpha}{c_w}(T_a - T_w) \tag{3.32}$$

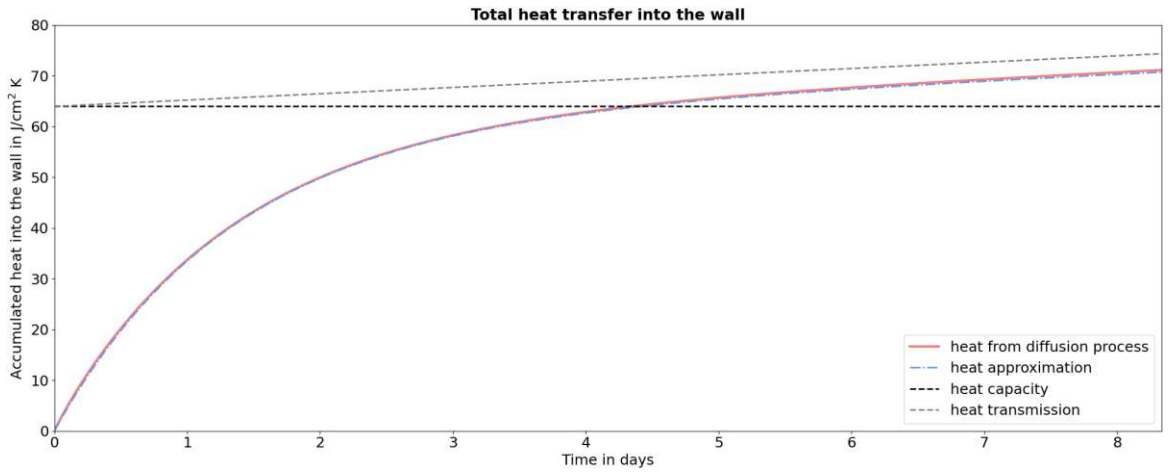

Figure 3.10: Accumulated heat transfer per cm^2 and K into the exterior wall calculated with finite difference method and an approximation with the theoretical heat capacity and transfer losses of 30 cm concrete and 20 cm polystyrene

An important parameter in this approximation is the combined heat capacity c_w, that includes both the concrete and insulation as well as the saturated temperature curve. With the heat transfer α not all of the temperature difference is in the wall itself. In order to estimate how much is in the wall and what ratio is in the coupling between air and wall, the transfer rates are treated as resistance and can thus be set in relation to each other. [1] This relation r is calculated with equation 3.33 and follows the idea of voltage at serial resistances. The thickness of the concrete and polystyrene $s_{c,p}$ as well as the thermal conductivity $\lambda_{c,p}$ and α are based on cm or cm^2.

$$r = \frac{\frac{s_c}{\lambda_c} + \frac{s_p}{\lambda_p}}{\frac{s_c}{\lambda_c} + \frac{s_p}{\lambda_c p} + \frac{1}{\alpha}} \tag{3.33}$$

The combined heat capacity of the exterior wall c_w per cm^2 can then be calculated using the relation r as well as the assumption, that the entire temperature difference in the wall is within the insulation, resulting in equation 3.34 with the specific heat capacity per volume $\rho_{c,p} c_{c,p}$. Due to the temperature drop in the insulation, only half of it stores heat as illustrated in Figure 3.9a.

$$c_w = r \left(\rho_c c_c s_c + \frac{\rho_p c_p s_p}{2} \right) \tag{3.34}$$

The result is also plotted in Figure 3.10 as a constant, for a reference. With no heat losses through the wall, the accumulated heat transferred into the wall per cm^2 and K should theoretically be exactly c_w. To take the heat losses as well into account the U-value U_w is calculated based on equation 3.6 for the exterior wall as in equation 3.35.

$$U_w = \frac{1}{\frac{s_c}{\lambda_c} + \frac{s_p}{\lambda_c p} + \frac{1}{\alpha}} \tag{3.35}$$

This heat is plotted as a linear curve on top of the combined heat capacity of the exterior wall in Figure 3.10. It is expected that the accumulated heat into the wall asymptotically approaches this line, with a small offset due to less heat losses to the ambient air at the beginning of the diffusion process, when the wall is not yet warm.

When combining equation 3.32 and heat losses from equation 3.35 an approximation for the heat transfer $\dot{q}$ per cm^2 can

be expressed 3.36 as well as the temperature of the wall T_w 3.37 with inside air temperature T_a and exterior temperature of T_e. In order to match the diffusion process a correction factor f of 0.71 needs to be applied to the literature heat transfer coefficient α_i on the inside of walls, for the transfer into the wall, which corrects the assumption that the temperature in the wall is the same everywhere, when in fact it is higher at the inside of the wall, leading to less heat transferred into it.

$$\dot{q} = f \cdot \alpha_i \left(T_a - T_w(t_j)\right) \tag{3.36}$$

$$T_w(t_{j+1}) = T_w(t_j) + \frac{\Delta t}{c_w} \left(\dot{q} - U_w(T_w(t_j) - T_e)\right) \tag{3.37}$$

Figure 3.10 shows the performance of the approximation to the diffusion process using equations 3.36 and 3.37. The coupling between the air and walls with α_i f has both a physical relevance to the heat transfer coefficient, but allows also for tuning to expected behavior. The total heat capacities of the building structure are by far the biggest as shown in 3.7 but include not only exterior walls. To include floors and interior walls as well, the combined heat capacity can be adjusted as well as the coupling factor to match the total system closely and not loose the computational benefits of one temperature in the wall over finite differences or resistance and capacitance elements as done in other grey box models.

The combination of the entire building structure, walls and floors, to one heat mass with one temperature works best for one climate zone. When having different temperature levels in different parts of the building the thermal conduction in the concrete and building structure will not be enough to keep temperature levels at the same level in the materials. But for well insulated building envelopes and similar heated rooms, this approach will estimate the dynamic behavior well, based on the analysis done in Figure 3.10.

Chapter 4

Model Implementation

This chapter presents the implementation of the proposed grey box model (GBM). It begins with a general overview of the simulation environment architecture and the model, followed by a detailed description of the calculations for each individual component. These calculations are grounded in the findings from the previous Chapter 3.

In addition to the model itself, the preparation of data for predictions related to flexibility is examined, alongside the development of a heat pump model for converting heat demand into electrical power. Finally, the logic governing the decision making process for heating or cooling mode of the HP is outlined, as it is essential for simulating a realistic behavior of building heating and cooling.

4.1 Environment

The simulation environment is Bifrost [77] introduced in Section 2.4. As described, it consists of a core module, linking any desired modules together. By calling each of them in a defined order via REST-API simulation data is transferred and aggregated between them. The most relevant modules, for the introduced heat demand model (HDM) in this thesis, are the community controller (CC) (managing and optimizing local energy communities) and the building model (consisting of Load Class, Battery Class, Photovoltaic Class and Heat Pump Class). This structure is depicted in Figure 2.2 together with the setup for cross-location optimization.

In addition to the discussed models many others are essential for a functioning simulation and modeling of a power grid, such as a weather model or load flow simulator. Since these are not directly relevant for implementing the proposed HDM, those models are not further discussed and it is assumed, that all relevant data for implementing the introduced model is available.

A more detailed overview of the communication between the models is illustrated in Figure 4.1 with the existing modules in blue and the implemented HDM in blue. The proposed GBM is written as two Python classes, that work as one module, therefore not using a REST-API. The first class handles the interface to the existing building model as well as data preparation and implementing a simple heat pump model. The second class implemented the proposed HDM with different methods for calculating losses and updating room and wall temperatures. A more detailed description of the functional structure of the model is given in Section 4.3.

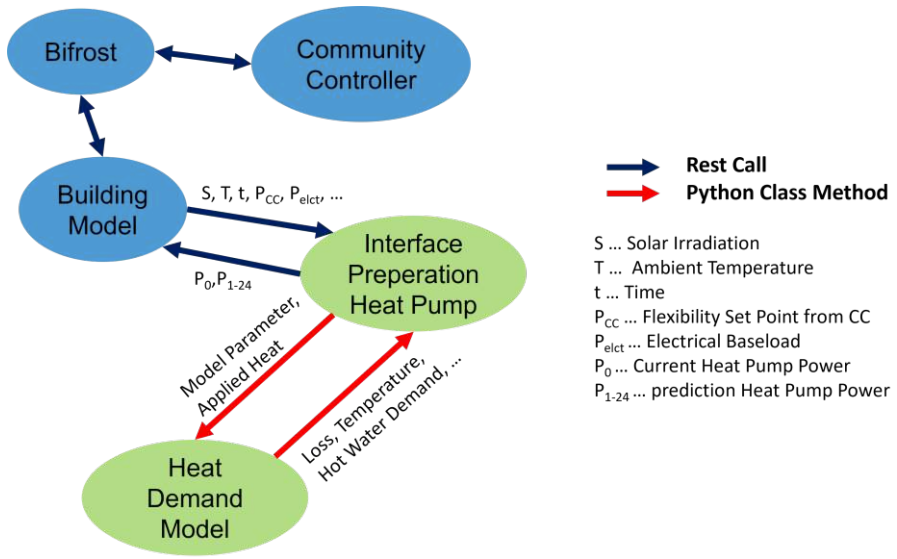

Figure 4.1: Architectural structure of the simulation environment with the focus on the communication between the relevant modules, with blue as the existing modules and green the proposed implementation of a GBM

4.2 Model Parameters

The implemented heat demand model based on the analysis from Chapter 3 requires several parameters and data for calculating heat losses, gains and temperature changes. Figure 4.1 shows an example of transferred values between the building model and the GBM. But some of the needed parameters are static building properties, such as geometry or U-Values for the buildings' envelop. They are defined in tables previous to the simulation and can be selected for each building individual. In addition to building properties the desired indoor temperature profiles with the respected flexibilities need to be defined and selected as well, allowing for individual behavior of each building. All static parameters are stored in a csv-file, combined to different household profiles.

In contrast to the static parameters, the HDM requires data of influencing factors, such as ambient temperature or solar irradiation. These values are provided by other modules in the Bifrost environment and are received via REST-API each simulation step. This data is then preprocessed to provide the required information before being used to calculate heat losses and gains.

The results of the GBM include the applied heat, the electrical power demand of the HP, a prediction of the electrical power demand with flexibilities to enable optimization, and the updated room and wall temperature for the next simulation step. A detailed overview of all parameters for the static properties, the input values and return data is shown in Table 4.1.

4.3 Model Structure

Based on the insides from Section 3.3, uniform temperature levels for all building zones and an even distribution of temperature within exterior walls and the building structure are assumed, thus, simplifying the model to two temperatures, each associated with corresponding heat capacities. These temperatures are represented by two internal state values of the model and are updated each simulation step. As shown in Figure 4.1 the HDM itself is controlled via a second Python class. This ensures the initialization of the GBM at the start of each simulation step for the each building. The process of one simulation update involves multiple steps illustrated in Figure 4.2.

Name	Unit	Description
		Static building properties
Humans	-	Amount of people living in this household
Footprint	m^2	The total area of the footprint of the building
Proportion	-	The proportion between the two sides of a rectangular footprint
Floors	-	Amount of floors in the building
Floor Height	m	The hight of each floor including the floor structure
Window Area	%	Percentage of the external walls that are windows
Absorption Wall	%	Percentage of absorbed solar irradiation by the buildings' envelop
Absorption Window	%	Percentage of absorbed solar irradiation through the windows
U-Value$_{wall}$	$W/m^2 K$	Heat transmittance through exterior walls
U-Value$_{window}$	$W/m^2 K$	Heat transmittance through windows
U-Value$_{floor}$	$W/m^2 K$	Heat transmittance through ground floor
Water Consumption	l	Daily hot water consumption per person
Shift	h	Time offset for hot water profile, occupancy model and ventilation
Noise	-	Standard deviation of an overlaying noise for behavior models such as hot water consumption, human dissipation and ventilation
Heat Pump Size	kW	Maximum electrical power of the HP
Temperature Profile Min	array of °C	The minimum temperature profile for an entire day each hour
Temperature Profile Max	array of °C	The maximum temperature profile for an entire day each hour
		Dynamic values provided by Bifrost modules
Time	s	Current time of simulation step in seconds
Ambient Temperature	°C	The ambient air temperature
Solar Angle	°	The altitude and azimuth angles of the position of the sun
Direct Irradiation	W/m^2	The direct solar irradiation
Diffuse Irradiation	W/m^2	The diffuse solar irradiation
Electricity	W	The electric power of devices in this building
Flexibility	kW	The requested electrical power from the community controller for the HP
		Return values with the results from the HDM
Applied Heating	kW	The resulting heat applied in this step, based on the HP model
Electrical Power	array of kW	The desired electrical power for the HP for the next 24 hours
Flexibilities Min	array of kW	Prediction for the next 24 hours of the minimum possible electrical power for the HP to meet temperature requirements
Flexibilities Max	array of kW	Prediction for the next 24 hours of the maximum possible electrical power for the HP to meet temperature requirements
Room Temperature	°C	Room temperature for the next simulation step
Structure Temperature	°C	Buildings' structure temperature for the next simulation step

Table 4.1: Overview of all parameters for the static properties, the input values and return data of the proposed grey box model

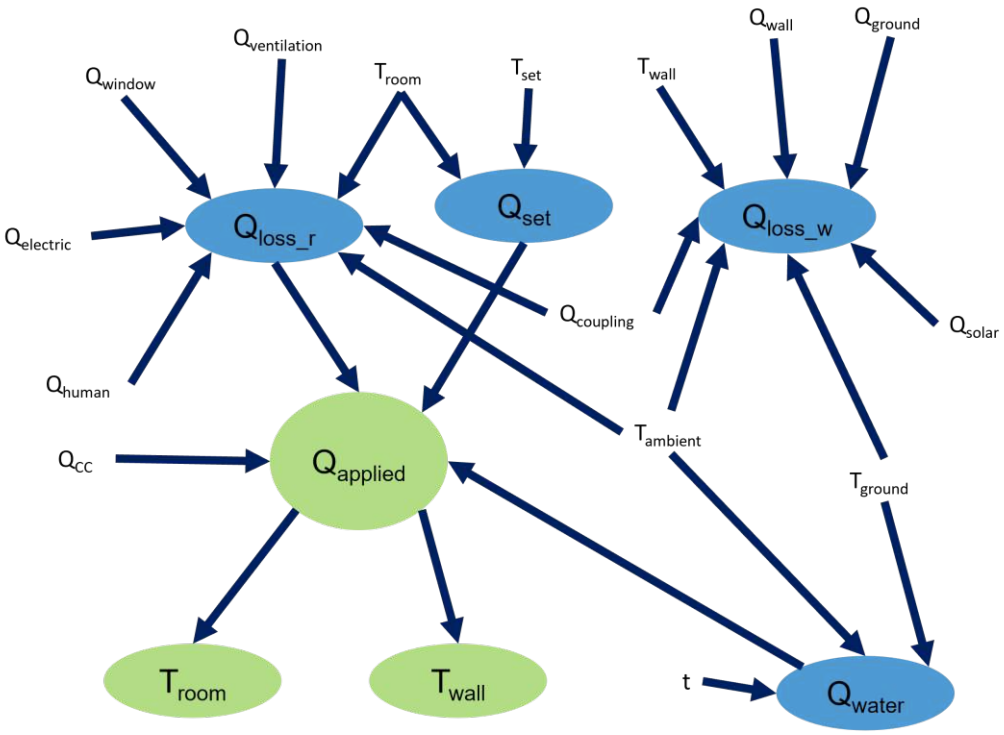

Figure 4.2: Functional process of one simulation step to calculate the HD, the applied heating and corresponding temperature changes in the rooms and the building structure, with returned values shown in green

At first the heat losses and gains are calculated for the given time step for the room and building structure individually. The heat balance for the room consists of heat transfer and solar irradiation through windows, ventilation, as well as internal heat gains, such as electrical devices and human dissipation. The building structure gets influenced by heat transfer through the buildings' envelop into the ambient air and soil, and solar irradiation onto the exterior walls. Both of them are coupled via the heat transfer coefficient α discussed in Section 3.3. Together with the required power for hot water generation, these aspects make up the static HD for this simulation step.

In a second method call, the temperature difference between set room limits and actual air temperature is calculated, resulting in an HD for lowering or raising the interior temperature. With the heat balance for the room, the required heat for changing the temperature and hot water demand, a total HD for space heating can be obtained. With a HP model described in 4.4 the HD is converted into an electrical power demand. Together with flexibilities requested by the community controller for optimization, and the power limits of the HP a resulting electrical load and applied heat is calculated.

In the last step, the temperatures of the room and building structure are updated, based on the applied heat and heat balances of losses and gains. Each of the described steps is implemented by one or multiple methods listed below, allowing for flexible application of the model.

4.3.1 Init - Method

This method initializes the HDM new for each building, by setting the static properties and defining fixed values for specific heat capacity, heat transfer coefficients and percentages of air, furniture or building structure of the total volume. The total volume of the building is calculated by multiplying the footprint with the amount of floors and the floor heights. The buildings' envelope is obtained by equation 4.1, with A_{foot} being the footprint, f the amount of floors, h_f the floor

height and p the proportion between the two sides of a rectangular footprint.

$$A_{envelope} = A_{foot} + f \cdot h_f \cdot 2 \left(\sqrt{A_{foot} \cdot p} + \sqrt{\frac{A_{foot}}{p}} \right) \tag{4.1}$$

With insides from Section 3.3 the heat capacity of the indoor environment is assumed to include not only the specific heat capacity of the air but also a portion of the heat capacity of furniture and other smaller thermal masses. Given a simulation resolution of 15 minutes, an approximation is made that these objects influence the heat capacity directly by being coupled to the air through a high surface area. The heat capacity of the buildings' structure is calculated with equation 3.34, considering temperature profiles in exterior walls.

4.3.2 Update Parameter - Method

For updating external factors influencing the HD between simulation steps, this method is used. Values for the solar irradiation, the ambient temperature and electrical power consumption of devices is set. In addition to that, the water tap temperature is set, by assuming a more inertial behavior, dampening the changes of ambient air temperature. Without using a dynamic system, the water tap temperature T_t is calculated with equation 4.2, presuming 15 °C for an ambient temperature T_a of 18 °C.

$$T_t = 15 + \frac{T_a - 18}{3.6} \tag{4.2}$$

4.3.3 Room Structure Coupling - Method

This method calculates the total exchanged heat between the air in the room and the building structure. The value represents the heat flow from the room to the building structure and needs to be considered as a negative factor for the heat balance for the indoor air and positive for the balance of the building structure. Equation 4.3 describes the heat flow $\dot{Q}_c$ due to coupling, based on equation 3.32, with the room temperature T_r, the temperature of the structure T_s, buildings' envelope area A_e, the footprint A_{foot}, the amount of floors f and the heat transfer coefficient α.

$$\dot{Q}_c = \alpha \left(T_r - T_s \right) \left(A_e + A_{foot} \cdot f \right) \tag{4.3}$$

4.3.4 Losses Room - Method

While this method is called losses, it also includes heat gains, resulting in a heat balance without space heating for the room. It includes the heat transfer through windows $\dot{Q}_w$, the solar gains through the windows $\dot{Q}_s$, human dissipation $\dot{Q}_h$, electrical power P_e, heat flow from coupling to the building structure $\dot{Q}_c$ and ventilation $\dot{Q}_v$. As shown in equation 4.4 these aspects need to be considered either negative as heat gains or positive as heat losses, to get a heat balance describing the total heat loss $\dot{Q}_l$ of the rooms.

$$\dot{Q}_l^r = \dot{Q}_w - \dot{Q}_s - \dot{Q}_h - P_e + \dot{Q}_c + \dot{Q}_v \tag{4.4}$$

The heat transfer through windows is obtained by equation 4.5, with the windows area A_w and the U-Value U_w of those as well as the temperature difference between indoor T_i and outside T_o.

$$\dot{Q}_w = A_w \cdot U_w \left(T_i - T_o \right) \tag{4.5}$$

In addition to that, the solar irradiation through the windows is calculated with the direct and diffuse heat gains calculated based on equations 3.9, 3.10. Furthermore, the human dissipation is based on the occupancy model, and the ventilation is pronounced in the morning and evening with a randomness based on equation 3.11.

4.3.5 Losses Structure - Method

The balance of the heat losses of the buildings' structure $\dot{Q}_l$ includes heat transfer through the buildings' envelope $\dot{Q}_e$ into the air, through a cellar or ground plate $\dot{Q}_g$ into the soil, as well as the solar heat gains $\dot{Q}_s$ and heat transfer with the rooms $\dot{Q}_c$ as shown in equation 4.6.

$$\dot{Q}_l^s = \dot{Q}_e + \dot{Q}_g - \dot{Q}_s \tag{4.6}$$

Similar to the heat balance of the rooms, the solar gains are obtained by equations 3.9, 3.10. The heat transfer trough the walls and ground plate is described in equations 4.7, 4.8, with the assumption that the soil temperature is equal to the tap water temperature T_t.

$$\dot{Q}_e = A_e \cdot U_e \left(T_s - T_o\right) \tag{4.7}$$

$$\dot{Q}_w = A_{foot} \cdot U_g \left(T_s - T_t\right) \tag{4.8}$$

The area of the buildings' envelope is represented by A_e, the footprint by A_{foot}, U_e and U_g are the U-Value for the exterior walls and the ground plate and the structure temperature is T_s.

4.3.6 Hot Water Demand - Method

The calculation of the hot water is based on Section 3.2 with a hourly hot water profile and the defined daily usage per person. The total power demand for the hot water generation $\dot{Q}_w$ is then calculated with equation 4.9 and multiplied with the coefficient of performance (COP) for the respective set point of the heat pump.

$$\dot{Q}_w = W_h \cdot V_p \cdot p \cdot c_w \left(T_h - T_t\right) \tag{4.9}$$

W_h stands for the percentage of water consumption per hour of the total water consumption per person over a day V_p, p for the amount of residents, c_w describes the volume specific heat capacity of water and T_t and T_h the temperature of the tap water and the hot water.

4.3.7 Temperature Change - Method

In order to allow dynamic behavior and therefore temperature changes, this function calculates the necessary heat to reach the desired room temperature in the next simulation step. Since the temperature profile is given with a maximum and minimum limit, the method calculates the required heat to reach both individually. With the mean between them, the optimal temperature in the middle of the minimum and maximum is reached. By using the minimum and maximum room temperatures, the flexibilities in heat are automatically obtained with maximum and minimum limits. Equation 4.10 calculates the required heat Q_{heat} to reach a set room temperature T_s from the current room temperature T_r. The equation is the same for calculating the minimum and maximum limits.

$$Q_{heat} = \left(T_s - T_r\right) c_r \tag{4.10}$$

The heat capacity of the room is given by c_r, combining the SHC of air and furniture pieces as previously described. In order to use this as power requirement, the heat Q needs to be divided by the simulation step time.

4.3.8 Update Room - Method

This method is used to update the room temperature with given losses and space heating for the next simulation step. While the previous methods did not require any arguments, the update method gets the heat balance and applied heating from outside the heat model. This allows for a separate logic on controlling the heating, in this case the upstream Python class. With the heat loss balance $\dot{Q}_l$ and the applied heating $\dot{Q}_h$ the updated temperature T_{+1} is given by equation 4.11. To get the total heat balance in one simulation step, the step size Δt is required, as well as the heat capacity of the room c_r for calculating the resulting temperature change.

$$T_{+1} = T_0 + \left(\dot{Q}_h - \dot{Q}_l\right) \frac{\Delta t}{c_r} \tag{4.11}$$

Additionally, a logic is implemented to assess whether the new temperature exceeds the defined temperature flexibility limits. In a real world scenario, an occupant is likely to open windows, if the room temperature becomes too high or too low, provided the ambient temperature is conducive to improvement. Therefore, if the room temperature exceeds the upper temperature flexibility limit and the ambient temperature is lower, it is assumed that ventilation occurs, and the new room temperature is adjusted to the ambient temperature. A similar logic is applied for the lower bound, where the room temperature is below the flexibility limit and the ambient temperature.

4.3.9 Update Structure Method

Similar to the method to update the room temperature, this function updates the buildings' structure temperature, without the ventilation functionality. It allows also for heating to be applied, with the benefit of enabling direct room heating via air conditioning or radiators, or underfloor heating as thermal component activation. With equation 4.11 the temperature of the buildings' structure can be calculated by using a different heat capacity c_s for the structure.

4.4 Heat Pump Model

Heat pumps are classified into various types based on the heat source and the type of energy used for operation. These include air-water, brine-water, water-water, direct condensation without ventilation function, and partially exhaust air-water systems. HPs can be powered either electrically or by gas engines, with each type offering distinct advantages depending on the application. The energy efficiency of a HP is heavily influenced by the operating conditions, especially the temperatures of the heat source and heat sink, the design parameters, and the system's controllability. Optimal efficiency is achieved when the temperature differences between the source and sink are minimized, and precise regulation of the system is maintained to adjust to varying thermal loads. [99]

HPs can operate in bivalent modes with a secondary heat generator assisting in providing heating. The three main modes are alternative, parallel, and partial parallel operation. In alternative operation, the HP supplies all heating until a set outdoor temperature, the bivalence temperature, is reached, after which the secondary heat generator takes over. In parallel operation, both units work together, with the secondary generator compensating for any shortfall in the HP's capacity. In partial parallel operation, the HP provides heating up to the bivalence temperature, and the additional

heating unit supplements the heat when necessary, with the secondary generator taking over entirely below a lower limit, resulting in a alternative operating mode. [99]

For this thesis the heat pump is assumed to work in a monovalent mode providing the entire heat demand without any additional heat generator. The efficiency of a HP is described by the coefficient of performance (COP) indicating the ratio of heat energy output to electrical energy input for heating, while energy efficiency ratio (EER) represents the same coefficient for cooling. COP/EER is influenced by both the source and sink temperatures, as well as the temperature spread between the supply and return temperatures of the HP. This means that the efficiency varies depending on the specific operating conditions. Additionally, HPs have limited capacities, which are also dependent on the operating point and do not correspond to a fixed electrical output power. Therefore, the performance of a HP is dynamic, changing with varying temperatures and system demands. [99]

To model the behavior of an air-water HP the proposed GBM implements the COP and EER utilizing values from the standard DIN V 18599-5 and 18599-7 [99, 100], which are dependent on the ambient and heated water temperatures. The electrical power P_e required for a given heat flow $\dot{Q}$ is obtained by equation 4.12 with $f(T_a, T_w)$ representing the implemented COP for heating and EER for cooling.

$$P_e = \frac{\dot{Q}}{f(T_a, T_w)} \tag{4.12}$$

While in reality the HP capacity depends on the operating point and does not correspond to a fixed electrical power, for an approximation of the behavior the limits of the HP's heating and cooling power $\min, \max(\dot{Q})$ is calculated via equation 4.13 with $\max(P_e)$ representing the maximum electrical power of a given HP.

$$\begin{aligned} \min(\dot{Q}) &= -\max(P_e) \cdot \mathrm{EER}(T_a, T_w) \\ \max(\dot{Q}) &= \max(P_e) \cdot \mathrm{COP}(T_a, T_w) \end{aligned} \tag{4.13}$$

4.5 Flexibility and Optimization

Section 4.3 describes the implementation of the heat demand model as a independent Python class. Together with the heat pump model presented in Section 4.4 these methods simulate a single time step. However, to facilitate optimization, a prediction of the HD is necessary.To achieve this, the parent Python class manages the data preparation and aggregation over 96 iterations of 15 minutes each, resulting in a prediction of 24 hours.

The community controller requires three values for each time step in the prediction, including the lower limit P_{min}, the upper limit P_{max} and the temperature optimal power P_{opt} for the HP. P_{opt} indicates the power required to restore the temperature to the arithmetic mean of the minimum and maximum temperature flexibilities in the next time step. In the absence of optimization, this power is applied at each simulation step, ensuring that the room temperature remains within the optimal range according to the upper and lower bounds, as long as the HP does not exceed its power limit.

Algorithm 1 outlines the steps involved in one simulation step, including the prediction. The HDM is called iteratively, calculating Q_l^r and Q_l^s as a heat balance, the power consumption for hot water, and the temperature change method to

Algorithm 1 one simulation step, with 24 hour prediction

Initialize module with the building parameter
Get weather and electrical demand prediction for 24 hour
for 96 prediction steps (24 hour a 15 min) **do**
  Calculate Q_l^r and Q_l^s
  Calculate power consumption for hot water demand
  Calculate $\min(\dot{Q}_{heat})$, $\max(\dot{Q}_{heat})$ for T_r flexibilities
  if first step **then**
    $\dot{Q}_{heat} \leftarrow$ requested flexibility
  else
    $\dot{Q}_{heat} \leftarrow \frac{\left(\min(\dot{Q}_{heat})+\max(\dot{Q}_{heat})\right)}{2}$
  end if
  Update T_r and T_s with Q_l^r and Q_l^s and $\dot{Q}_{heat}$
  Convert $\min(\dot{Q}_{heat}), \max(\dot{Q}_{heat}), \dot{Q}_{heat}$ to $P_{min}, P_{max}, P_{opt}$
end for
Decide on operation mode for next simulation step
return $P[i] = [P_{min}, P_{max}, P_{opt}], \forall i \in \{0, 1, .., 95\}$

maintain the bounds of the temperature flexibility. For the first time step the heating power is set according to a flexibility requested by the CC, after which the temperature optimal heat is applied. The HD values for upper $\max(\dot{Q}_{heat})$, lower $\min(\dot{Q}_{heat})$, and optimal heat flow $\dot{Q}_{heat}$ for each step are then converted into an electrical power demand of the HP and aggregated over all iterations. While algorithm 1 illustrates the procedure relevant for the flexibility calculation required for the optimization, the GBM returns additional values to the simulation environment according to Table 4.1.

4.6 Heating-Cooling Switch

This thesis assumes heat pumps operate in two distinct modes involving heating and cooling. However, they can only perform one mode at a time, with the system alternating between these modes. The mode selection process should be based on an operational logic, which could simple be based on the immediate heat demand. [100]

Driven by immediate demand, frequent mode switching in HPs can result in inefficiencies and unrealistic operation, as rapid alternation between heating and cooling is not typically desirable. For optimization this inconsistency leads to significant challenges. The community controller assumes a balance in power consumption, where using more power now would ideally lead to less power requirement in the future. However, mode switching can disrupt this balance, as transitioning between heating and cooling could reverse expected power usage patterns. For instance, increased heating at a given time step may lead to higher cooling demands in the future, complicating the optimization of energy consumption and potentially undermining the system's efficiency. Maintaining a consistent operational mode is thus critical for achieving optimal performance and energy efficiency over time.

Thus, a logic for deciding on the operation mode needs to be implemented, beyond the immediate HD. For this, the proposed GBM uses the predicted data of the HD, provided to the CC, and analyzes the total heating energy required in the next 24 hours. Together with a predefined threshold for switching between modes, this heat balance is used to decide on the mode. While the decision itself is important, so is ensuring that throughout the entire prediction horizon the operating mode stays the same. This is accomplished by switching modes only at the initialization of each simulation step.

This approach enables automatic mode switching with adjustable thresholds, leading to both more frequent and less frequent transitions between modes. However, alternative solutions may also be viable. Therefore, the option for manual mode selection is implemented, providing the ability to maintain constant modes, such as exclusive heating, in scenarios where cooling is not permissible for the modeled building, or exclusive cooling during the summer period, when heating should be disabled.

Chapter 5

Model Analysis

The WPuQ dataset [65] comprises of 68 single family houses with 38 of them providing separate measurements of electricity demand and heat pump power, as described in Section 2.3. In order to validate the introduced GBM a comparison is conducted between the measured data from these households and the simulation results, as presented in the following chapter.

The simulation data used is from 2020 and excludes two of the 38 households due to insufficient measurement data. To ensure comparability, weather data recorded during the same period and at the same location is used for the simulation. This requires the interpolation of missing measurement data to match the 15 minute resolution of the simulation. This interpolation was performed using Python, after which the data was imported into the simulation.

The dataset lacks detailed information on each building, providing only the living area and the number of residents. Since many of the buildings have similar parameters and do not provide sufficient data for a detailed analysis, Table 5.1 shows seven aggregated profiles from the WPuQ dataset for simulation purposes. This table only lists some of the needed input parameters required for the GBM, with the rest being provided in Table 5.2. These parameters are not fixed for each profile but are instead given as ranges within which they vary to account for randomized patterns over all profiles.

The simulation is done by setting up each of the households profiles in BIFROST [77], with varying parameters from Table 5.2, with the frequency of each profile's occurrence in the WPuQ dataset. The simulation duration is set for one full year, and the heat pump mode is configured exclusively for heating, to reflect the actual operational setup in the buildings.

Profile	Building Living Area in m^2	Residents	Occurrence in WPuQ Dataset
H1	100	1	5
H2	100	2	7
H3	100	3	3
H4	150	2	9
H5	150	3	5
H6	200	2	4
H7	200	4	3

Table 5.1: Seven aggregated profiles from the WPuQ dataset for simulation purposes, listing the living area size, the residents and the number of occurrence in the dataset

Parameter	Unit	Range
Proportion	-	$0.5 - 2$
Floors	-	$1 - 2$
Footprint	m^2	Living Area / Floors
Floor Height	m	$2.5 - 2.8$
Window Area	%	$15 - 30$
Absorption_{wall}	%	$2 - 3$
$\text{Absorption}_{window}$	%	$5 - 10$
U-Value_{wall}	$W/m^2\,K$	$0.35 - 0.45$
U-Value_{window}	$W/m^2\,K$	$1.2 - 1.5$
U-Value_{floor}	$W/m^2\,K$	$0.8 - 1.2$
Water per Day	l	$35 - 45$
Shift	h	± 1 h
Noise	-	± 0.2
Heat Pump Size	kW	3.6 kW
Temperature Min	array of °C	[18, 18, 18, 18, 18, 18, 21, 21, 21, 21, 20, 20, 20, 20, 20, 20, 21, 21, 21, 21, 21, 21, 18, 18]
for each hour		[19, 19, 19, 19, 19, 19, 21, 21, 21, 21, 21, 21, 21, 21, 21, 21, 21, 21, 21, 21, 21, 21, 19, 19]
Temperature Max	array of °C	[20, 20, 20, 20, 20, 20, 23, 23, 23, 23, 23, 23, 23, 23, 23, 23, 23, 23, 23, 23, 23, 23, 20, 20]
for each hour		[22, 22, 22, 22, 22, 22, 24, 24, 24, 24, 25, 25, 25, 25, 25, 25, 24, 24, 24, 24, 24, 24, 22, 22]

Table 5.2: Overview of the additional parameters for the simulation, including the ranges within which they vary to account for randomized patterns across all profiles, based on typical values for these parameters

5.1 Yearly Demand

The comparison between the WPuQ dataset and the introduced GBM is done on both an annual basis as well as daily profiles, as discussed in Section 5.2. Since the dataset only accounts for heating demands and hot water generation, the analysis is done only on the heating mode of the model. Although BIFROST offers extensive additional information regarding the simulated settlement, this chapter focuses only on the data related to the HPs for the verification of the heat demand model. Prior to analyzing the simulation, the dataset must be preprocessed.

The data preparation for comparison with simulation results involved addressing several challenges within the dataset. With the two excluded household due to unusable data, a total of 36 buildings is left for analysis. The dataset has missing values, which are imputed using the mean of the available data from the remaining households, ensuring that the interpolation change the overall trend of the dataset. To align the data with the simulation results, which are at 15 minute intervals, the data is interpolated to create evenly spaced time points over each household measurements. This approach ensured that the data points were consistent with the temporal resolution of the simulation, allowing for a direct and meaningful comparison between the WPuQ dataset and the simulated results.

Figure 5.1 presents the daily energy demand of all HPs aggregated from both the WPuQ dataset as well as the simulation. The first five days of the simulated year are not shown, due to a transient phase occurring at the beginning of the simulation. The internal states of the HDM, such as room and structure temperature, are initialized with default values at the start, leading to unrealistic behavior at the beginning of the simulation. With respect to the results from Section 3.3 on the dynamics of the system, several days are required for this transient process to stabilize.

It is evident that while the two curves do not align perfectly, the overall trends are similar. In addressing the first two research questions from Section 1.2 regarding the relevant factors for representation the behavior of the heat demand, Figure 5.1 demonstrates that the proposed GBM follows realistic behavior. The total energy consumption over an entire year of all 36 households in the measured data is **170602 kWh with a mean of 4739 kWh** per household and **162528 kWh with a mean of 4515 kWh** for the simulated settlement. This results in a relative error of **less than**

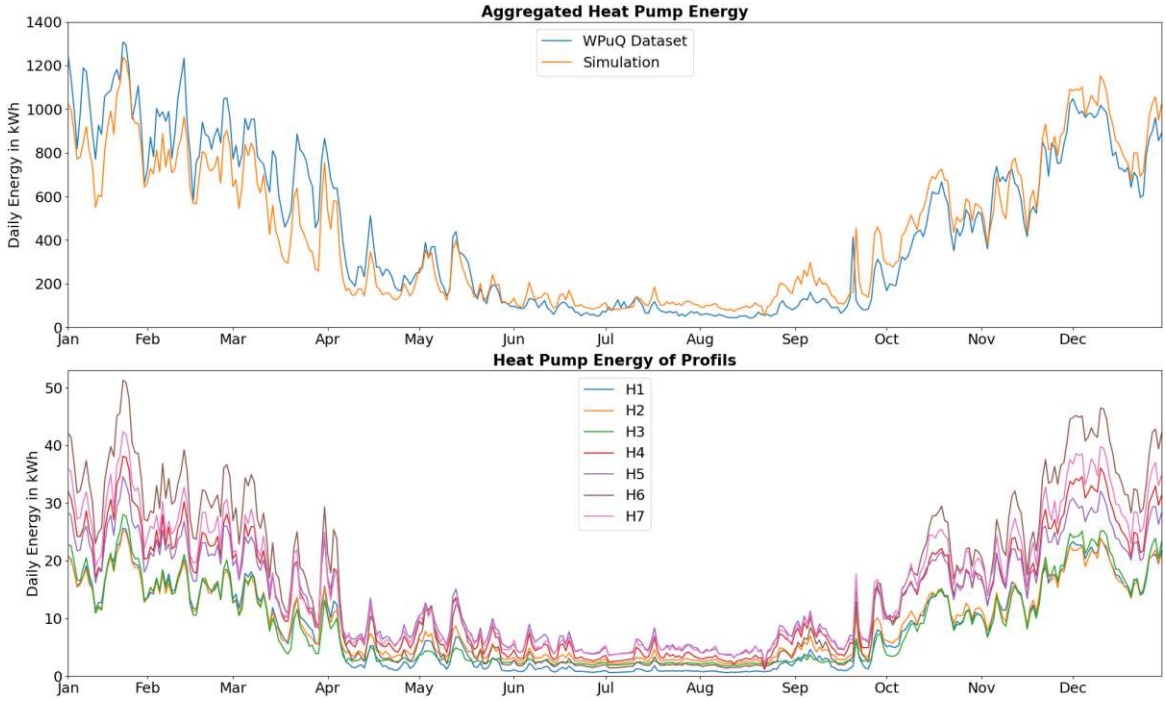

Figure 5.1: The daily energy demand of all HPs aggregated from both the WPuQ dataset and the simulation, as well as the mean daily energy demand of all seven profiles, over the course of an entire year

5 %. Considering the limited information and the great simplifications in the building parameters from the dataset, this result is satisfying.

Inconsistencies between the two data could result from the mentioned simplification in the parameters. Additionally, they may also stem from the inherent approximations within the model itself. For instance, the geometry of a building is assumed to be a cuboid, a simplification that does not accurately reflect real-world variations. Another factor influencing the HD of buildings is the surrounding vegetation. [87] Large trees, depending on the season and solar angle, can reduce heat gains from solar irradiation, due to shadows onto windows or entire exterior walls. A significant variable for HD is the residents' behavior, which is compensated by aggregating many households, thereby aligning with the statistical occupancy model discussed in Section 3.1. However, there may still be weeks or months, such as during holidays when many residents are not at home, resulting in an overall reduce in HD. While these factors contribute to discrepancies between the simulation and the measured data, the benefit of a simplified GBM with significantly less configuration parameters, while still resulting in a realistic behavior, is apparent.

The second plot inf Figure 5.1 shows the mean daily energy demand for all seven profiles over the course of a year. As listed in Table 5.1, the size of the building increases or remains constant, with higher profile numbers, resulting in a higher HD. Although larger living areas generally result in greater HD, the daily energy consumption for the HP does not always increase proportionally with the number of residents. For instance, during winter profile H6 has a higher demand than profile H7, similar to the trends observed by H1 - H3 and H4 - H5, during summer however, this pattern is reversed. This could be explained by the increased hot water usage among more residents, but also greater heat dissipation from human occupants and electrical devices. During the summer, the energy demand for the HP is predominantly driven by hot water consumption, whereas in winter, the HD constitutes the majority of the HP's energy usage.

The comparison between all profiles and their corresponding mean annual HP energy demand is listed in Table 5.3.

Profile	HP's annual energy demand	
	Simulation in kWh	WPuQ Dataset in kWh
H1	3101	5322
H2	3411	3340
H3	3214	1572
H4	5148	3577
H5	5093	5513
H6	6103	6043
H7	5767	9191

Table 5.3: Comparison between all seven profiles and their corresponding mean annual HP energy demand, including each a single household from the WPuQ dataset with equivalent building size and number of residents

Each profiles is also compared to a single household from the WPuQ dataset with equivalent building size and number of residents. It is evident, that the GBM does not accurately match the energy demand for a specific single building. This is apparent, when considering the limited information on the real household used for simulating the HD. Discrepancies may arise from factors previously discussed, but they have a much greater impact on individual households than on entire settlements. This highlights the intended application for this model, to analyze the influence of HPs on the electrical grid of larger settlements, while acknowledging its limitations in accurately simulating individual buildings.

5.2 Daily Profile

For a more in-depth analysis of the introduced GBM, both the energy consumption and room temperature profiles are examined on a daily basis. To highlight periods of high load on the heat pumps and illustrate intervals with notable behavior, January 20th is selected in this section. During this time, outdoor temperatures remain close to zero, and the heating demand of the building is predominant over hot water consumption. Figure 5.2 shows three plots with the first one depicting the aggregated power of all HPs from the WPuQ dataset and the simulation, the second comparing the data of a specific household with the profile H4 in each case and the third displaying the applied heat flow and room temperature of the simulation household only.

While the daily energy demand over the course of the year aligns with the real measured data, Figure 5.2 demonstrates that the aggregated electrical power of the HPs, recorded in 15 minute intervals, does not match between the simulation and the WPuQ dataset. The proposed GBM leads to a higher power spike in the morning, to heat up the buildings to the desired room temperatures during the day. In contrast, both the measured data and the simulation show a reduction in power around midday, resulting from decreased heat losses, increased solar heat gains and, in some cases, deactivation of the heating system when residents are absent. In the evening, both power consumption increases again, for reasons opposite to those observed during midday, and additionally a rise in hot water demand for activities such as showering and dish washing. Throughout the night, the GBM does not lead to relevant energy consumption, as temperature requirements are lower and hot water consumption is minimal. Interestingly, the measure data shows no significant reduction in power over the night. Possible explanations for this include households maintaining a constant temperature overnight, with the HPs working to sustain high temperature levels. This could also account for the absence of a morning power peak, as the GBM heats the building again, while the WPuQ dataset data does not show this behavior. Another factor could be small hot water buffers, typically installed with HPs to provide minimal heat storage. However, without knowledge of the specific temperature settings and system configurations, these hypotheses cannot be conclusively verified.

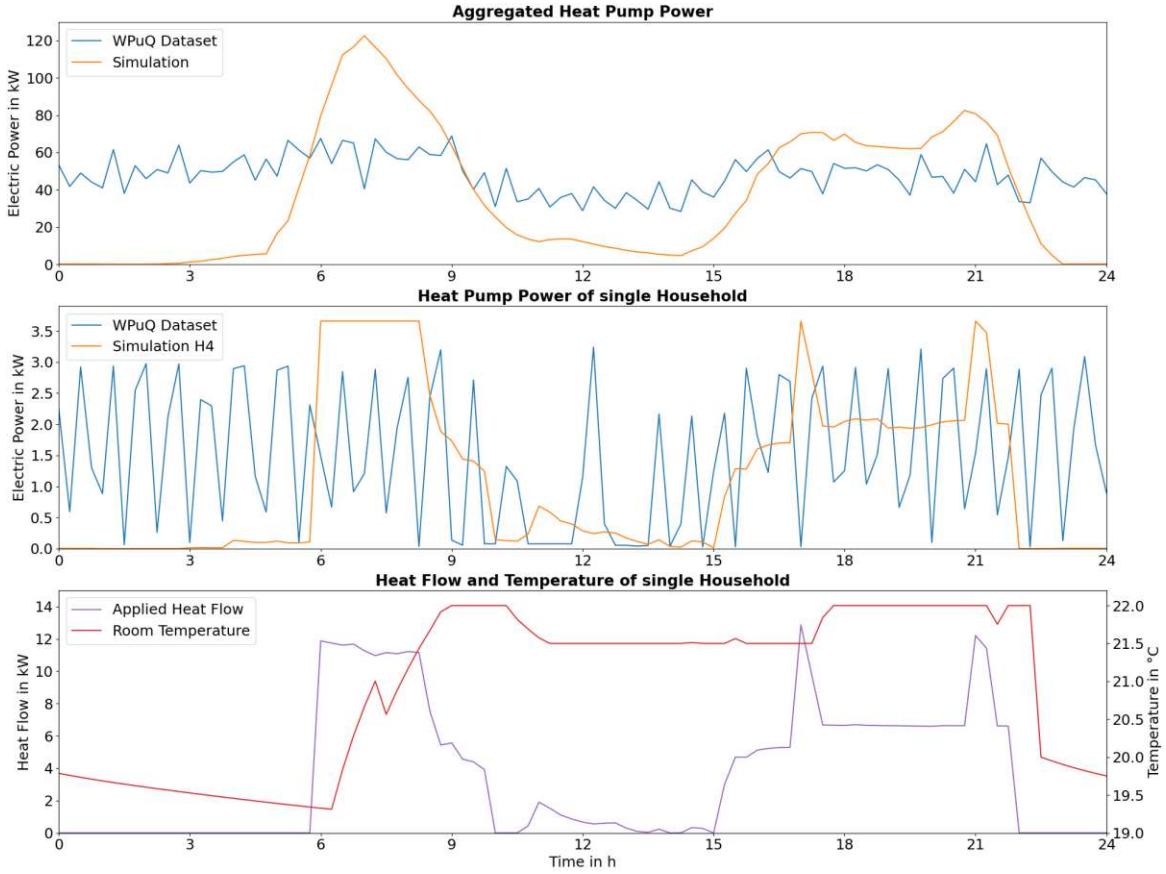

Figure 5.2: Electrical Power of all HPs aggregated over the course of an entire day and the power profile of a single household for both the simulation and the WPuQ dataset, as well as the heat flow and room temperature of one building in the simulation on January 20th

The second plot, illustrating the power consumption of a specific household from both the simulation and the dataset, shows comparable behavior to the aggregated power above. The power consumption of individual households appears to follow similar patterns, resulting in a smoothed yet equivalent profile for the aggregated power. The simulation data displays a peak in the morning, where the HP reaches its capacity of 3.6 kWh, followed by another increase in power during the evening. In contrast, the measured data demonstrates volatile power fluctuations, suggesting that the HP operates in two or three discrete stages, switching on and off multiple times. This behavior may be attributed to insufficient measurement resolution, potentially failing to meet the Nyquist Criteria. However, information regarding the operation of HPs suggests, that they do not provide continuous heating power, but rather operate at different discrete set points. [81] Consequently, HPs are often paired with small hot water buffers, as described previously, to mitigate the fluctuations in their operational mode. Given the significant power fluctuations in the measured data, it is challenging to extract visually a mean energy consumption for a given time period. However, the density of power peaks provides insights into the this. Higher activation frequencies of the HP correlate with increased energy consumption. This results in a similar pattern to the simulation data, with reduced consumption during midday.

The third plot in Figure 5.2, shows the applied heat flow and room temperature, which are compared with the electrical power and heating data from the second plot. The relationship between the electrical power and the applied heat flow is given by the COP of the HP, although the coupling is not perfectly linear. Variations in the HP's set point cause changes in the COP, leading to deviations from a strictly linear relationship between electrical power and heat output. Additionally, the electrical power associated with hot water demand is reflected in the power data, however, it

is not represented in the applied heat flow in the heating system. This distinction highlights that while both electrical power and applied heat flow are influenced by the performance of the HP, the electrical power reflects both the heating demand and the hot water demand, while the applied heat flow represents only the portion of the heat energy that directly influences the temperature change in the room.

With the applied heat flow directly influencing the temperature of the room, a relationship between these can be seen in the third plot. In the morning the peak in applied heat flow results in a rise in temperature. In the morning, the peak in applied heat flow leads to a rise in temperature. Although the heat remains nearly constant during this period, the temperature increase is not linear, as the heat transfer into the building's structure increases with the rising room temperature. Initially, the room temperature is similar to the structure's temperature, resulting in negligible heat transfer. As the heating system raises the room temperature, the temperature differential between the indoor air and the building's structure increases. Due to the significantly higher thermal heat capacity of the building's structure, its temperature remains nearly constant during this period, not rising with the room's.

The small temperature drops observed in the morning and evening are attributed to the building's ventilation. During midday, the room temperature decreases, representing the deactivation of the heating system when residents are absent. In the evening, as the temperature requirement lowers, heating to keep the temperature constant stops. Initially, the room temperature drops rapidly to the structure's temperature at approximately 20 °C, and then gradually follows the slow cooling of the structure due to its high heat capacity. Throughout the night, this results in an additional temperature drop of about 0.5 °C, implying a fluctuation of around 0.5 °C of the structure temperature over the course of the entire day.

The implemented grey box model demonstrates a good fit when compared to the measured dataset, particularly in terms of certain trends, such as the lower power consumption observed during midday. However, discrepancies are seen in the HP power, where real data exhibits significant power fluctuations, whereas the model predicts continuous power usage. This difference may be attributed to the absence of a hot water buffer in the model, which could smooth out these fluctuations in the real world scenarios. Despite these variations, the behavior of the implemented GBM is consistent with the intended goals of the simulation, producing a temperature profile that aligns well with expected results.

5.3 Heating Cooling Logic

The WPuQ dataset consists solely of households equipped with heating systems that are capable of heating but not cooling, therefore, a fixed operating mode was selected for the simulation as well. To analyze the behavior of the introduced GBM in relation to the switching decision, a separate simulation was conducted using the same settlement and weather data, but with adaptive mode switching for the HPs. The analysis is limited to the period from April 1st to April 20th, due to the notable simulation results observed during this time frame, with three distinct threshold settings for the switching logic. The threshold is defined relative to the HP's capacity, using 10 %, 4 % and no threshold, based on the maximum electrical heating energy that the heat pump can provide over the next 24 hours. The accumulated predicted heat demand, thus including positive and negative heat requirements with respect to their sign, is compared to the threshold and a mode switch is only performed, when the HD deviates beyond the threshold in the opposite direction of the current operating mode.

Figure 5.3 presents three different plots over the same period of time, with the first plot depicting the electrical power

Figure 5.3: HPs electrical power for three different switching thresholds of HP's operation mode for profile H2, as well as the applied heating flow for profile H2 and H6 from April 4^{th} to April 14^{th}

by a HP based on profile H2, including the three different threshold setting. High threshold corresponds to 10 % of the maximum energy, medium to 4 % and no threshold describes the case for solely picking the operating mode based on the sign of the accumulated predicted HD over the next 24 hours. The second and third plots illustrate the applied heating flow, indicating the operating modes for both the H2 profile and the H6 profile, which corresponds to a larger building with an equal HP capacity.

In the second plot, mode switches are evident due to changes of the sign in the applied heat flow. In the case of no threshold, frequent switches are observed. The operating mode transitions up to twice per day, with heating in the morning, cooling during midday, heating in the afternoon, and cooling again in the evening to lower the temperature for sleeping. This pattern is atypical for a residential household, where temperature deviations from the set point are generally tolerated, with the expectation of saving energy on heating or cooling later in the day.

The medium threshold of 4 % already significantly reduces the frequencies of mode switches, with no switching occurring between 5^{th} to April 12^{th}. However, around 4^{th}, multiple mode switches from heating to cooling are observed. With a higher threshold, as represented by the high threshold curve, these fluctuations are further mitigated, with only one switch to cooling occurring between 8^{th} to April 14^{th}. Due to the higher threshold though, the switching does not only occur less, but also delayed, as the building first needs to heat up, resulting in higher cooling requirements to overcome the threshold. Consequently, the later switching and heating of the building leads to minimal heating requirements prior to mode switching, thus reducing the electrical power demand for the heat pump, as seen in the first plot from 5^{th} to April 8^{th}. With the building structure heated up before the mode switch, the model with a higher threshold,

Profile	HP's total electrical energy demand in kWh		
	No Threshold	Medium Threshold	High Threshold
H1	246	160	136
H2	108	199	183
H3	332	230	220
H4	396	335	271
H5	405	384	263
H6	450	424	275
H7	536	459	384

Table 5.4: Comparison between all seven profiles and their corresponding HP's total electrical energy demand, in the time interval from April 1st to April 20th, for three different thresholds deciding on mode switching

consequently, shortly requires more electrical energy for cooling it down again after the switch.

As depicted in the third plot, the building profile significantly influences the behavior of the switching logic. While the HP's capacities for the H6 profile are identical to those of the H2 profile, the threshold corresponds to the same heating energy in both cases. However, due to the larger building size of the H6 profile, the heating demand is considerably higher, the threshold being reached more likely. It can be seen, that the high threshold still results in realistic behavior, with the mode switch occurring just a few days earlier. It is observed that the high threshold still results in realistic behavior, with the mode switch occurring just a few days earlier. In contrast, the medium threshold exhibits behavior similar to that of the no threshold scenario, leading to unrealistic behavior. One might conclude, that simply applying higher thresholds would achieve the desired results. However, for a smaller building, such as the H2 profile, an excessively high threshold could lead to delayed mode switching, potentially violating temperature limits by letting the building heat up too much before switching, thus resulting also in unrealistic behavior. Therefore, the threshold needs to be calibrated to the building's parameters and weather conditions, to represent realistic behavior of the GBM.

5.4 Real-time Behavior

Real-time capability of the GBM is essential for real applications, predicting HD in multiple buildings over a 24 hour period at 15 minute intervals. It allows for optimized heating schedules, reducing energy waste while maintaining comfort. Real-time data helps adjust predictions based on changing environmental conditions, occupancy, and other factors, ensuring heating systems are responsive and efficient. This flexibility is critical when managing diverse HDs across several buildings, addressing the research questions.

In scheduling heating systems on small hardware platforms, as utilized for many application in building management, real-time capability ensures optimal system performance. Furthermore, faster than real-time simulations, allowing for long term analysis as shown in this and following chapters, is crucial for the proposed GBM.

Figure 5.4 presents a violin plot depicting 2664 measured times for computing a single simulation step, involving 96 predictions as outlined in algorithm 1, for each of the seven profiles introduced in this chapter. The data reveals that the average time for one calculation step is approximately 3 ms, with all profiles showing a maximum of 10 ms. For real-time applications a task executed every 15 minutes with a maximal duration of 10 ms is more than real-time capable, even when applied for multiple buildings.

The distribution observed in the violin plots suggests, that majority of simulation steps require between 2 and 4 ms, with a minority of measurements exceeding this range. This variability is likely due to hardware scheduling, as mul-

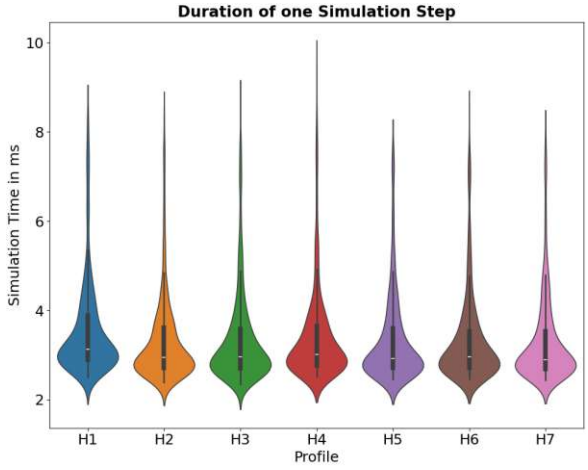

Figure 5.4: A violin plot depicting 2664 measured times for computing a single simulation step, involving 96 predictions, for each of the seven profiles introduced in Chapter 5

tiple models within the BIFROST simulation run concurrently, and task preemption by higher-priority processes can lead to occasional, significantly longer computation durations. The algorithm itself should not introduce substantial variations in computation time, as the code path is designed to ensure similar execution times, with conditional statements performing analogous procedures. This can be seen when comparing the different profiles, presented in Figure 5.4, indicating same statistical distribution of the measurements for different parameters settings.

Chapter 6

Flexibilities and Optimization Potential

As part of the second set of research questions in this thesis, the proposed grey box model is employed to assess the potential of cross-location optimization. The two research questions are as follows:

RQ 3: What dynamic behavior is required from a grey box model to model temperature changes due to energy shifts for optimization purposes?

RQ 4: What potential does cross-location optimization offer over local optimization, particularly by leveraging different weather conditions across various locations?

The first question was addressed in sections 3.3 and 5.2, but requires further investigation regarding its flexibility potential. This chapter analyzes the flexibility potential of local optimization using the introduced GBM in relation to HP capacities, drawing an analogy to batteries. Subsequently, the potential benefits of cross-location optimization are compared with local optimization by simulating two settlements with varying weather conditions. For both analyses, the community controller proposed by [78] is utilized, incorporating a higher-level decision making unit for the cross-location optimization. The CC optimizes the scheduling for all participants in one energy community (EC), including batteries, HP or PV systems, based on energy demand predictions for the next 24 h. Based on these schedules, the DMU determines an schedule of energy shifting between the two settlements or ECs, instructing the CC on the set point for the aggregated power at the substation that the EC should optimize at.

6.1 Flexibility for Local Optimization Potential

The simulation setup for analyzing the potential of local optimization in heat demand using the proposed heat demand model is based on the low-voltage grid topology and consumer classifications from the semi-urban SimBench dataset [63] introduced in Section 2.3. This dataset offer a realistic representation of grid configurations, with different future grid development stages. Two scenarios are used, corresponding to the years 2024 and 2034 in the dataset, with adapted grids to only analyze residential buildings. The key difference between the two used scenarios is the PV size, with a summary of the scenarios listed in Table 6.1. The grid topologies are essential for understanding how the distribution of decentralized resources affects the overall HD and energy consumption at the local level and offer comparability between studies using the same datasets.

Parameter	2024	2034
Number of Households	30	30
Number of PV	1	5
PV Capacity in kWh	6.5	43.4
Annual Power in MWh	94.88	94.44

Table 6.1: Summary of the adapted grid development scenarios used in the simulation of local optimization based on the SimBench dataset for only residential buildings

For weather data, two future climate scenarios from the SecuresMet dataset [101] are used to capture the effects of climate change on building heating demand. This dataset is for the modeling of electricity production and demand, as future emission scenarios RCP 4.5 and RCP 8.5, both from 1951 to 2100 and different spatial aggregation levels. The two selected short time scenarios of each 20 days, representing a heat wave with all nights above 20 °C and a cold spell with temperatures below -5 °C, are based on the RCP 4.5 emissions scenario and correspond to Vienna at the NUTS 3 level. These extreme weather events provide a challenging context for HPs, highlighting their performance under stressful conditions. The analysis is conducted for each grid development stage, with the HPs capacity ranging from 1.2 kW to 12.0 kW, to assess their potential in optimizing HD under varying climatic and grid conditions. The capacity of the HPs is equal for all buildings through one simulation and separate simulations are performed for each HP capacity.

The temperature targets for households are set at 20 °C during night-time and 22.5 °C during day-time, with added flexibility during midday of ± 2 °C and other times ± 1 °C. To reflect real-world variability, the day and night cycles for each building are randomly shifted within a range of ± 1 hour following a normal distribution. This adjustment ensures that the simulation incorporates realistic patterns of heating demand, with individual household schedules varying slightly.

6.1.1 Impact of Heat Pump utilization on Grid

Figure 6.1 presents a comparison of the aggregated power load at the substation for representative hot and cold temperature extremes across different HP sizes, over the curse of one day. The reference curve represents the substation load when all HPs operate continuously according to their optimal temperature power demand, as would occur in the absence of grid wide control, thereby maintaining the set temperature target. In contrast, the curves labeled "optimized" show the substation power load under the objective of minimizing peak loads while closely adhering to the desired temperature profile, as determined by the optimize schedule provided by the community controller. It is important to note that, in cold spell scenarios, a 3.6 kW HP is necessary to adequately maintain the set temperature target and prevent continuous operation at its maximum power capacity.

The results indicate that, overall, optimization smooths the aggregated power at the substation by controlling only the HPs, which affects not only the HD but also the electric load from other devices and energy generation from photovoltaic. When comparing the hot day scenario across different grid development stages, the primary difference is the PV generation during midday, which results in energy feedback from low to medium grid levels as shown in the 2034 scenario. Although the 2.4 kW HPs have the potential to smooth the total power profile, in the 2034 scenario their flexibility is insufficient to fully utilize the electric power generated by the PV system. In this case, a 7.2 kW HP capacity is necessary to prevent negative power consumption at the substation.

While higher HP capacity, therefore, results in more flexibility that can be utilized, it is also evident, that it leads to

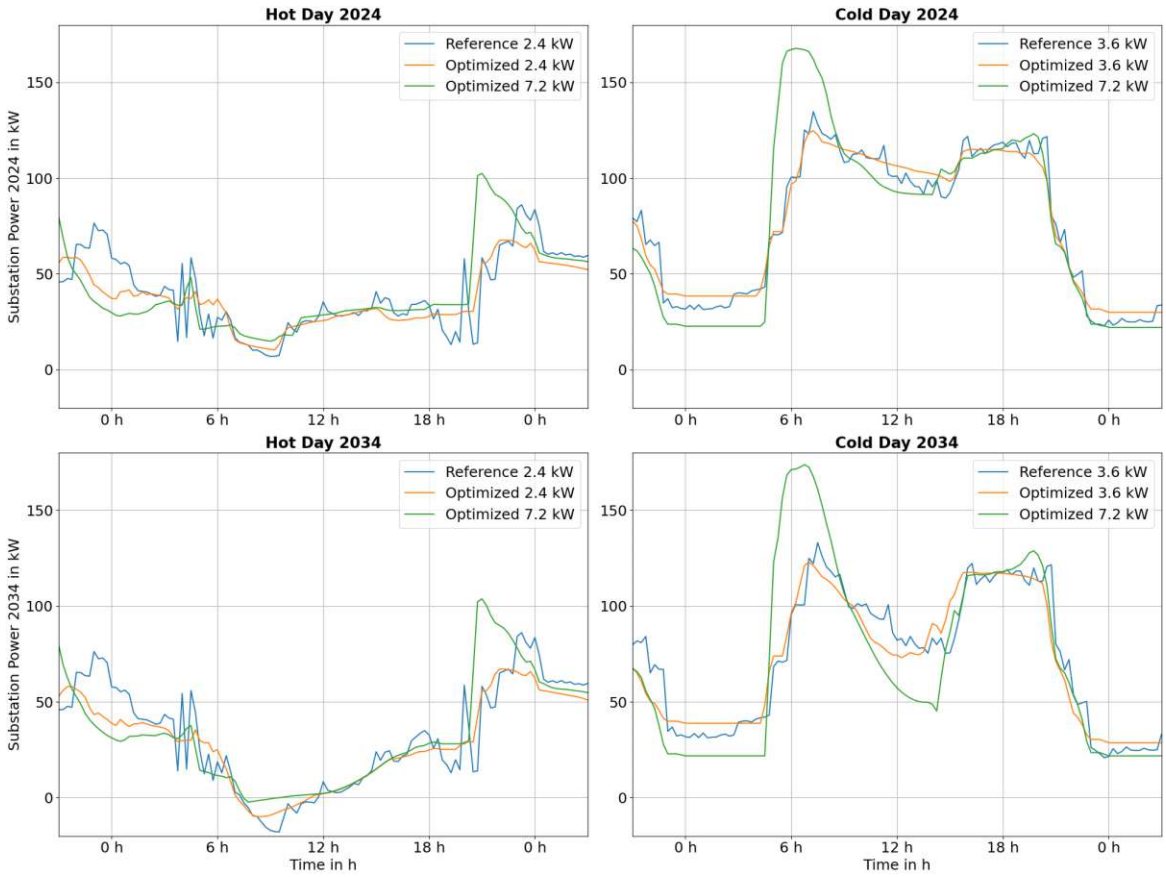

Figure 6.1: Comparison of the aggregated power load at the substation for hot and cold temperature extremes across different HP sizes and operation modes, for both grid development stages, over the curse of a representative day

higher peaks in power. This is particularly evident during cold spells, where the morning power demand is significantly higher with the 7.2 kW HPs. This occurs due to the opposing objectives of controlling room temperature while limiting the total power demand. When the lower capacity HPs reach their power limit in the morning, when the HD exceeds their capacity to heat the building, the higher capacity HPs tend to provide the required heat, resulting in increased electrical demand. The balance between these two optimization objectives can be adjusted through parameter tuning of the optimization algorithm in the CC, however, this issue will always be present.

In summary, it is evident that higher HP capacity provides greater flexibility but also results in higher peaks during periods of high HD. Optimization of HP power consumption leads to a smoother power profile compared to a reference curve, which represents the absence of grid-wide control, and offers the potential to compensate for fluctuations in electrical demand and PV power generation by leveraging the thermal mass of the building structure.

6.1.2 Individual Heat Pump Flexibilities

The previous subsection examines the impact of optimized HPs on the aggregated electrical power demand at a substations. For residential applications, an individual analysis of single HPs and their impact on the corresponding household is important. Subsequently, Figure 6.2 presents an analysis of the optimization effects on the power consumption of a single HP. The shaded areas in the figure visually represent the positive and negative energy shifts resulting from the optimization process. It demonstrates how system flexibility allows the repositioning of active cycles in alignment with the electrical power generated by other loads, such as PV systems.

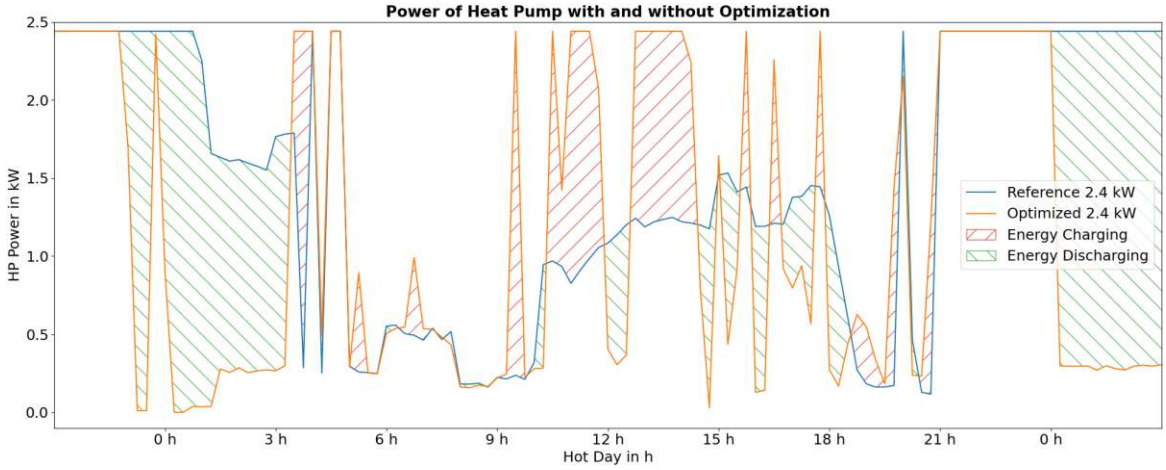

Figure 6.2: Comparison of the power consumption of a single optimized and uncontrolled HP, over the curse of a hot day with the grid development stage 2034

It is evident that the optimization of a HP results in significant fluctuations in power consumption, with operational points typically corresponding to either maximum or minimum power. This behavior is not unusual for a real HP, as demonstrated in Section 5.2. The observed fluctuations comes from the compensation of other loads and their distribution across multiple HPs. The overall energy shift occurs from nighttime to daytime, capitalizing on the high power availability during daylight hours due to PV system overproduction. The majority of the highlighted areas in red occur during midday, allowing surplus PV energy to be utilized at the time of generation without the need for intermediate storage. This strategy enables efficient building cooling without causing any carbon emissions or violating the room temperature constraints. During the night, power consumption is reduced due to the pre-cooled building structure.

When the optimized and reference power demand of the HP overlap, it indicates that no flexibility is being utilized. This could result from a lack of demand for flexibility or the absence of potential flexibility in the heat demand. For example, in the evening, the temperature profile is configured in a way, so that the room must be cooled from 22.5 °C to 20 °C. The temperature flexibility is limited to ± 1 °C at this time, resulting in a step from 21.5 °C to 21 °C in the maximum utilization of these flexibilities. Consequently, a HD is required during this step, with no opportunity for flexibility in the electrical demand of the HP.

When the HP operates at its maximum capacity of 2.4 kW for extended periods, it indicates the limitations in either controlling room temperature or providing flexibility. The maximum utilization observed during midday highlights the insufficient power of HPs with 2.4 kW capacity to fully utilize the power generated by the PV, as demonstrated in Figure 6.1 during the hot day and the 2034 gird development stage. The evening peak, coupled with the lack of flexibility during this period, as discussed previously, indicates a higher energy demand with HPs providing a higher capacity, as also illustrated in the same plot in Figure 6.1 during the evening hours.

6.1.3 Battery Size Analogy

The interpretation of heat flexibility in terms of the theoretically required capacity of a battery system provides a valuable means for performance quantification and estimation. In battery system planning, critical factors include the required capacity and the associated costs of energy charged and discharged over the system's lifespan. While a HP does not support bidirectional energy flow, as it solely facilitates energy usage without the ability to charge or discharge, it can

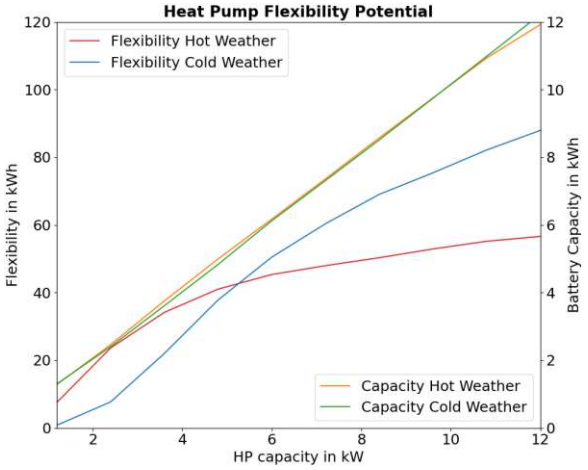

Figure 6.3: The average daily energy flexibility and equivalent battery capacity for both hot and cold weather scenarios over a 20-day period in the 2034 grid development stage, as a function of varying HP capacities

still be compared to a battery, which operates in both modes. Flexibility in heating is fundamentally related to the temporal shift in energy demand. By consuming more energy at a given point, the expectation is that the demand for energy will decrease later. In this context, the reduced energy demand of a HP in the future is analogous to the role of a battery providing energy during that time. Consequently, although a HP lacks the capacity for energy generation, it functions as a bidirectional energy buffer when considering energy usage over time.

Figure 6.3 illustrates the mean average daily energy flexibility for both hot and cold weather scenarios over a 20-day period and all HPs in the 2034 grid development stage, as a function of varying HP capacities. The total energy flexibility utilized is derived by integrating the absolute area between the reference and optimized power of the HP, as shown in Figure 6.2. Additionally, the corresponding equivalent battery capacity is provided in Figure 6.3. The maximum capacity of the equivalent battery can be determined by summing the colored areas in Figure 6.2, accounting for the respective sign, resulting in a maximum stage of charge for a equivalent battery.

It is observed, that the equivalent battery capacity increases linear with the HP's capacity, regardless of the weather scenario, representing a short term energy shift. This is not surprising, since higher HP capacities are expected to result in an increase in the maximum flexibility peak, as they enable the consumption of more electrical power by the HPs. However, the total average energy shifts over a day do not increase linearly with the HP capacity. Although the flexibility for both weather scenarios increases, it appears to approach a limit, suggesting that higher short term power flexibility is less efficiently utilized in terms of total energy shifted.

During a heat wave, flexibility is higher than during a cold spell for smaller HP capacities, but the rate of increase in flexibility decreases with larger capacities. This difference is attributed to the varying operating modes of the HPs, with cooling during the heat wave and heating during the cold spell, resulting in different efficiencies for heat generation. For smaller HP capacities, the lower coefficient of performance for heating is insufficient to meet the high HD while maintaining flexibility. In contrast, during a heat wave, the higher energy efficiency ratio allows the HP to provide a higher flow of heat (cooling) with the same electrical capacity, offering greater flexibility. With increasing capacities of HPs, the limiting factor in flexibility results from the thermal capacity of the room's air and the building structure. In this case, a higher EER, which reflects the efficiency of converting HD to electrical power demand, leads to reduced electrical flexibility for the same thermal flexibility compared to the cold spell with the COP. This indicates that the

flexibility provided by a HP is not only dependent on its capacity but also on the building's characteristics and thermal capacities, weather conditions and the HP's operating modes.

6.2 Flexibility for Cross-Location Potential

In order to investigate the potential of cross-location optimization over local optimization between two citizien communities, a simulation was conducted with two BIFROST instances and corresponding settlements. The concept and setup are depicted in Figures 2.3 and 2.2. For a simple representative settlement, four buildings are instantiated, each corresponding to heat demand, base load, and photovoltaic profiles that represent four equal residential households. This configuration results in a settlement representing 16 households with a total PV capacity of 60 kWp.

Both settlements share an identical setup, with the only difference being the weather data. The weather data used is based on data from the SecuresMet dataset [101], as previously introduced, with weather predictions for March and April of the year 2049. The two locations are both situated in Tyrol, one in East Tyrol (ET) and the other in the Tyrolean Oberland (TO), with the potential for energy exchange. The weather data in the SecuresMet dataset is provided at a spatial resolution of NUTS level 3, which does not capture local weather conditions at specific locations. These weather data are used to illustrate the potential of cross-location optimization based on the proposed GBM, without focusing on a specific real-world scenario. With higher resolution data, there could be the potential for even more significant weather differences for nearby locations, such as between two valleys. he selected weather data shows high temperatures up to 15 °C and significant solar irradiation in the TO, while ET experiences cooler temperatures and less solar irradiation. Consequently, one settlement faces an energy deficit due to higher heat demand, while the other generates more energy with PV than it can consume.

6.2.1 Flexibility in one Location

To assess the impact and potential of cross-location optimization, the settlements are first simulated individually with only the CC optimizing locally. Figure 6.4 depicts the total electrical power at the substation for each settlement, along with the ambient temperature and solar irradiation over the period from March 20th to April 2nd is depicted, as this timeframe contains the most relevant and significant data.

The ambient temperature and the solar irradiation highlight the energy intensive scenario in ET, where HPs are required to supply significantly more heat due to lower solar gains and reduced electrical power generation from PVs. In contrast, TO experiences higher solar irradiation and milder temperatures, reaching up to 17°C, which likely results in an overproduction of electrical energy. Indeed, ET exhibits a substantially higher power load at the substation compared to TO, with the power consumption behavior primarily driven by the characteristics of the HPs' energy profile. This indicates that in ET, the electrical energy demand from HPs is the dominant factor, while in TO, the midday power load is predominantly influenced by PV production.

Without the DMU, the CC in both settlements attempts to flatten the substation power load. In TO, the flexibilities of the HPs are fully utilized, reaching their operational limit, and are unable to prevent feedback into the grid. In ET, the substation power load exhibits morning peaks and slight increases in the evening, with a relatively flat and stable power load during midday. During the night, both settlements show similar electrical power demands, with no variation in solar irradiation and reduced heat requirements due to the reduction of the room temperature.

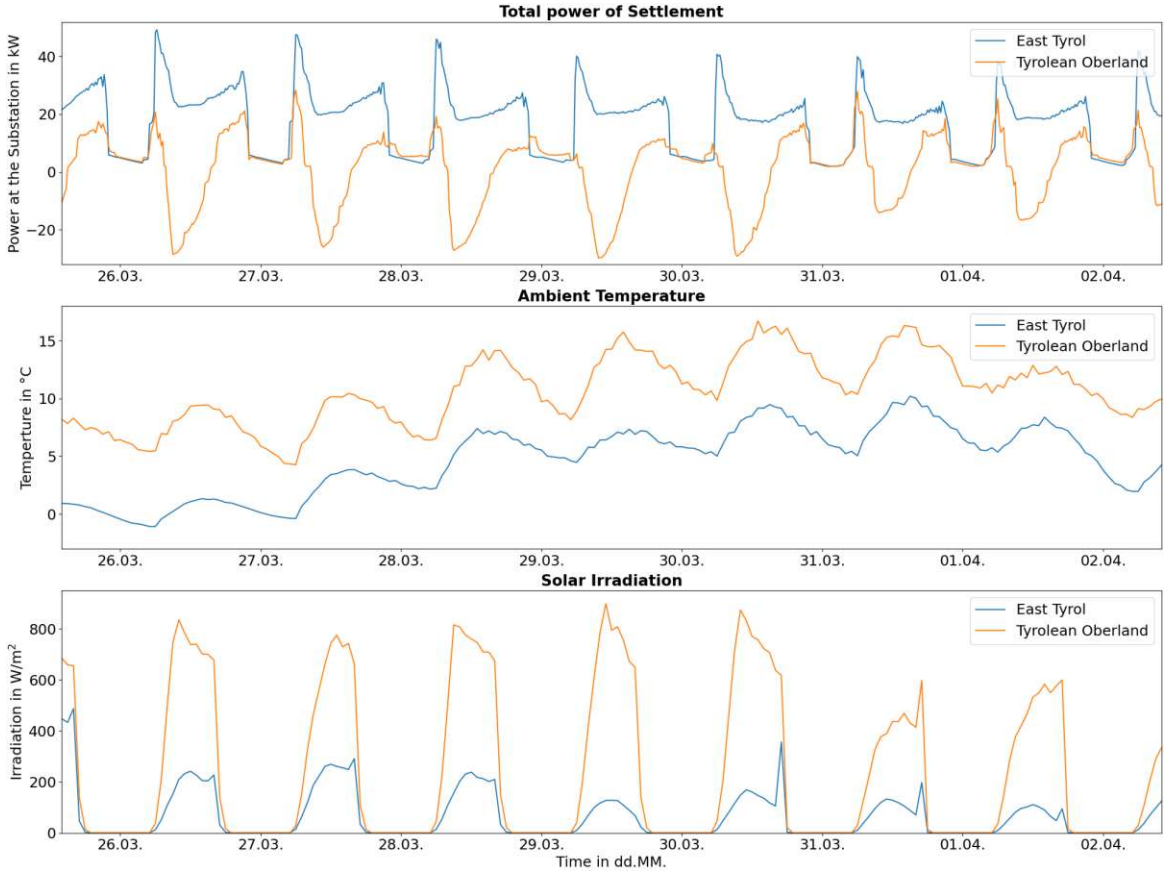

Figure 6.4: The total electrical power at the substation for East Tyrol and Tyrolean Oberland, along with the ambient temperature and solar irradiation over the period from March 20th to April 2nd with local optimization only

6.2.2 Flexibility over both Locations

Previously, the settlements were simulated using only local optimization. However, both settlements' CC are now connected to a higher level DMU, enabling cross-location optimization.Based on the predictions for each settlement provided through the CC, the DMU schedules set points for each settlement, directing the local optimization to converge towards them. Figure 6.5 depicts the electric power loads for each of the substations in the case of cross-location optimization, along with the set points provided by the DMU. These set points are complementary, due to the conservation of energy in the grid representing the desired power shift between both settlements.

With the scheduled set points, East Tyrol no longer experiences smooth and flat power loads during midday, but instead aligns with the overproduction from Tyrolean Oberland, utilizing the flexibility of HPs. This demonstrates that, although ET does not require the increased power demand during midday, its HPs are being leveraged to compensate for the generated power by PVs in TO.

In contrast, TO shows no significant differences between the local optimized power load at the substation illustrated in Figure 6.4 and the cross-location optimization in Figure 6.5. In both cases the flexibility of its HPs is fully utilized to encounter the PV production. The only additional flexibility option controlled by the CC in TO would involve the PV modules themselves, limiting their power generation to reduce feedback into the grid. However, in this scenario, such an adjustment is not enabled, to focus solely on the flexibility provided by the HPs.

To fully assess the potential of cross-location optimization, the second plot in Figure 6.5 shows the aggregated power of both settlements, for both the local and cross-location optimization. In the absence of a DMU, the overproduction from

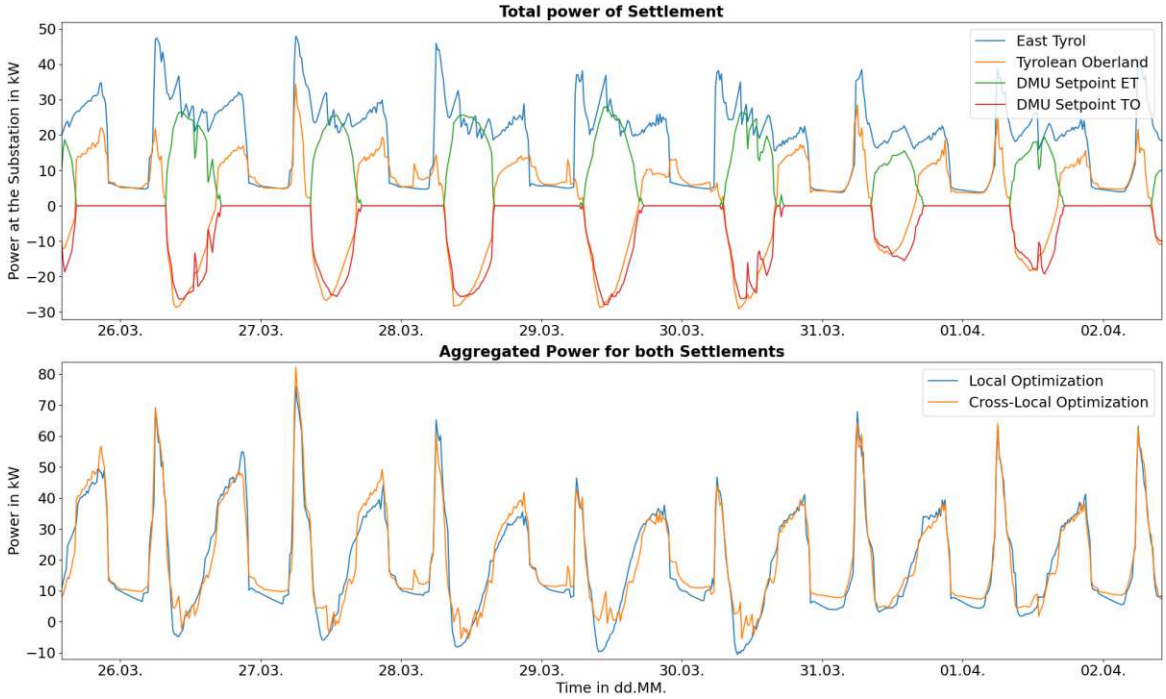

Figure 6.5: The electric power loads for each of the substations in East Tyrol and Tyrolean Oberland in the case of cross-location optimization, along with the set points provided by the DMU, as well as the total aggregated power of both settlements, comparing the energy balance between local and cross-location optimization

TO is naturally partially used by ET to meet its power demand. However, cross-location optimization demonstrates an increased utilization of the power generated by the PV systems. Especially between March 29th and 31th, the otherwise negative power balance is encountered by the flexibilities of the HPs in ET, resulting in reduced or no grid feedback for the combination of both settlements.

This is important for a grid-oriented control of the settlements, as it reduces the reliance on energy buffers provided by the grid operator, while also offering economic benefits to citizen communities across different cities. The total shifted energy between both settlements with cross-location optimization amounts to **1088 kWh** in the depicted time period, with a combined **total demand of 3555 kWh**, resulting in an **energy shift of 31 %** of the total energy demand. Although the absolute values may have limited significance due to the hypothetical nature of the settlements, these figures clearly highlight the potential of cross-location optimization and the crucial role of flexibility provided by HPs in such scenarios. Consequently, the proposed GBM offers the necessary tools and framework to further explore various scenarios and optimization strategies for cross-location optimization, as the current implementation of the DMU is focused solely on minimizing the total grid feedback from both settlements.

Chapter 7

Summary

In this chapter, the results previously discussed are summarized and aligned with the research questions. The aim of this thesis was to develop a grey box model for simulating the heat demand in residential buildings, with the goal of integrating it into the BIFROST [77] simulation environment, to be used in further studies. The motivation for creating a heat demand model stemmed from the growing prevalence of HPs, as they are considered a key solution for achieving climate-neutral heat supply by 2045. These systems are integral to sector coupling strategies designed to integrate electricity, heating and cooling, which will significantly increase decentralized loads in electrical distribution networks, particularly in urban areas. Consequently, this trend necessitates accurate predictions of HDs and electrical loads to maintain grid stability. One advantage of sector coupling is that HP systems can utilize the substantial thermal capacity of building structures as a source of flexibility for grid-oriented energy optimization. This, in turn, creates a need for the dynamic behavior of the proposed GBM, which links room temperature flexibilities to heat and, subsequently, electrical flexibilities.

To summarize this thesis, each proposed research question is presented along with a brief discussion of the corresponding results. The first question states:

RQ 1: Which factors influencing a household's HD significantly affect the overall HD profile, particularly in the context of grid-oriented energy optimization?

The relevant aspects affecting HD in the context of grid-oriented energy optimization are primarily the characteristics and dependencies of the HD. In this regard, the exact total value of HD is less critical than the peak loads and variations driven by weather and other external factors, as these ar critical for grid stability. Chapter 3, and particularly sections 3.1 and 3.2, focused on the influencing factors and resulting profiles in HD. The most relevant aspects in HD influenced by external conditions are the thermal transmittance and solar irradiation. Although these can be calculated based on building parameters and weather conditions, it was observed that many other factors are highly dependent on occupant behavior, such as human heat dissipation, ventilation, hot water consumption and heat from electrical devices. Consequently, accurately matching the HD profile of a single household is challenging without extensive knowledge of the resident's behavior. However, statistical models provide a reasonable approximation for an aggregated HD, as demonstrated in Chapter 5.

These approximations bridge to answer the second research question:

RQ 2: To what level of detail and using which methods should these factors be estimated to provide a general representation of HD while enabling real-time calculation?

Given that many of these aspects have been extensively studied in white box model, the aim of this thesis was to facilitate fast simulations using a limited parameter set for each building, in the form of a GBM. This approach allows for physics-based calculations, enabling the analysis of future or hypothetical scenarios without the need for extensive knowledge or parametrization of the model. All necessary model parameters are listed in Section 4.2, with each parameter having a clear physical interpretation. The implemented approximations and estimations, as discussed in Chapter 3, rely on statistical or empirical models derived from the literature. As illustrated in Section 5.4, these approximations result in minimal computational effort, enabling the prediction of HD for multiple buildings 24 h into the future at a resolution of 15 minutes, which is a de-facto standard in the smart grid sector, fast than real-time.

In addition to these literature-based approximations, an extensive analysis of the dynamic behavior of the building's thermal capacity and its coupling with room temperature was presented in Section 3.3, addressing the third research question:

RQ 3: What dynamic behavior is required from a GBM to model temperature changes due to energy shifts for optimization purposes?

While most state of the art GBMs model dynamic behavior using a lumped capacitance and resistance element approach, this thesis investigated a more computationally efficient method. Section 3.3 demonstrated the reasonable approach of assuming uniform temperature levels within the buildings' structure, with an empirical corrections factor for the coupling between the room temperature and the building's thermal mass. The dynamic behavior of the GBM, as presented in Section 5.2, follows the expectations, with room temperatures rapidly dropping in the evening without heating, matching the building structure's temperature, and then decreasing slowly throughout the night due to the high thermal capacity of the building's mass. The dynamic behavior of the GBM for temperature changes resulting from energy shifts for optimization purposes was shown in Section 6.1. This involves an increased load during midday, reducing the electrical power required by the HPs at night to maximize the utilization of power generated by the photovoltaic systems.

The final research question explores the potential of cross-location optimization over local optimization, specifically by leveraging different weather conditions at various locations:

RQ 4: What potential does cross-location optimization offer over local optimization, particularly by leveraging different weather conditions across various locations?

Section 6.2 compared local and cross-location optimization optimization strategies for two settlements with differing weather scenarios. The comparison highlighted the potential of utilizing the flexibility provided by HPs in both locations to take advantage of an overproduction by PV in one settlement, resulting in a load profile for the combined power of both settlements. The proposed GBM thus facilitates simulation and analysis in these emerging areas of interest.

7.1 Results

Overall the results from Chapter 5 and 6 demonstrated a strong correlation between the introduced GBM model and the compared WPuQ dataset, and align with the expected behavior. Although the HD for an individual household does not perfectly match the reference data, the aggregated electric load at the substation level for the entire settlement is well approximated. In terms of cumulative daily energy demand, the simulated HPs using the GBM exhibit a high degree of accuracy when compared to the dataset across an entire year, with relative errors remaining below 5 %.

The power profile at a 15 minute resolution showed differences between the GBM profile and the dataset, with actual HPs fluctuating between two or three distinct power consumption states, while the model predicts a continuous power load throughout the day. This discrepancy may arise from the presence of small hot water tanks, which buffer the continuously varying HD over short periods, as they are typically installed in combination with HPs. Given their limited size, these tanks were not modeled in this thesis, but they may account for the observed differences in behavior over short time intervals.

The efficient design of the GBM minimizes computational effort, thereby enabling rapid simulations and consequently, real-time predictions for multiple buildings. This capability is essential for enabling optimization for utilizing flexibilities provided by the thermal heat capacity of building structures and flexible room temperature profiles. The connection between temperature flexibility and corresponding heat and electrical power flexibilities is key for further investigating the potential of leveraging HPs to utilize PV generation, as occupant comfort primarily depends on room temperature.

The effectiveness of cross-location optimization in enhancing optimization potential compared to local optimization underscored the role of the GBM in assessing HD across various locations influenced by differing weather conditions. The introduced GBM provides the opportunity to simulate and analyze these scenarios, with the potential for more sophisticated optimization methods at a higher level, based on the decision making unit. In this thesis, a basic approach for shifting energy between settlements is implemented, offering the possibility to unlock further optimization potential through more complex functionalities within the DMU.

Overall, the analyses conducted on flexibility potentials for optimizing HPs together with PV systems highlighted the critical role of flexibility provided by HPs in these scenarios. Consequently, the proposed GBM offers the necessary tools and framework to explore various scenarios and optimization strategies, thereby ensuring grid stability and optimizing self-sufficiency with emerging on-site renewable energy sources.

7.2 Outlook

Building upon the results and analysis presented in the previous section, this section outlines several potential areas for further investigation. These topics aim to enhance the introduced GBM, expanding its functionality and broadening the range of supported scenarios.

7.2.1 Heating System

For this thesis a heating system via air conditioning or radiators was assumed, coupling the provided heat directly with the air. This approach relies solely on the building's thermal mass in an indirect manner, with the room temperature

coupling heat into the structure. Many modern heating systems, however, are based on the thermal activation of building elements, such as floor heating, which allows for indirect heating. These systems offer significantly greater flexibility as they are designed to store and buffer heat due to their high thermal capacity. Nevertheless, such systems necessitate a more complex control system to account for the heat release over a long period of time and the extended heating times associated with activated elements. Additionally, these systems do not allow for rapid room temperature changes and control, due to the indirect heating and high capacity.

Moreover, the inclusion of a hot water tank could introduce further flexibility. While modern HPs do not always require one, a hot water tank is commonly implemented for domestic hot water usage. This addition could enable the GBM to better align with the distinct power consumption patterns observed in the WPuQ dataset. However, incorporating such an energy buffer would increase the complexity of the heating control system, as it would necessitate a physical model of the hot water tank and an internal optimization and control strategy to balance the heating of the tank while ensuring adequate heating for the building and meeting the required flexibilities set by the community controller.

Both the thermal activation of building elements and the integration of a hot water tank increase the complexity of the overall heating system. Nevertheless, they have the potential to substantially enhance the flexibility of HPs, leveraging existing applications in the residential sector.

7.2.2 Switching Logic

Another area of further investigation is given by the switching logic, governing the operating mode of the HP. Currently, the implemented GBM computes the total heat requirement for the next 24 h and, based on a parameterized threshold, decides whether to activate heating or cooling. As discussed in Section 5.3, realistic behavior requires careful calibration based on the building's parameters and consideration of weather conditions.

Consequently, an alternative approach may lead to a more robust GBM with reduced reliance on parametrization. For instance, a decision process based on violations of predefined minimum and maximum temperature thresholds would eliminate the need for additional parameters and may better reflect actual occupant behavior by switching modes in response to room temperature. Another possibility involves incorporating past operating modes, which would necessitate a memory function to store previous time steps and prevent toggling between modes based on this historical information.

A more robust implementation would enhance the reliability of simulation behavior, reducing the need for detailed analysis of the operation modes of the HP. Additionally, it would offer the potential for varying room temperature profiles associated with the mode of the HP, as different temperature settings are often employed during winter and summer seasons.

7.2.3 Occupancy and Heated Water Model

As a final topic for further study, the statistical models from the literature concerning occupancy probability and hot water usage throughout the day exhibit potential for improvement. While these models are computationally efficient and demonstrate a good fit between real data and simulation for aggregated power demand, they lack the ability to parametrize households based on occupant behavior. There may be variations in the HD based on the age of the population or other key characteristics, such as an older population, due to differences in occupancy probability and hot

water usage.

The ability to configure additional profiles would also allow for the expansion of the implemented GBM to commercial buildings, where the majority of occupants are present during working hours. In conclusion, it can be stated that the proposed GBM offers a robust foundation for a diverse range of scenarios and is capable of supporting their analysis. Coupled with the identified future areas of development, this enables a more comprehensive investigation and simulation of the HD for various settlements and flexibility requirements.

Glossary

cross-location optimization Optimization across multiple locations in a global sense with different objectives such as grid-oriented or cost efficiency, in contrast to purely local optimization.

differential equation Differential equations are equations that relate functions to their derivatives, with either on or more unknowns [96].

electromagnetic waves An electromagnetic wave is a wave of coupled electric and magnetic fields with no medium required for propagation [102].

Energy Performance of Buildings Directive A set of standards that aims to promote the improvement of the energy performance of buildings within the European Union [103].

grid-oriented With the goal of minimizing the peak loads on the power grid, in contrast to cost-orientated.

HDF5 The Hierarchical Data Format Version 5 is an open source file format that supports large, complex, heterogeneous data by using a file directory-like structure that allows data to be organized within the file [104].

iso-process The isoprocess describes a process in thermodynamics in which it is assumed that a state variable is kept constant as well as that the mass in the system always remains constant [105].

nearly zero energy buildings A requirement introduced by the Energy Performance of Buildings Directive EU/31/-2010 stating that all new buildings – as of 2020 - must have a high energy performance and very low-energy needs, covered largely by onsite and nearby renewable energy sources [106].

NUTS NUTS (Nomenclature des unités territoriales statistiques) is a hierarchical system used to uniquely identify and classify spatial reference units in official statistics across EU member states, with NUTS 1 representing larger socio-economic regions, NUTS 2 referring to basic regions for regional policy, NUTS 3 for smaller regions used for specific data collection [101].

Nyquist Criteria The Nyquist Criteria in signal processing, named after Harry Nyquist, refers to the Nyquist frequency, which is half the sampling frequency, ensuring that a continuous signal below this frequency remains free of aliasing when being discretized [107].

parabolic partial differential equation A parabolic partial differential equation is used to describe a variety of dynamic phenomena and is a partial derivative function that consists of at least two independent variables [96].

Python Python is a common object-oriented programming language with many extensions as packages that enable quick and easy implementation of problems [108].

RCP RCP (Representative Concentration Pathway) are greenhouse gas concentration trajectories used in climate modeling to project different future climate scenarios, with the numbers (such as 4.5 or 8.5) representing the expected radiative forcing in W/m^2 by the year 2100, correlating to the greenhouse gas concentration [101].

real-time Real-time refers to the operation of a computer system in which programs for processing incoming data are constantly ready for use in such a way that the processing results are available within a certain period of time dictated by the physical system that it interacts with [109].

renewable energy Energy from renewable natural resources that are replenished on a human timescale [110].

REST-API A REST-API is an application programming interface that follows the design principles of the REST architectural style (Representational State Transfer), offering a flexible, lightweight way to integrate applications and connect components [111].

solar constant The solar constant describes the amount of energy that would be emitted to the earth by solar radiation at an average distance from the sun and without an air envelope and is around $1.4\,kW/m^2$ [81].

Stefan-Bolzmann constant Stefan-Bolzmann constant was introduced together with the Stefan-Bolzmann law and is a constant of 5.67 $W/m^2\,K^4$ as a proportion between the radiation of a ideal black body and the temperature T^4 [112].

Stefan-Bolzmann law Stefan-Bolzmann law was found by Josef Stefan and Ludwig Bolzmann and describes the intensity of the thermal radiation emitted from a object based on its temperature [112].

Taylor series The Taylor series of a function is an infinite sum of terms expressed by the derivatives of the function at a single point to approximate the function value at a distance, introduced by Brook Taylor [96].

WPuQ WPuQ is a joint project with the name Wind-Solar-Wärmepumpen-Quartier - Erneuerbar betriebene Wärmepumpen zur Minimierung des Primärenergiebedarfs with the goal to analyze the behavior and effects of operating many heat pumps within a local network [113].

Zenodo platform Zenodo is a platform for providing open source data as open science, that was launched 2013 out of CERN, an OpenAIRE partners [114].

Bibliography

[1] Nikolaos A. Efkarpidis, Georgios C. Christoforidis, and Grigoris K. Papagiannis. "Modeling of Heating and Cooling Energy Needs in Different Types of Smart Buildings". In: *IEEE Access* 8 (2020), pp. 29711–29728. DOI: 10.1109/ACCESS.2020.2972965.

[2] Energy Information Administration. *International Energy Outlook 2016*. 2016.

[3] European Commision. "Directive (EU) 2018/ of the European Parliament and of the Council of 30 May 2018 amending Directive 2010/31/EU on the energy performance of buildings and Directive 2012/27/EU on energy efficiency". In: *Official Journal of the European Union* 156 (June 19, 2018), pp. 75–91.

[4] European Commision. "Directive 2010/31/EU of the European Parliament and of the Council of 19 May 2010 on the energy performance of buildings". In: *Official Journal of the European Union* 153 (June 18, 2010), pp. 13–53.

[5] Bundesministerium für Wirtschaft und Klimaschutz. *Für mehr klimafreundliche Heizungen*. Sept. 27, 2024.

[6] Dominik J Storch et al. *Modelling the Electrical Power Demand of Different Heat Pump Systems: Approaches for Simplified and Detailed Load Assessment*. Feb. 16, 2024.

[7] Mehmet Hazar Cintuglu et al. "A Survey on Smart Grid Cyber-Physical System Testbeds". In: *IEEE Communications Surveys & Tutorials* 19.1 (2017), pp. 446–464. DOI: 10.1109/COMST.2016.2627399.

[8] Kevin Mets, Juan Aparicio Ojea, and Chris Develder. "Combining Power and Communication Network Simulation for Cost-Effective Smart Grid Analysis". In: *IEEE Communications Surveys & Tutorials* 16.3 (2014), pp. 1771–1796. DOI: 10.1109/SURV.2014.021414.00116.

[9] Lukas G. Swan and V. Ismet Ugursal. "Modeling of end-use energy consumption in the residential sector: A review of modeling techniques". In: *Renewable and Sustainable Energy Reviews* 13.8 (Oct. 2009), pp. 1819–1835. DOI: 10.1016/j.rser.2008.09.033.

[10] Austrian Standards International. *Energetische Bewertung von Gebäuden - Berechnung des Energiebedarfs für Heizung und Kühlung, Innentemperaturen sowie der Heiz- und Kühllast in einem Gebäude oder einer Gebäudezone - Teil 1: Berechnungsverfahren (ISO 52016-1:2017)*. ÖNORM 52016-1. Komitee 175: Wärmeschutz von Gebäuden und Bauteilen. 2018.

[11] DIN Deutsches Institut für Normung. *Thermal protection and energy economy in buildings — Part 6: Calculation of annual heat and annual energy use*. DIN 4108-6. Normenausschuss Bauwesen (NABau). 2003.

[12] VDI Verein deutscher Ingenieure. *Referenzlastprofile von Wohngebäuden für Strom, Heizung und Trinkwarmwasser sowie Referenzerzeugungsprofile für Fotovoltaikanlagen*. VDI 4655. VDI-Gesellschaft Energie und Umwelt (GEU). 2021.

[13] Henrik Aalborg Nielsen and Henrik Madsen. "Modelling the heat consumption in district heating systems using a grey-box approach". In: *Energy and Buildings* 38.1 (Jan. 2006), pp. 63–71. DOI: 10.1016/j.enbuild.2005.05.002.

[14] A Thür et al. *Das Gebäude als Energieschwamm - Strom rein - Wärme raus.*

[15] Österreichsiche Koordinationsstelle für Energiegemeinschaften. *Energiegemeinschaften in der Europäischen Union.* 2022.

[16] ISO International Organisation for Standardization. *Energy performance of buildings — Overarching EPB assessment.* ISO 52000-1:2017. ISO technical committees. 2017.

[17] ISO International Organisation for Standardization. *Energy performance of buildings — Energy needs for heating and cooling, internal temperatures and sensible and latent heat loads.* ISO 52016-1:2017. ISO technical committees. 2022.

[18] Austrian Standards International. *Heizungsanlagen in Gebäuden - Verfahren zur Berechnung der Norm-Heizlast.* ÖNORM EN 12831. Komitee 058: Heizungsanlagen. 2003.

[19] VDI Verein Deutscher Ingenieure e.V. *VDI-Richtlinien: Standards setzen – auf dem aktuellen Stand der Technik.* [Online]. URL: https://www.vdi.de/richtlinien (visited on 02/04/2025).

[20] VDI Verein deutscher Ingenieure. *Wirtschaftlichkeit gebäudetechnischer Anlagen Nutzenergiebedarf für die Trinkwassererwärmung.* VDI 2067. VDI-Gesellschaft Bauen und Gebäudetechnik (GBG). 2017.

[21] DIN Deutsches Institut für Normung. *DIN - kurz erklärt.* [Online]. URL: https://www.din.de/de/ueber-normen-und-standards/basiswissen?etcc_cmp_onsite=din-kurz-erklaert-onsite&etcc_med_onsite=homepage-teaser&etcc_cu=onsite&et_cmp_seg2=https%3A%2F%2Fwww.din.de%2Fde (visited on 02/04/2025).

[22] Clara Büttner et al. "Open modeling of electricity and heat demand curves for all residential buildings in Germany". In: *Energy Informatics* 5 (S1 Sept. 7, 2022), p. 21. DOI: 10.1186/s42162-022-00201-y.

[23] Octavio Loyola-Gonzalez. "Black-Box vs. White-Box: Understanding Their Advantages and Weaknesses From a Practical Point of View". In: *IEEE Access* 7 (2019), pp. 154096–154113. DOI: 10.1109/ACCESS.2019.2949286.

[24] Tjarko Tjaden. *Repräsentative elektrische Lastprofile für Wohngebäude in Deutschland auf 1-sekündiger Datenbasis.*

[25] David Fischer et al. "A stochastic bottom-up model for space heating and domestic hot water load profiles for German households". In: *Energy and Buildings* 124 (July 2016), pp. 120–128. DOI: 10.1016/j.enbuild.2016.04.069.

[26] Francesco Lombardi et al. "Generating high-resolution multi-energy load profiles for remote areas with an open-source stochastic model". In: *Energy* 177 (June 2019), pp. 433–444. DOI: 10.1016/j.energy.2019.04.097.

[27] H. Farahbakhsh. "A residential end-use energy consumption model for Canada". In: *International Journal of Energy Research* 22 (1998), pp. 1133–1143.

[28] V. Ismet Ugursal and Alan S. Fung. "Impact of appliance efficiency and fuel substitution on residential end-use energy consumption in Canada". In: *Energy and Buildings* 24.2 (July 1996), pp. 137–146. DOI: 10.1016/0378-7788(96)00970-X.

[29] Julia Sachs et al. "Clustered spatially and temporally resolved global heat and cooling energy demand in the residential sector". In: *Applied Energy* 250 (Sept. 2019), pp. 48–62. DOI: 10.1016/j.apenergy.2019.05.011.

[30] Hai-xiang Zhao and Frédéric Magoulès. "A review on the prediction of building energy consumption". In: *Renewable and Sustainable Energy Reviews* 16.6 (Aug. 2012), pp. 3586–3592. DOI: 10.1016/j.rser.2012.02.049.

[31] M. Bauer and J.-L. Scartezzini. "A simplified correlation method accounting for heating and cooling loads in energy-efficient buildings". In: *Energy and Buildings* 27.2 (Apr. 1998), pp. 147–154. DOI: 10.1016/S0378-7788(97)00035-2.

[32] Karl-Erik Westergren, Hans Högberg, and Urban Norlén. "Monitoring energy consumption in single-family houses". In: *Energy and Buildings* 29.3 (Jan. 1999), pp. 247–257. DOI: 10.1016/S0378-7788(98)00065-6.

[33] Jens Pfafferott, Sebastian Herkel, and Jeannette Wapler. "Thermal building behaviour in summer: long-term data evaluation using simplified models". In: *Energy and Buildings* 37.8 (Aug. 2005), pp. 844–852. DOI: 10.1016/j.enbuild.2004.11.007.

[34] Yuan Ma et al. "Study on Power Energy Consumption Model for Large-Scale Public Building". In: *2010 2nd International Workshop on Intelligent Systems and Applications*. 2010 2nd International Workshop on Intelligent Systems and Applications (ISA). Wuhan, China: IEEE, May 2010, pp. 1–4. DOI: 10.1109/IWISA.2010.5473608.

[35] Sung-Hwan Cho et al. "Effect of length of measurement period on accuracy of predicted annual heating energy consumption of buildings". In: *Energy Conversion and Management* 45.18 (Nov. 2004), pp. 2867–2878. DOI: 10.1016/j.enconman.2003.12.017.

[36] Subodh Paudel et al. *Support Vector Machine in Prediction of Building Energy Demand Using Pseudo Dynamic Approach*. Version Number: 1. 2015. DOI: 10.48550/ARXIV.1507.05019.

[37] Eiman Tamah Al-Shammari et al. "Prediction of heat load in district heating systems by Support Vector Machine with Firefly searching algorithm". In: *Energy* 95 (Jan. 2016), pp. 266–273. DOI: 10.1016/j.energy.2015.11.079.

[38] Milan Protić et al. "Forecasting of consumers heat load in district heating systems using the support vector machine with a discrete wavelet transform algorithm". In: *Energy* 87 (July 2015), pp. 343–351. DOI: 10.1016/j.energy.2015.04.109.

[39] J. F. Kreider et al. "Building Energy Use Prediction and System Identification Using Recurrent Neural Networks". In: *Journal of Solar Energy Engineering* 117.3 (Aug. 1, 1995), pp. 161–166. DOI: 10.1115/1.2847757.

[40] Abdullatif E. Ben-Nakhi and Mohamed A. Mahmoud. "Cooling load prediction for buildings using general regression neural networks". In: *Energy Conversion and Management* 45.13 (Aug. 2004), pp. 2127–2141. DOI: 10.1016/j.enconman.2003.10.009.

[41] S. A. Kalogirou. "Artificial neural networks in energy applications in buildings". In: *International Journal of Low-Carbon Technologies* 1.3 (July 1, 2006), pp. 201–216. DOI: 10.1093/ijlct/1.3.201.

[42] Ryohei Yokoyama, Tetsuya Wakui, and Ryoichi Satake. "Prediction of energy demands using neural network with model identification by global optimization". In: *Energy Conversion and Management* 50.2 (Feb. 2009), pp. 319–327. DOI: 10.1016/j.enconman.2008.09.017.

[43] Yan Cheng-wen and Yao Jian. "Application of ANN for the prediction of building energy consumption at different climate zones with HDD and CDD". In: *2010 2nd International Conference on Future Computer and Communication*. 2010 2nd International Conference on Future Computer and Communication. Wuhan, China: IEEE, 2010, pp. V3–286–V3–289. DOI: 10.1109/ICFCC.2010.5497626.

[44] Jin Woo Moon and Jong-Jin Kim. "ANN-based thermal control models for residential buildings". In: *Building and Environment* 45.7 (July 2010), pp. 1612–1625. DOI: 10.1016/j.buildenv.2010.01.009.

[45] Rocío Escandón et al. "Thermal comfort prediction in a building category: Artificial neural network generation from calibrated models for a social housing stock in southern Europe". In: *Applied Thermal Engineering* 150 (Mar. 2019), pp. 492–505. DOI: 10.1016/j.applthermaleng.2019.01.013.

[46] Xinyi Li and Runming Yao. "A machine-learning-based approach to predict residential annual space heating and cooling loads considering occupant behaviour". In: *Energy* 212 (Dec. 2020), p. 118676. DOI: 10.1016/j.energy.2020.118676.

[47] Chengchu Yan et al. "A simplified analytical model to evaluate the impact of radiant heat on building cooling load". In: *Applied Thermal Engineering* 77 (Feb. 2015), pp. 30–41. DOI: 10.1016/j.applthermaleng.2014.12.017.

[48] Amirreza Fateh et al. “A State-Space Analysis of a Single Zone Building Considering Solar Radiation, Internal Radiation, and PCM Effects”. In: *Applied Sciences* 9.5 (Feb. 26, 2019), p. 832. DOI: 10.3390/app9050832.

[49] M Deru, R Judkoff, and J Neymark. *Whole-Building Energy Simulation with a Three-Dimensional Ground-Coupled Heat Transfer Model: Preprint.*

[50] Li Mei et al. “Thermal modelling of a building with an integrated ventilated PV façade”. In: *Energy and Buildings* 35.6 (July 2003), pp. 605–617. DOI: 10.1016/S0378-7788(02)00168-8.

[51] Choongwan Koo et al. “An estimation model for the heating and cooling demand of a residential building with a different envelope design using the finite element method”. In: *Applied Energy* 115 (Feb. 2014), pp. 205–215. DOI: 10.1016/j.apenergy.2013.11.014.

[52] Toke Rammer Nielsen. “Simple tool to evaluate energy demand and indoor environment in the early stages of building design”. In: *Solar Energy* 78.1 (Jan. 2005), pp. 73–83. DOI: 10.1016/j.solener.2004.06.016.

[53] Mattia De Rosa et al. “An Iterative Methodology for Model Complexity Reduction in Residential Building Simulation”. In: *Energies* 12.12 (June 25, 2019), p. 2448. DOI: 10.3390/en12122448.

[54] Xianmin Wang et al. “Gray predicting theory and application of energy consumption of building heat-moisture system”. In: *Building and Environment* 34.4 (July 1999), pp. 417–420. DOI: 10.1016/S0360-1323(98)00037-7.

[55] J.J. Guo, J.Y. Wu, and R.Z. Wang. “A new approach to energy consumption prediction of domestic heat pump water heater based on grey system theory”. In: *Energy and Buildings* 43.6 (June 2011), pp. 1273–1279. DOI: 10.1016/j.enbuild.2011.01.001.

[56] Qiang Zhou et al. “A grey-box model of next-day building thermal load prediction for energy-efficient control”. In: *International Journal of Energy Research* 32.15 (Dec. 2008), pp. 1418–1431. DOI: 10.1002/er.1458.

[57] Oluwaseyi T. Ogunsola, Li Song, and Gang Wang. “Development and validation of a time-series model for real-time thermal load estimation”. In: *Energy and Buildings* 76 (June 2014), pp. 440–449. DOI: 10.1016/j.enbuild.2014.02.075.

[58] Shengwei Wang and Xinhua Xu. “Parameter estimation of internal thermal mass of building dynamic models using genetic algorithm”. In: *Energy Conversion and Management* 47.13 (Aug. 2006), pp. 1927–1941. DOI: 10.1016/j.enconman.2005.09.011.

[59] Byung-Ki Jeon et al. “Learning-Based Predictive Building Energy Model Using Weather Forecasts for Optimal Control of Domestic Energy Systems”. In: *Sustainability* 11.1 (Dec. 28, 2018), p. 147. DOI: 10.3390/su11010147.

[60] Gilles Fraisse et al. “Development of a simplified and accurate building model based on electrical analogy”. In: *Energy and Buildings* 34.10 (Nov. 2002), pp. 1017–1031. DOI: 10.1016/S0378-7788(02)00019-1.

[61] A. Tindale. “Third-order lumped-parameter simulation method”. In: *Building Services Engineering Research and Technology* 14.3 (Aug. 1993), pp. 87–97. DOI: 10.1177/014362449301400302.

[62] Mattia De Rosa et al. “Heating and cooling building energy demand evaluation; a simplified model and a modified degree days approach”. In: *Applied Energy* 128 (Sept. 2014), pp. 217–229. DOI: 10.1016/j.apenergy.2014.04.067.

[63] Steffen Meinecke. *SimBench.* [Online]. URL: https://simbench.de/de/ (visited on 02/10/2025).

[64] Harry Wagstaff et al. “SimBench: A portable benchmarking methodology for full-system simulators”. In: *2017 IEEE International Symposium on Performance Analysis of Systems and Software (ISPASS).* 2017 IEEE International Symposium on Performance Analysis of Systems and Software (ISPASS). Santa Rosa, CA, USA: IEEE, Apr. 2017, pp. 217–226. DOI: 10.1109/ISPASS.2017.7975293.

[65] Marlon Schlemminger et al. “Dataset on electrical single-family house and heat pump load profiles in Germany”. In: *Scientific Data* 9.1 (Feb. 15, 2022), p. 56. DOI: 10.1038/s41597-022-01156-1.

[66] Theresa Müller and Dominik Möst. "Demand Response Potential: Available when Needed?" In: *Energy Policy* 115 (Apr. 2018), pp. 181–198. DOI: 10.1016/j.enpol.2017.12.025.

[67] Andreas Weglage et al. *Energieausweis - Das große Kompendium*. 3rd ed. Wiesbaden: Vieweg+Teubner, 2010. 569 pp.

[68] Ying Han, Xiao Liu, and Li Chang. "Comparison of software for building energy simulation". In: (2014).

[69] MathWorks. *MATLAB*. [Online]. URL: https://de.mathworks.com/ (visited on 02/04/2025).

[70] Angela Sasic Kalagasidis et al. "The International Building Physics Toolbox in Simulink". In: *Energy and Buildings* 39.6 (June 2007), pp. 665–674. DOI: 10.1016/j.enbuild.2006.10.007.

[71] MathWorks. *Neuronale Netze*. [Online]. URL: https://de.mathworks.com/discovery/neural-network.html (visited on 02/04/2025).

[72] TRNSYS. *Transient System Simulation Tool*. [Online]. URL: https://www.trnsys.com/ (visited on 02/04/2025).

[73] {and} managed by the National Renewable Energy Laboratory (NREL) U.S. Department of Energy's (DOE) Building Technologies Office (BTO). *EnergyPlus*. [Online]. URL: https://energyplus.net/ (visited on 02/04/2025).

[74] University of Strathclyde Glasgow. *Energy Systems Research Unit*. [Online]. URL: https://www.strath.ac.uk/research/energysystemsresearchunit/applications/esp-r/ (visited on 02/04/2025).

[75] U.S. Department of and Energy. *SUNREL Software*. [Online]. URL: https://labpartnering.org/technologies/ad38f992-966f-4b1b-a5f6-3ba192b3c790 (visited on 02/04/2025).

[76] James J. Hirsch. *Welcome to DOE2*. [Online]. URL: https://www.doe2.com/ (visited on 02/04/2025).

[77] Siemens. *Bifrost*. [Online]. URL: https://bifrost.siemens.com/en (visited on 02/03/2025).

[78] Thomas Leopold et al. "Simulation-based methodology for optimizing Energy Community Controllers". In: *2021 IEEE 30th International Symposium on Industrial Electronics (ISIE)*. 2021 IEEE 30th International Symposium on Industrial Electronics (ISIE). Kyoto, Japan: IEEE, June 20, 2021, pp. 1–6. DOI: 10.1109/ISIE45552.2021.9576277.

[79] Wirtschaftsuniversität Wien. *EnergyDec*. FFG Projektdatenbank. [Online]. URL: https://projekte.ffg.at/projekt/4174815 (visited on 02/04/2015).

[80] Thomas Leopold, Paul Bauer, and Thomas Reisinger. *Optimierung des Energietransferpotentials von Energiegemeinschaften*. IEWT 2025. [Online]. Feb. 2025. URL: https://iewt2025.eeg.tuwien.ac.at/ (visited on 03/13/2025).

[81] Hermann Recknagel et al. *Taschenbuch für Heizung+Klimatechnik*. 77th ed. Vol. 1. 2 vols. DIV Deutscher Industrieverlag GmbH, 2015.

[82] Benoit Delcroix. "Modeling of Thermal Mass Energy Storage in Buildings with Phase Change Materials". PhD thesis. École Polytechnique de Montréal, 2015.

[83] G. Ziskind, V. Dubovsky, and R. Letan. "Ventilation by natural convection of a one-story building". In: *Energy and Buildings* 34.1 (Jan. 2002), pp. 91–101. DOI: 10.1016/S0378-7788(01)00080-9.

[84] Francisco José Sánchez De La Flor et al. "Solar radiation calculation methodology for building exterior surfaces". In: *Solar Energy* 79.5 (Nov. 2005), pp. 513–522. DOI: 10.1016/j.solener.2004.12.007.

[85] Simon Ruben Drauz. *Synthesis of a heat and electrical load profile for single and multi-family houses used for subsequent performance tests of a multi-component energy system*. 2016.

[86] Meral Ozel. "The influence of exterior surface solar absorptivity on thermal characteristics and optimum insulation thickness". In: *Renewable Energy* 39.1 (Mar. 2012), pp. 347–355. DOI: 10.1016/j.renene.2011.08.039.

[87] Hermann Recknagel et al. *Taschenbuch für Heizung+Klimatechnik*. 77th ed. Vol. 2. 2 vols. DIV Deutscher Industrieverlag GmbH, 2015.

[88] DIN Deutsches Institut für Normung. *Ergonomie der thermischen Umgebung - Analytische Bestimmung und Interpretation der thermischen Behaglichkeit durch Berechnung des PMV- und des PPD-Indexes und Kriterien der lokalen thermischen Behaglichkeit (ISO 7730:2005)*. DIN EN ISO 7730. Arbeitsausschuss NAErg AA 7 "Klima" im NAErg. 2005.

[89] Ian Richardson, Murray Thomson, and David Infield. "A high-resolution domestic building occupancy model for energy demand simulations". In: *Energy and Buildings* 40.8 (Jan. 2008), pp. 1560–1566. DOI: 10.1016/j.enbuild.2008.02.006.

[90] Eoghan McKenna, Michal Krawczynski, and Murray Thomson. "Four-state domestic building occupancy model for energy demand simulations". In: *Energy and Buildings* 96 (June 2015), pp. 30–39. DOI: 10.1016/j.enbuild.2015.03.013.

[91] Ulrike Jordan et al. "Realistic Domestic Hot-Water Profiles in Different Time Scales". In: (2001).

[92] Nidal H. Abu-Hamdeh. "Thermal Properties of Soils as affected by Density and Water Content". In: *Biosystems Engineering* 86.1 (Sept. 2003), pp. 97–102. DOI: 10.1016/S1537-5110(03)00112-0.

[93] Defoe C. Ginnings and George T. Furukawa. "Heat Capacity Standards for the Range 14 to 1200°K." In: *Journal of the American Chemical Society* 75.3 (Feb. 1953), pp. 522–527. DOI: 10.1021/ja01099a004.

[94] John Crank. *The Mathematics of Diffusion*. 2nd ed. Oxford University Press, 1975.

[95] T. N. Narasimhan. "Fourier's heat conduction equation: History, influence, and connections". In: *Reviews of Geophysics* 37.1 (Feb. 1999). Publisher: American Geophysical Union (AGU), pp. 151–172. DOI: 10.1029/1998rg900006.

[96] J. W. Thomas. *Numerical Partial Differential Equations: Finite Difference Methods*. Springer Science & Business Media, 2013.

[97] R. Heinzl. *Finite Differences*. [Online]. URL: https://www.iue.tuwien.ac.at/phd/heinzl/node27.html (visited on 01/26/2025).

[98] S.G. Bankoff. *Heat Conduction or Diffusion With Change of Phase*. ISSN: 0065-2377. Elsevier, 1964. DOI: 10.1016/s0065-2377(08)60007-1.

[99] DIN Deutsches Institut für Normung. *Energy efficiency of buildings – calculation of the net, final and primary energy demand for heating, cooling, ventilation, domestic hot water and lighting – Part 5: Final energy demand of heating systems*. DIN V 18599-5. DIN-Normenausschuss Bauwesen (NABau) DIN-Normenausschuss Heiz- und Raumlufttechnik sowie deren Sicherheit (NHRS). 2018.

[100] DIN Deutsches Institut für Normung. *Energy efficiency of buildings – Calculation of the net, final and primary energy demand for heating, cooling, ventilation, domestic hot water and lighting – Part 7: Final energy demand of air-handling and air- conditioning systems for non-residential buildings*. DIN V 18599-7. DIN-Normenausschuss Bauwesen (NABau) DIN-Normenausschuss Heiz- und Raumlufttechnik sowie deren Sicherheit (NHRS). 2018.

[101] Herbert Formayer et al. *SECURES-Met - A European wide meteorological data set suitable for electricity modelling (supply and demand) for historical climate and climate change projections*. Version 1.0.0. May 15, 2023. DOI: 10.5281/ZENODO.7907883.

[102] Adalbert Prechtl. *Vorlesung über die Grundlagen der Elektrotechnik*. 2nd ed. Vol. 2. 2 vols. SpringerWienNewYork, 2008.

[103] EPB Center. *The Energy Performance of Buildings Directive (EPBD)*. [Online]. URL: https://epb.center/epb-standards/energy-performance-buildings-directive-epbd/ (visited on 02/02/2025).

[104] Leah A. Wasser. *Hierarchical Data Formats - What is HDF5?* [Online]. URL: https://www.neonscience.org/resources/learning-hub/tutorials/about-hdf5#:~:text=The%20Hierarchical%20Data%20Format%20version,with%20files%20on%20your%20computer. (visited on 02/10/2050).

[105] Ingo Müller. *Grundzüge der Thermodynamik: mit historischen Anmerkungen*. 3rd ed. Springer Berlin Heidelberg, 2001.

[106] European Commision. *Nearly-zero energy and zero-emission buildings*. [Online]. URL: https://energy.ec.europa.eu/topics/energy-efficiency/energy-efficient-buildings/nearly-zero-energy-and-zero-emission-buildings_en (visited on 02/02/2025).

[107] Enders Robinson and Dean Clark. "Sampling and the Nyquist frequency". In: *The Leading Edge* 10.3 (Jan. 3, 1991), pp. 51–53. DOI: 10.1190/1.1436812.

[108] *python*. [Online]. URL: https://www.python.org/ (visited on 02/01/2025).

[109] ISO/ICE. *Information technology — Vocabulary*. ISO/IEC 2382:2015. ISO (the International Organization for Standardization) and IEC (the International Electrotechnical Commission). 2022.

[110] United Nations. *What is renewable energy?* [Online]. URL: https://www.un.org/en/climatechange/what-is-renewable-energy (visited on 02/02/2025).

[111] Adeel Ehsan et al. "RESTful API Testing Methodologies: Rationale, Challenges, and Solution Directions". In: *Applied Sciences* 12.9 (Apr. 26, 2022), p. 4369. DOI: 10.3390/app12094369.

[112] Mark Wellons. "The Stefan-Boltzmann Law". In: *Physics Department, The College of Wooster* (May 2007).

[113] Tobias Ohrdes et al. *Wind-Solar-Wärmepumpen-Quartier - Erneuerbar betriebene Wärmepumpen zur Minimierung des Primärenergiebedarfs (WPuQ)*. Institut für Solarenergieforschung Hameln, Sept. 2021.

[114] European Organization For Nuclear Research. *zenodo*. [Online]. URL: https://zenodo.org/ (visited on 02/02/2025).

Erklärung

Hiermit erkläre ich, dass die vorliegende Arbeit ohne unzulässige Hilfe Dritter und ohne Benutzung anderer als der angegebenen Hilfsmittel angefertigt wurde. Die aus anderen Quellen oder indirekt übernommenen Daten und Konzepte sind unter Angabe der Quelle gekennzeichnet.

Die Arbeit wurde bisher weder im In- noch im Ausland in gleicher oder in ähnlicher Form in anderen Prüfungsverfahren vorgelegt.

Copyright Statement

I, Benedikt Herold, hereby declare that this thesis is my own original work and, to the best of my knowledge and belief, it does not:

- Breach copyright or other intellectual property rights of a third party.
- Contain material previously published or written by a third party, except where this is appropriately cited through full and accurate referencing.
- Contain material which to a substantial extent has been accepted for the qualification of any other degree or diploma of a university or other institution of higher learning.
- Contain substantial portions of third party copyright material, including but not limited to charts, diagrams, graphs, photographs or maps, or in instances where it does, I have obtained permission to use such material and allow it to be made accessible worldwide via the Internet.

Signature: Benedikt Herold

Vienna, Austria, 20th March 2025 Benedikt Herold